CHARACTERIZATION OF URBAN MORPHOLOGY AND ITS EFFECT ON WEATHER UNCERTAINTY IN BUILDING ENERGY SIMULATION

A Dissertation
Presented to
The Academic Faculty

by

Mayuri Rajput

In Partial Fulfillment
of the Requirements for the Degree
Doctor of Philosophy in the
School of Architecture

Georgia Institute of Technology
December 2020

[THESIS TITLE GOES HERE]

CHARACTERIZATION OF URBAN MORPHOLOGY AND ITS EFFECT ON WEATHER UNCERTAINTY IN BUILDING ENERGY SIMULATION

Approved by:

Prof. Godfried Augenbroe, Advisor
College of Design
Georgia Institute of Technology

Dr. Kamran Paynabar
School of Industrial Engineering
Georgia Institute of Technology

Dr. Tarek Rakha
College of Design
Georgia Institute of Technology

Dr. Santiago Grijalva
School of Electrical Engineering
Georgia Institute of Technology

Dr. Brian Stone
School of City and Regional Planning
Georgia Institute of Technology

Dr. Joe Huang
White Box Technologies Inc.

Date Approved: Dec 3, 2020

To my father, Dr. Roop Singh Rajput and my husband, Mr. Mayank Agarwal for their unconditional love and support in this long endeavor

ACKNOWLEDGEMENTS

This journey of PhD has been truly life altering for me where I met some wonderful people, who, supported and guided me to the conclusion of my doctoral studies.

I was extremely lucky to have found Prof. Augenbroe as my advisor and benefit from his vast knowledge and experience in the field. His deep vision for research and dry wit made every discussion an intellectual treat that one cannot have enough of. I would also like to thank Prof. Jason Brown for teaching the course of Building Physics with so much dedication. It helped me with understand the basics of building energy dynamics down at the molecular level.

I am grateful to my committee members for their valuable suggestions that helped to improve the quality of this thesis.

Besides the faculty at Georgia Tech, I would like to thank Dr. Mostafa Reisi, Dr. Evan Mallen, and Dr. Jianli Chen for guiding me through disciplines that I had no prior knowledge about. Without their sheer help and support, some parts of this thesis would have been nearly impossible to accomplish.

I would also like to thank my lovely colleagues, YunJoon, Alya, Mohanned, Raunak and Devashree who almost made the lab my second home.

Last but not the least, I thank my husband, Mayank for being patient and bearing with me in all the ups and downs this journey brought with itself.

TABLE OF CONTENTS

LIST OF TABLES

LIST OF FIGURES

LIST OF SYMBOLS AND ABBREVIATIONS

AHS	American Housing Survey
ANOVA	Analysis of Variance
AOGCM	Atmosphere Ocean General Circulation Model
ASHRAE	American Society of Heating, Refrigerating and Air Conditioning Engineers
CAPEX	Capital Expenditure
CFD	Computational Fluid Dynamics
CLM	Community Land Model
DC	Direct Current
DEM	Digital Elevation Model
DOE	Department of Energy
EIA	Energy Information Administration
ELA	Effective Leakage Area
EPA	Environmental Protection Agency
EPC	Energy Performance Coefficient Calculator
EPI	Energy Poverty Index
ET	Exposure Temperature
EUI	Energy Use Intensity
GCM	Global Climate Model
GHG	Greenhouse Gas Emission
GIS	Geographical Information System
HVAC	Heating, Ventilation and Air Conditioning
HVI	Heat Vulnerability Index
IRR	Internal Rate of Return
LBC	Living Building Challenge
LHS	Latin Hypercube Sampling
MARS	Multi-Adaptive Regression Splines
MCDM	Multi-Criteria Decision Making
MTOT	Multiple Tensor on Tensor
NEMS	National Energy Modeling System
NPV	Net Present Value
NREL	National Renewable Energy Laboratory
NWP	Numeric Weather Prediction
OOP	Object Oriented Programming
PNNL	Pacific Northwest National Laboratory
PV	Photovoltaic
QoI	Quantity of Interest
RECS	Residential Energy Consumption Survey
ROI	Return on Investment
SA	Sensitivity Analysis
SMSE	Standardized Mean Square Error
TEB	Town Energy Balance

TMY	Typical Meteorological Year
TOU	Time of Use
UA	Uncertainty Analysis
UHI	Urban Heat Island
UMI	Urban Modeling Interface
UQ	Uncertainty Quantification
Usim	Urban Simulation
UWG	Urban Weather Generator
WRF	Weather Research and Forecasting
WSM	Weighted Sum Method
WUDAPT	World Urban Database

SUMMARY

The application of building simulation serves to assess the performance of a building throughout its lifetime. But the proper use of these applications relies heavily on the boundary conditions under which the behavior of a model is simulated. One of the most important inputs for simulation models is the stimulus by the weather conditions (actual or typical) in which it is supposed to operate.

Traditionally, weather data for building simulation is a composed of 8760 hourly values of weather variables (temperature, humidity, solar insolation etc.) derived through statistical means from historical weather data acquired conventionally from remote (usually airport) weather stations. The derived data is taken to represent a typical weather year for a city. However, due to rapid increase in urbanization, weather in city centers with high urban density is significantly different from rural areas, a large part of which is due to localized effects, e.g. urban heat islands, increased albedo of man-made surfaces and anthropogenic emissions. This thesis investigates the relative importance of spatial weather variability in predicted building performance simulation outcomes. Ranking the importance cannot be looked at in isolation but needs to be determined relative to all other sources of uncertainty, predominantly in the parameters of the energy model which in this thesis is EnergyPlus. The latter stem from lack of information or ignorance about many physical and scenario of use parameters. Together they are the ensemble of sources of uncertainties that need to be recognized in any simulation. A sensitivity analysis is conducted to reveal their relative ranking. An inspection of the resulting rank of the effect of spatial weather variability reveals whether the knowledge of local weather, in contrast to the assumption of uniform

weather throughout the city, significantly reduces the overall uncertainty in the outcomes of the simulation.

It should be recognized that there is only limited availability of localized weather data that reflect variability of urban contexts throughout a city. This recognition leads to the first contribution of this thesis: the development of a high fidelity statistical urban weather model fitted on local urban morphology and recorded weather. This is accomplished with a Multiple Tensor on Tensor (MTOT) regression model. The model can be applied universally and enables building modelers to create a synthetic meso scale weather data for their site, essentially putting the individual building in the urban fabric of the city.

The resulting model is a new cornerstone in the uncertainty analysis of the building simulation with inclusion of spatial weather variability. It is consequently used to inspect the role of spatially diverse weather in two critical applications. First, at the single building scale it is verified in three applications whether spatially diverse weather plays an important role when the assessment is conducted for a non-specific location in the city. Secondly, the role of spatial variability is tested in three urban decision making cases where the question is answered whether decisions should be diversified per location.

The thesis offers answers to both questions that elevate our understanding of the role of meso scale weather information in building simulation practice.

Throughout the research, Chicago is used as the demonstration region due to the availability of quality data both for urban morphology as well as weather from multiple distributed weather stations.

CHAPTER 1. INTRODUCTION

1.1 Background

Since the start of civilization, the primary function of buildings has been to provide refuge to its dwellers from the external weather conditions. As societies progressed, more and more functions were added to modern buildings. To date, providing comfortable environment to building occupants is still second to none in terms of priority of building functions. This is affirmed by the fact that providing indoor thermal comfort accounts for the bigger share of energy consumption in today's world of built space.

Building simulation models are used in virtual experiments to study how different building systems, including building fabric, air conditioning systems and its occupants react to the external forces of nature to meet all its functionalities. Weather data is needed to provide boundary conditions to drive these experiments. Although there can be numerous external environment factors, Table 1 shows the environmental variables that are mandatory, even in routine applications;

Table 1 Weather variables and their use in building simulation

Environmental Variable	Use in building model
Dry Bulb Temperature	• External surface heat transfer through conduction, convection and radiation • Infiltration/Ventilation through façade openings (sensible heat transfer)
Humidity	• Moisture transfer through building skin→latent heat transfer

Table 1 continued

Environmental Variable	Use in building model
Wind speed	• Ventilation and Infiltration • Exterior surface conductive heat transfer
Solar irradiation	• Solar heat load on exterior surfaces • Heat ingress through fenestrations • Yield from onsite PV systems
Cloud cover/ Sky cover	• Daylight access and illumination
Ground and sky temperature	• Below grade heat transfer • Radiative heat transfer between façade and exterior: ground and sky
Ground albedo	• Daylight access and illumination

Weather data finds application in the following targets of building simulation;

i. ***Making architectural design choices:*** A building envelope can be visualized as a valve that couples outdoor environment to indoor environment and controls the effect of weather on thermal and visual comfort of occupants. Decisions like window to wall ratio, daylight autonomy, envelope tightness and choice of construction material have a profound impact on comfort and operational energy of a building through its lifetime.

ii. ***Sizing of Air Conditioning systems:*** Weather variables that directly influence heat transfer across building fabric and provide the air that must be conditioned, play a key role in ascertaining heat loads for the whole system which is typically followed up by standard compliance and benchmarking for air-conditioned buildings.

iii. ***Performance of naturally cooled buildings:*** Indoor comfort conditions are assessed in passive and low energy architecture to study the effect of passive solar heating and cooling strategies. Such studies also complement resiliency studies for overheating and thermal stress inside the built space for critical events like heatwaves and/or power outages.

iv. ***Performance of Distributed Energy Generation:*** Yield of on-site energy generation such as Photovoltaic systems and in some cases, wind driven generators, are predicted based on weather variables such as wind speed and availability of direct and diffuse solar insolation on site. This assessment is required in design of net zero energy buildings as well as in larger policy designs such as determination of feed-in tariffs and introduction of incentives based on energy generation potential of a geographical area.

v. ***Daylighting Analysis:*** The solar irradiance component and its coupled sky dome luminance allows the building modeler to study the amount of daylight that will make its way inside the built space that may have both positive consequences such as daylight autonomy, better visual environment, increased productivity and energy savings as well as negative consequences such as glare and visual discomfort.

1.2 Weather data for Building Simulation: A walkthrough

Recording of weather patterns began when early civilizations adopted agriculture as primary means of food production where successful yield of crops depended heavily on rainfall and optimum temperature for crops. With the advent of industrial revolution and debut of the aviation industry, weather recordings were done daily usually and increasingly

hourly. Thus, airports became the de-facto location of repositories of historical weather data. The use of historical weather data in engineering applications came much later when advancements in computation allowed scientists to run physics-based models for building performance simulations.

With the rapid developments in the field of building simulation, boundary conditions, representing outdoor weather as an external stimulus was needed for detailed models. For such models, the best boundary conditions are provided by a weather station situated at the site itself. However, it incurs significant cost and manpower to collect that data. Furthermore, there is always the associated risk that the year in which data would be recorded will not be an average representative weather for the location.

As an alternative, historic recorded data was used to construct weather files that could be deemed representative for the given location and thereby were suitable enough to conduct routine studies on a (projected) building in that location. This led to creation of Typical Reference Years which have since evolved to Typical Meteorological Year (TMY) data published by National Renewable Energy Laboratory (NREL) with its latest release in 2008. A building energy modeler may pick the TMY weather data that is closest to the proposed site of the building. Since most cities have only two to three TMY locations corresponding to regional airports, the building site location may happen to be quite far from the weather station. Regardless, weather files generated from historic weather data for a remote location, if used for the whole city may not be adequate for a building in parts of the city that have their unique microclimate.

The issue of spatial variability has compounded with the increase in population and compactness of cities which altered the land use in cities in lieu of their natural environment and wilderness. In addition to Urban Heat Island effect (UHI) and wind canyons, climate change is posing new challenges to the definition of a "typical" weather boundary conditions for a building to be simulated.

1.3 Research questions and hypothesis

The research focuses on the spatial variability of (meso)weather and develops a statistical model to derive it based on morphological parameters and data from nearby weather stations. The hypothesis is that the increased fidelity of the spatial representation compared to the use of airport weather increases the value of predictions generated by the building energy model. The spatial variability is modeled as local deviation from airport weather. It is adjusted according to urban parameters of the building's location. The primary aim of the thesis is to test above hypothesis in general, and then verify it in the specific context of a set of application cases. This translates to the following research questions;

i. How does an urban setting, at the meso-scale, affect the performance of buildings in the selected application cases and how can that be quantified?

ii. What are the decision scenarios in which the higher fidelity of the developed weather model leads to a significant improvement in assessment and decision-making?

1.4 Motivation

The increase in urban sprawl all over the world necessitates an examination of superannuated method of using typical weather as boundary condition for building performance simulation practice. In particular it should be investigated whether altered weather conditions that account for emplacement of the building in a particular location in its unique urban morphology setting, is required to reach better informed decisions. Intuition tells us that this may be true in some cases but not in other. It is therefore appropriate to look at different situations with different decision scenarios to conduct the investigation.

There are two aspects of the decision scenarios covered by this study, namely,

- The variance in building simulation outcomes if the location of a building is not specific and the weather derived from an open space like airport is assumed uniform over all possible locations. If this variance is acknowledged and baked into the virtual experiment to study the behavior of a building along with other sources of inputs that the modeler has limited knowledge about, would weather stand out as a notable factor? A set of 3 hypothetical cases are simulated and results are discussed to reflect these assumptions
- If the location of a building or cluster of buildings is known, and the decision scenarios demand the outcomes to be latched to relative position of a building in the city, does the use of higher resolution data impact decision outcomes? A set of 3 application cases are formulated, modeled and discussed to imitate these conditions.

There is ample literature about the impact of immediate surroundings such as wind variation and shading due to adjoining structures on a building's behavior, referred as micro-climate of the site. However, the impact of larger scale urban morphology on buildings, referred to as meso-climate in this thesis, is fragmented in UHI and wind canyon research communities that compel the modelers to use sophisticated tools such as Computational Fluid Dynamics (CFD) and Weather Research and Forecasting (WRF) to arrive at a climate that is more representative of the city tract where the building will be located.

Additionally, there are very few studies that inspect the consequence and extent of both alteration in UHI as well as wind simultaneously on building performance measures in presence of other uncertainties as discussed in Chapter 2.

As a first step thesis also develops a model for the creation of local meso-scale weather for applications in building simulation practice. The prime target is a fast and efficient model, provided that enough local weather station data and regional morphology data are available for the city in consideration. Based on this model this thesis first performs the inquiry described above by performing detailed multi-aspect performance simulations on different building types to answer the question,

"How important is it to place building in its local meso weather versus city wide average weather for everyday building simulation practice?"

For the thesis to be all encompassing, the role of weather is not limited to individual building level but expanded to novel and ballooning field of urban simulation with three illustration case studies at the urban scale for parts of a synthetically populated city with

building archetypes. Multi aspect studies are performed aimed at policy and urban decision scenarios.

1.5 Broader Impact

The research aims to bridge the gap between (1) data and analysis tools that pertain to urban planning and (2) routine building simulations that are executed for the smallest element in the larger urban fabric. The broader impact of this research may be summarized in following points;

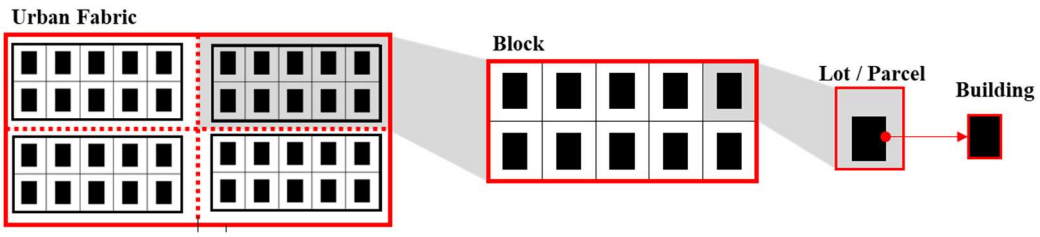

Figure 1 Buildings as element of urban fabric

i. The disconnect between these two fields is resolved by providing a framework to translate the effect of urban features as alterations in site weather using statistics. The weather thus altered can then be digested by building simulation programs to better reflect the impact of urban location on building performance than current methods.

ii. The derivation of the statistical model that can be packaged to be re-used in any city based on access to morphological data and dispersed weather station data.

iii. The spatial variability of weather, once quantified, will find its application in studies at the broader urban scale, for example in impacting socio-economic policy decisions, resilience studies and other.

CHAPTER 2. LITERATURE REVIEW

2.1 Weather in Building Simulation

2.1.1 Business as Usual- Typical Meteorological Year

The most conventional output of building simulation is the prediction of a building's annual energy consumption when operational. This could be achieved either through the arduous task of performing each building simulation with multi-year data or by distilling the weather data to a generic single year weather year that may be used for any simulation. Most widely available "distilled" weather data used in building science practice is published by NREL in the form of "Typical Meteorological Year" abbreviated as TMY, and distributed as data files with hourly (8760) records in a standard format.

To date, 4 versions of TMY data have been published, of these, TMY-1 digested the data for 26 US locations from 1952 to 1975. Refinements in weighted averages were made for TMY-2 data for a period spanning from 1961 to 1990. In 2005, the DOE introduced TMY3 files. This newest release puts greater emphasis on solar radiation data as well as the inclusion of precipitation data.

TMY3 weather data are based on the algorithm formulated by Sandia National Laboratories which processes weather at a location for longer periods, usually 30 years. Five candidate months are selected for each of the 12 months of a year based on their closeness to long term CDF's by using Finkelstein-Schafer statistics. For example, to find a typical June for the city of Chicago, 5 months of June are selected from different years which are then ranked with respect to their closeness to the long term mean and median of

all 30 June months. The highest-ranked June is then concatenated with the highest ranked July and so forth to compose a full year. Each month is smoothed over 6 hours at the month to month transition point. The result is a typical weather file (Wilcox & Marion, 2008b). The TMY3 method is the currently accepted approach for generating energy outcomes through building simulation in the United States and its territories.

There are 16 climate zones classified by the DOE for the USA, each having their representative cities. For example, Chicago is the representative city for climate zone 5A and has its own unique TMY derived from long term weather data recorded at the Chicago O'Hare airport.

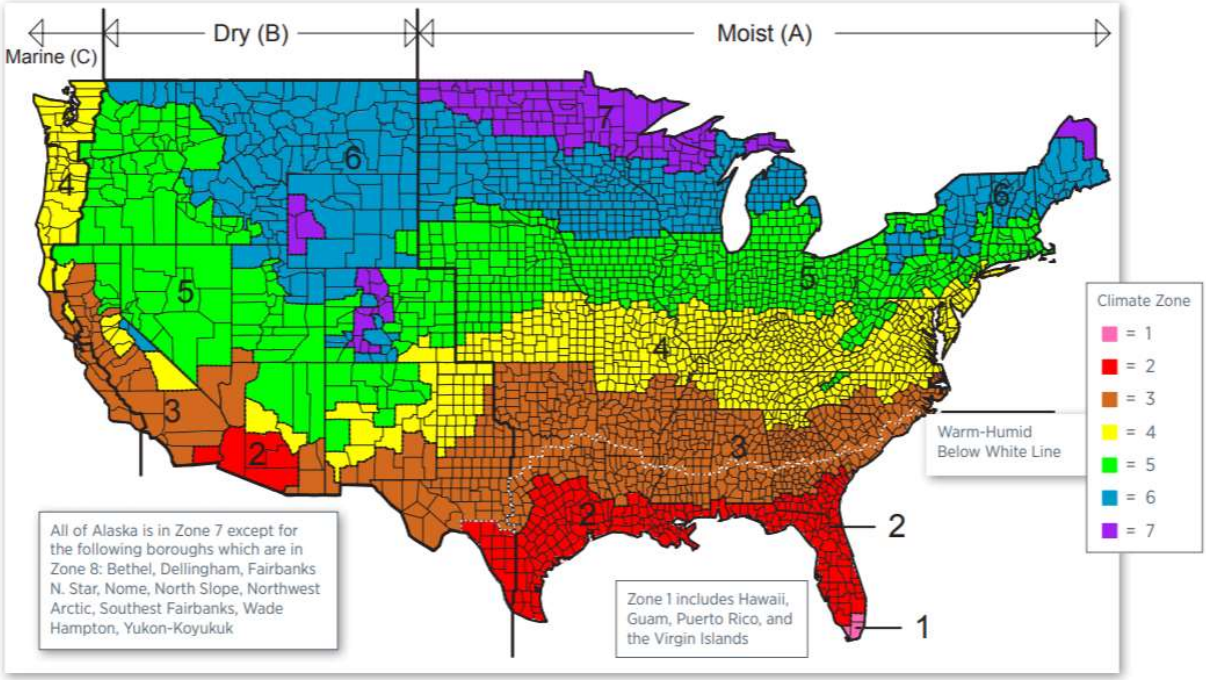

Figure 2 International Energy Conservation Code (IECC) climate regions

It is to be noted that using the derived TMY as the representative, "typical" or "averaged", weather year of a location has limited value. It may for instance only be useful for routine

building simulation application, and not be suitable for comfort or resiliency studies which should include a better representation of the statistical occurrence of extreme weather conditions in a given time span (Pernigotto, Prada, & Gasparella, 2019)(Crawley & Lawrie, n.d.).

Despite these shortcomings, there is good reason to assume that TMY data is adequate for many types of simulation studies. At the same time, there is increasing recognition of the variability of weather across metropolitan areas spanning rural, semi-rural and high-density areas, with large variations in vegetation and impermeable surfaces. This has led to an increasing number of efforts to model local weather phenomena as discussed in the following section, especially for investigations at the urban scale.

2.1.2 Spatial variation in weather

Section 2.1.1 describes how TMY captures the temporal span of weather patterns based on observed data from weather stations primarily located in open spaces. It, however, misses on the spatial variability that is caused by natural forces such as diurnal wind variations like land and sea breezes and mountain breezes or localized evapotranspiration from forests affecting the humidity of a nearby location. Weather files generated solely from historic weather data collected at an airport, if used for the whole city may not be adequate for a building which is proposed or exists in parts of the city that have their unique weather.

The issue of spatial variability has compounded with the increase in population and compactness of cities which altered the land use in cities in lieu of their natural environment and wilderness. Rapid urbanization of cities has two major impacts on the microclimate which alters the input to building simulation models, namely;

i. ***Urban Heat Islands:*** Densely populated parts of cities see a build-up of thermal energy due to activity of population, waste heat from cars and buildings, thermal storage of paved and built area delaying the release of absorbed heat, decreased reflection due to roads and roofs, and loss of green cover.

Stored heat energy is naturally dissipated back to the universe at night. Rural areas are more open which allows more radiative heat transfer between earth and sky. In contrast, in urban areas, high thermal mass of buildings and pavements holds and thus accumulates the heat. In addition, radiative heat transfer is trapped due to reduced sky view factors while paved surfaces inhibit evaporative cooling in contrast with rural areas where water retained in the soil enhances latent heat flux. This results in high day and night temperatures compared to open areas such as airports. Figure 3 from (Shahmohamadi, Che-Ani, Maulud, Tawil, & Abdullah, 2011) lists the factors that intensify the Urban Heat Island effect in a city.

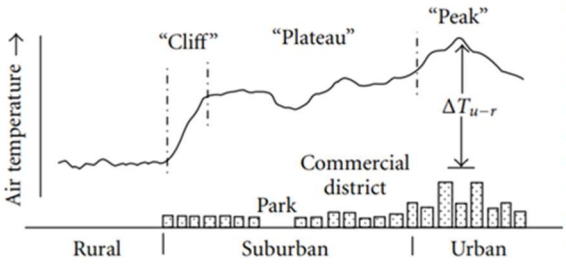

Characteristic contributing to UHI formation	Effect on the energy balance
Lack of vegetation	Reduced evaporation
Widespread use of impermeable surfaces	Reduced evaporation
Increased thermal diffusivity of urban materials	Increased heat storage
Low solar reflectance of urban materials	Increased net radiation
Urban geometries that trap heat	Increased net radiation
Urban geometries that slow wind speeds	Reduced convection
Increased levels of air pollution	Increased net radiation
Increased energy use	Increased anthropogenic heat

Figure 3 (a) Cross section of an UHI (b) Urban characteristics and their effects on energy balance of city

ii. ***Wind canyons:*** Wind or street canyons are formed when skyscrapers influence the speed and direction of wind in urban surroundings. These canyons are characterized

by aspect ratio i.e., height to width ratio of a canyon (Memon, Leung, & Liu, 2010). The impact on wind is directly proportional to the aspect ratio in addition to radiation trapping. An alteration of wind also has an acute impact on temperature by flushing out the heat and pollutants. The variation in air speed and its effects increase locally when air is channeled through a small opening known as venturi effect. The alteration of wind can have an impact on weather on all three levels, i.e., at the scale of continents (macro), at the scale of city tracts (meso) and at the scale of individual buildings (micro). section 2.4 details the difference in these scales and the scope of this thesis in this context.

2.1.3 Temporal variation in weather (Climate Change)

As mentioned in section 2.1.1, typical year weather is based on data acquired from observations in the past. For example, TMY3 is based on data recorded between 1991 and 2005 which is already 15 to 29 years in the past. The average temperature in North America is expected to rise by 1.3 °C by mid-century as compared to the start of century with the AOGCM[1] model in B1 storyline (best case scenario) implying rapid economic growth and introduction to clean, sustainable and resource efficient technologies. About a third of that warming due to climate change has already been committed (Meehl, Stocker, Collins, & Friedlingstein, 2007). Further, the warming is more pronounced in urban areas as compared to remote locations where the land use has not been altered due to anthropogenic activities resulting in higher heat risk in city centres and metropolitan regions (Stone et al., n.d.). Thus, acceleration in climate change with time calls for the building simulation community

[1] Atmosphere-Ocean General Circulation Model

to inculcate climate change scenarios in the development of future typical weather years with the onus of scenario selection on the modeler in view of the building lifecycle and extent of performance prediction risk that the modeler intends to cover.

2.2 Accounting for spatial variations of weather in Building Simulation applications

2.2.1 Stochastic weather generation

Stochastic weather generators are used to assess the what-if scenarios in building simulation wherein synthetic weather is created by overlaying a baseline typical weather scenario with statistically generated random noise to create multiple longitudinal scenarios that mimic the temporal randomness in real weather. The generated time series are often referred to as synthetic weather data.

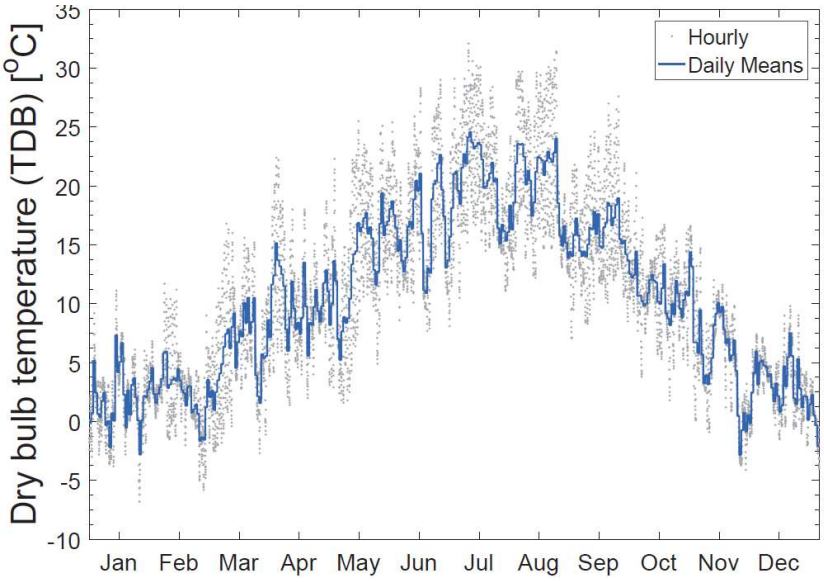

Figure 4 Dry bulb temperature for Geneva (Rastogi, 2016)

Auto-Regressive models (Lee, Sun, Hu, Augenbroe, & Paredis, n.d.; Rastogi, 2016) are the most widely used to preserve correlations between seasons and diurnal cycles. These

generated weather files are then used in Uncertainty Analyses to estimate the impact on performance indicators obtained with building simulation. This approach, however, typically lacks attention to the spatial variation in local weather as it focuses on capturing the temporal variation for a dynamic analysis of the building response.

2.2.2 Adjustments for spatial variation

Computation of site specific weather for building simulation has seen some rapid advancements over the last decade where physics-based energy balance models are used to compute the temperature and humidity variations owing to change in land use in city centers (Dorer et al., 2012). The computation time for an energy and mass balance model depends on the number of objects that part-take in the energy dynamics of a region and the choice of time-step for the solution of equations. Setting up the experiment itself takes a substantial amount of time as detailed information about thermal properties of each object is required for the model. This manifests itself in scalability of the model if one wishes to increase the area of the experiment. Figure 2 (a) shows the 3D editor for surface energy balances in the routinely used micro-climate simulator ENVI-MET (Bruse, 2004). Figure 2(b) illustrates the variation in energy use intensity of buildings in an urban environment calculated by urban modeling interface (Reinhart et al., 2013).

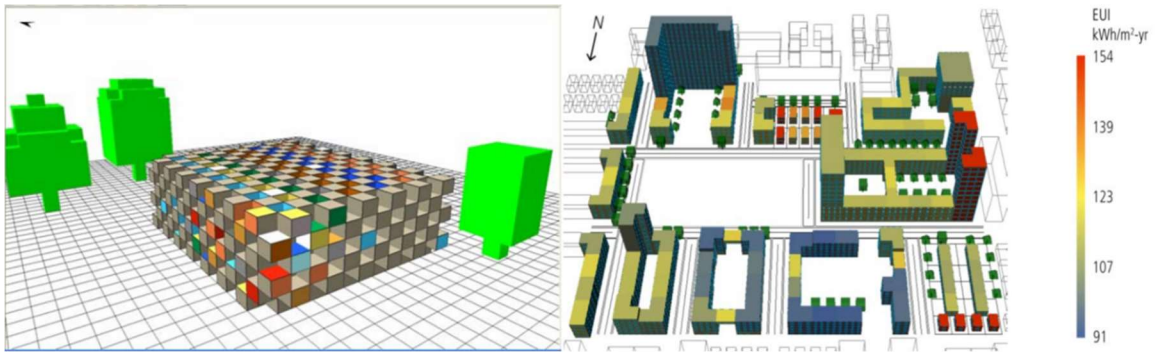

Figure 5 (a) Screen capture of ENVI-MET, different colors show different facade materials (Bruse, 2004) (b) Urban Modeling Interface energy use intensity (Reinhart et al., 2013)

Wind canyon effects require special attention and several modeling approaches have been reported in literature. One popular approach is to use CFD in a shape representation of urban settings (Liu et al., 2017). This is appropriate for applications such as pedestrian comfort and some special cases of building energy modeling, e.g. when natural ventilation phenomena are dominant. The simulation modeling requires structures in the urban setting to be modeled in detail as shown in Figure 6, i.e. with fairly detailed geometries and surface properties of all exposed skins/facades. A mesh is created around buildings and on their surfaces where the equations of fluid dynamics are solved to capture the heat and mass exchanges at the domain boundaries, i.e. between the environment and the building. Like physics-based models for UHI, the computation time for CFD studies is directly proportional to the number of cells in the mesh, and hence the resolution of the urban geometry description. When the urban area under consideration is scaled up, run time increases dramatically.

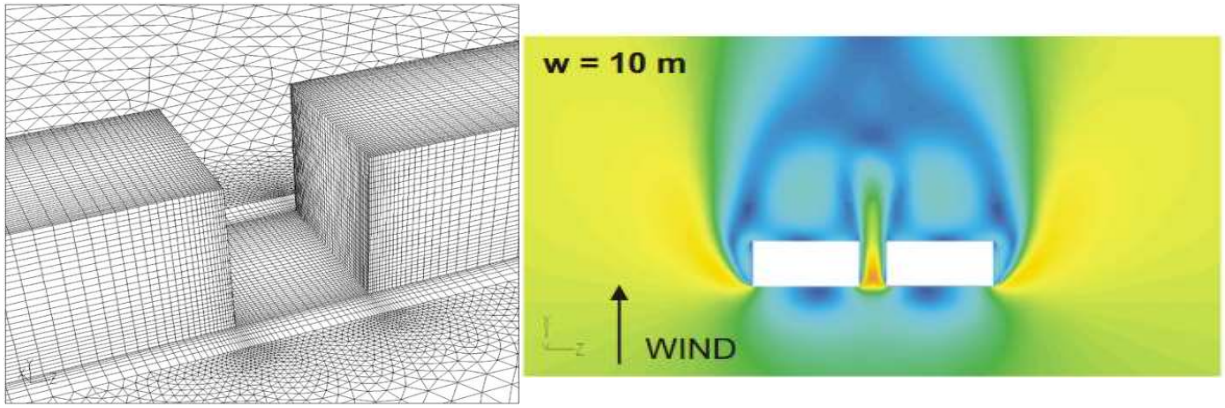

Figure 6 (a) Mesh for CFD simulation (b) Visualization of wind behavior in the presence of obstructions (Blocken, Carmeliet, & Stathopoulos, 2007)

To elaborate on the scalability issue, ASHRAE mentions the use of weather research and forecasting (WRF) for computation of local weather, the scale of which varies from one study to the next in its Handbook but, as the resolution of the WRF model is increased (see Figure 4), it becomes both labor as well as computationally very expensive. For example, to simulate 1 km x 1 km grid resolution for a year for the city of Atlanta would take approximately 36 days on a standard 8 core Linux machine. Additionally, to construct a TMY for each grid would need multiple-year simulation making it an astronomical effort to construct TMY's for the whole city at a given resolution.

One other physics-based model, the Urban Weather Generator (Bueno, Norford, Hidalgo, & Pigeon, 2013) was built to create weather adjustments to reflect UHI in urban city locations over the baseline of recorded weather outside the city. It works by coupling four distinct modules that compute the energy balances using the RC-circuit analogy to calculate adjustment in temperature owing to the urban fabric.

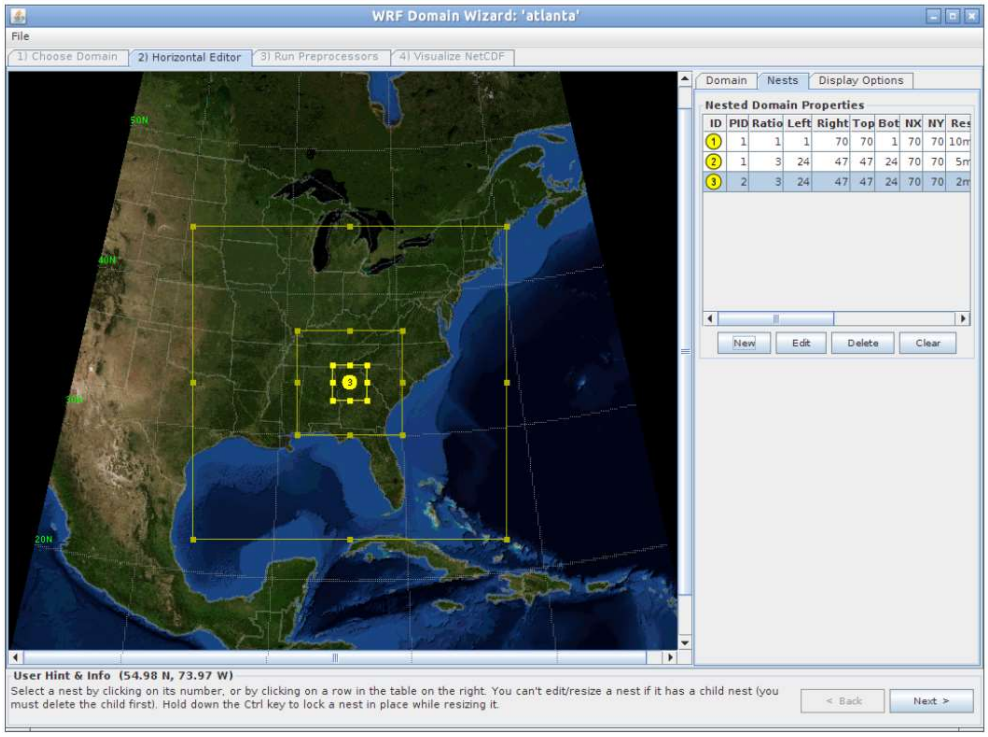

Figure 7 Domains of WRF model (Klimaat Consulting & Innovation Inc., 2016)

Other widely used methods to ascertain weather in places with no nearby weather station is using interpolation and extrapolation techniques with statistical models based on Kriging or Inverse Distance Weighing (IDW) algorithms (Shahraiyni & Sodoudi, 2017). They too have their limitations such as:

- If the number of automatic weather stations (AWS) are sparse and not geographically distributed across the city, spatial interpolation of weather variables may be marred by considerable uncertainties and errors owing to edge effects of extrapolation.

- Interpolation techniques don't take into consideration the spatial heterogeneity of urban features; therefore, it can miss the micro-climate created by land features such as forests and water bodies. (Shahraiyni & Sodoudi, 2017) use interpolation techniques to find air temperature in the city of Berlin and compare it with recorded data from weather

stations. It is concluded that the interpolation technique completely missed the lower temperatures in parts of city with green urban areas and water bodies.

Another popular statistical approach is morphing which was developed by (Belcher, Hacker, & Powell, 2005) to create urban local weather from a baseline weather file which is combined with monthly mean values of weather variables obtained from Regional Climate Models. Concepts of shifting and linear stretching are used to convert monthly mean variables to hourly values. (Lin, Huang, Lin, & Hwang, 2019) used the same model to create the effect of UHI on temperature and relative humidity in Tainan city. In this study, the weather baseline is obtained from the Tainan weather station and monthly mean temperature values are computed from the regression model based on GIS data and weather stations across the city.

2.2.3 Adjustment for climate change

Since the typical lifecycle of buildings span multiple decades, the systems that incur significant capital investments such as HVAC, renewable energy systems and plumbing are designed for long term use based on outputs of predictions generated with building simulation. But, the rapid pace of climate change has cast a doubt on the effectiveness of systems designed on past weather data for predicting their future performance. (Chinazzo, Rastogi, & Andersen, 2015; Tian & De Wilde, 2011) employ the probabilistic projections of climate change and propagate the uncertainties in climate of the future through building simulation studies. These studies highlight the importance of incorporating climate change scenarios in the sizing of building systems. To aid to the studies that make an attempt towards studying effects of climate change on building simulation outcomes, (Jentsch,

James, Bourikas, & Bahaj, 2013) proposed a simple future weather generator based on coarse GCM outputs and the morphing approach already discussed in section 2.2.2. Although this method too has its limitations such as the representativeness of coarse GCM data for a particular site, as well as the validity of underlying GCM data and the disaggregated treatment of weather variables in the process of morphing.

2.3 Impact of imprecise weather on simulation outcomes

The discipline of Uncertainty Analysis (or UA) is of growing importance in the field of building simulation as it enables the quantification of potential "errors" in predictions that are attributed to incomplete knowledge of the properties of the simulated object and its environment. As briefly discussed in section 2.2.3, errors in simulation outcomes and hence in the performance measures derived from them can have far-reaching consequences such as buildings that underperform their predictions leading to higher than expected operational costs and sub-par thermal comfort, which can lead to high costs of rectification.

(Domínguez-Muñoz, Cejudo-López, & Carrillo-Andrés, 2010) describe the abstraction of building model as a function f that digests input vector $\vec{x}$ and produces an output vector $\vec{y}$;

$$\vec{y} = f(\vec{x}) = f(x_1, x_2, x_3, x_4, x_5, x_6)$$

Traditionally, both inputs as well as outputs were considered to be deterministic quantities implying that when the experiment is repeated, it produces the same output, which represents ideal conditions and perfect information.

However, reality is plagued by a lack of knowledge and natural randomness injecting unavoidable uncertainties in building simulation. This section focuses on the role of uncertainties in weather in predictive simulations.

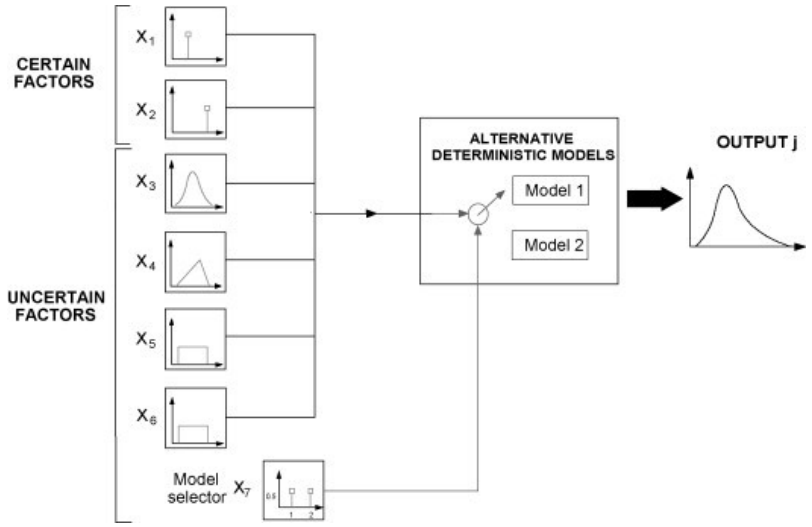

Figure 8. Scheme of framework for stochastic simulation (Domínguez-Muñoz et al., 2010)

Uncertainty in weather due to urban characteristics has been covered in ASHRAE [2]Handbook Chapter 24.4. However, it gives only broad guidelines about alteration in weather variables in accordance with the arrangement of land use around the site of proposed building. For example, the wind speed near a proposed building site is altered to accommodate the effect of surrounding buildings characterized by the urban boundary layer parameters according to the following formula;

$$U_H = U_{met}\left(\frac{\delta_{met}}{H_{met}}\right)^{\alpha_{met}}\left(\frac{H}{\delta}\right)^{\alpha}$$

[2] ASHRAE: American Society of Heating, Refrigerating and Air-conditioning Engineers

Where, U_H= Approach wind speed at uphill wall height (m/s)

U_{met}= Wind speed at nearby meteorological station

H= Height of the wall

δ =Boundary layer thickness

α=Exponent

δ and α are derived from the following table;

Table 1 Atmospheric Boundary Layer Parameters

Terrain Cate-gory	Description	Exponent a	Layer Thickness δ, m
1	Large city centers, in which at least 50% of buildings are higher than 25 m, over a distance of at least 0.8 km or 10 times the height of the structure upwind, whichever is greater	0.33	460
2	Urban and suburban areas, wooded areas, or other terrain with numerous closely spaced obstructions having the size of single-family dwellings or larger, over a distance of at least 460 m or 10 times the height of the structure upwind, whichever is greater	0.22	370
3	Open terrain with scattered obstructions having heights generally less than 9 m, including flat open country typical of meteorological station surroundings	0.14	270
4	Flat, unobstructed areas exposed to wind flowing over water for at least 1.6 km, over a distance of 460 m or 10 times the height of the structure inland, whichever is greater	0.10	210

Figure 9. Boundary layer parameters (ASHRAE)

(Yuming Sun, Gu, Wu, & Augenbroe, 2014) use Actual Meteorological Years (AMY's) from 1982-2013 to account for variabilities in weather and compare it with a widely accepted design day methodology (Hong, Chou, & Bong, 1999) for system sizing ignoring all other uncertainties as the first crude step. It is found that systems designed using design day calculations were grossly oversized for heating loads and significantly oversized for

cooling requirements. The study is then repeated with additional sources of uncertainty in occupancy, infiltration, convective heat transfer coefficients etc., and it is observed from a sensitivity analysis that weather was amongst the top three sources of uncertainty in load calculations, thus highlighting the role of weather, as one form of scenario uncertainty, when building simulation is used for HVAC sizing.

(Yuming Sun, Heo, et al., 2014) quantified the expanse of uncertainty due to incomplete knowledge of microclimate variables in diverse urban settings ranging from open grasslands to densely built urban environments. Their approach is based on a standard uncertainty quantification (UQ) technique where the results from the low fidelity models used in current standard simulations are compared with results from a higher fidelity model. Quantification of the difference ("Diff") between the predictions with both low and high-fidelity models for a range of different settings are then used to quantify the uncertainty distribution and express correlations with certain case parameters. In their study, the low fidelity model is based on microclimate wind speeds based on ASHRAE recommendations as shown earlier, (Yuming Sun, Heo, et al., 2014). Their high fidelity microclimate model uses wind speeds derived from the Community Land Model (CLM) (Oleson, Bonan, Feddema, Vertenstein, & Grimmond, 2008)while temperature variation is based on the Town Energy Balance Model (TEB) (Masson, Grimmond, & Oke, 2002). TEB is one of many physics-based urban weather generators used to transform meteorological data to weather in a specific urban location. Again, although this model covers all the possibilities of land use, the majority of inputs in these models are either hypothetical or very labor intensive to construct. The computation time is exponentially dependent on the size of the urban area and number of grid cells in the finite element model.

The mentioned study provides a good baseline to assess the variability caused by urban land use in meteorological data which is usually recorded in open areas away from the settlement like airports. A large range of hypothetical settings (samples) is constructed by varying urban parameters. The low and high-fidelity predictions for all samples of urban variables are used to quantify the Diff as a probability distribution to subsequently construct the correlations between the Diff and specific urban parameters.

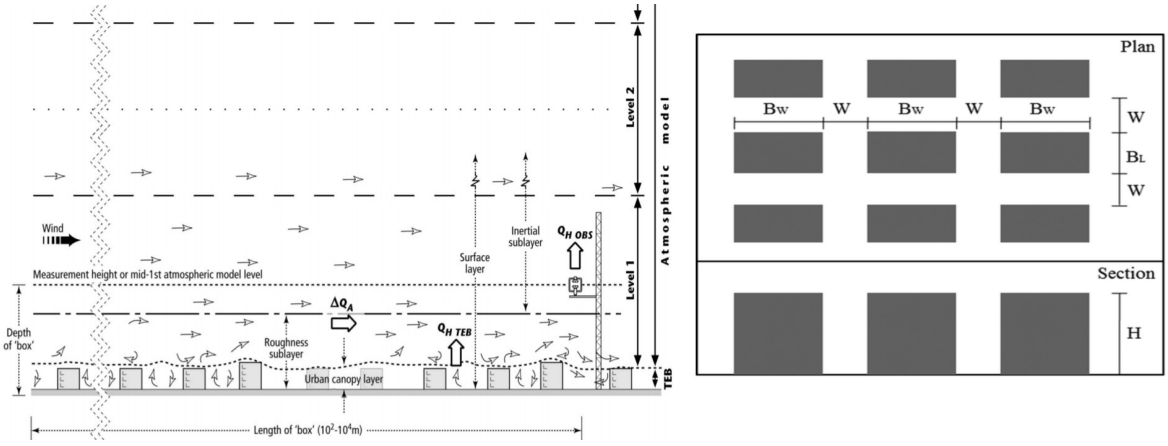

Figure 10 (a)Town Energy Balance Model (TEB)(Masson et al., 2002) (b) Urban parameterization scheme in Community Land Model (CLM) (Sun, Heo, et al., 2014)

2.4 Delineating meso from micro scale: defining the scope of this thesis

As mentioned in (Fujita, Newstein, & Tepper, 1956), there is no consistent strict definition of scale for the terms macro, meso and micro in literature and they are used relative to each other with the axiom that macro is more closely related to meso scale and micro is more intimately connected to meso. The scales of meso and micro becomes even more fuzzy when seen in the context of atmospheric phenomena.

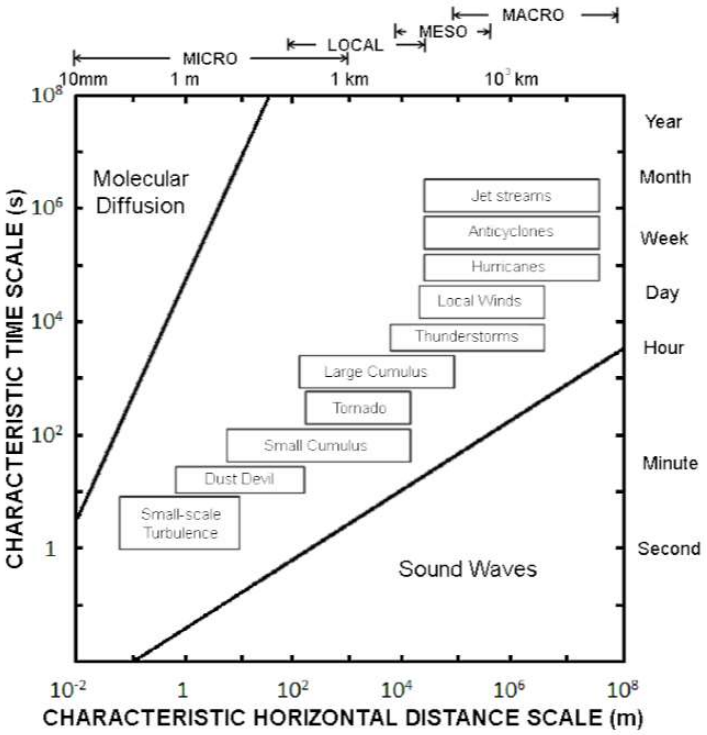

Figure 11 Time and space scales of different atmospheric phenomena (Ahmet, 2014)

For example, in the context of positioning wind turbines (Ahmet, 2014), the scale of wind analysis is important for up to 30 meters (termed as micro in some studies) to assess the energy yield from it. However, to reach the 30 m scale, one must downscale via CFD from meso scale models, i.e., between 1 km to 10 km resolution of wind characteristics as shown in Figure 11 which is usually derived from Numerical Weather Predicting (NWP) models such as WRF.

In the scope of this thesis, the difference between micro-climate and meso-climate is understood to be similar to the terminology that distinguishes climate and weather. Climate is linked to the over-arching scale of landmass such as continents whereas weather is more local in nature affected by geography of an area.

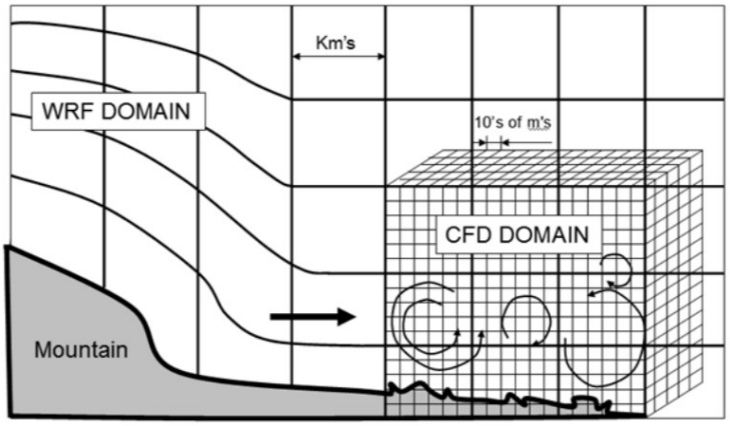

Figure 12 Coupling of WRF with CFD (Ahmet, 2014)

Along the same lines, meso-climate refers to the weather that is influenced by urban features at the scale of tracts or neighborhoods, typically 1 km to 3 km. On the other hand, micro-climate is the local weather that is directly affected by the external form of the building and immediately surrounding structures and vegetation, i.e. roughly at the scale the individual building and typically distinguishing different parts and orientations of the building perimeter.

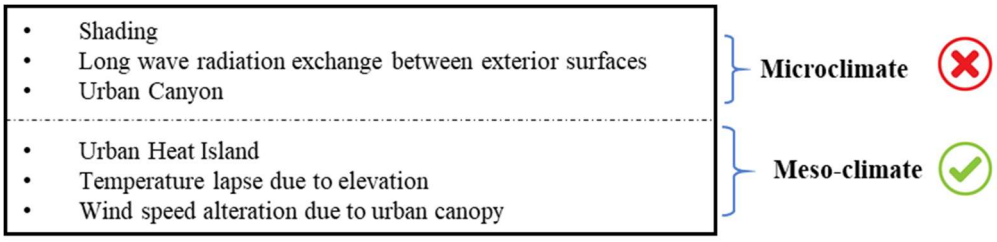

Figure 13 Domains of weather scale

Many studies have been conducted to study the micro-climate in relation to the immediate surroundings of an individual building, studying effect on boundary conditions in terms of convective heat transfer, wind pressures and of course solar shading by nearby obstacles (Mirsadeghi, Cóstola, Blocken, & Hensen, 2013)(Futcher, Kershaw, & Mills, 2013).

(Nor&n, Westberg, Jernberg, Haagenrud, & Sjiistriim, n.d.) discuss the methodology for correction of meteorological weather data for predicting the amount of degradation that happens to a building's performance over time.

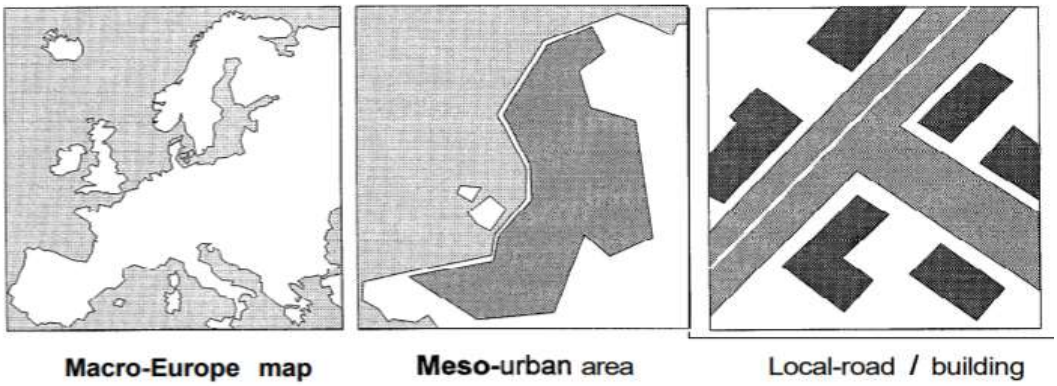

Figure 14. Environments classified at different scales

The scope of this thesis is ***not*** to simulate the environment in the neighborhood of building in question, which, often is considered as the micro-climate of building, often to analyze phenomenon of smaller dimension such as pedestrian thermal comfort with respect to temperature, shading and wind canyons around the structure. The use of physics based models is imperative to scale down from meso weather to micro weather for studies that aim to assess impact of weather alterations within few meters of the building.

The thesis in no way negates the effect of micro-climate on building performance but tries to focus on meso climate that is affected by clusters of urban features rather than individual units of them and have been referred to as "meso" or "local" weather throughout the document.

2.5 Conclusion

From an exhaustive review of the literature that deal with the choice of weather in building simulation, it can be concluded that perhaps weather is one of the most important inputs for the “virtual experiment” to analyze the behavior of a building and make predictions about its performance.

Even though there are ample studies that drive home the said conclusion, there are very few that take into account the relative placement of building in the fabric of a city without the use of bulky micro and meso weather generators, missing the effect of localized urban morphology information in the process.

This thesis identifies this gap and attempts to find a simple and dexterous method to do the same by proposing a statistical method to create local weather and test its effectiveness by simulating case studies around accepted performance indicators of building simulation community at building as well as urban scale.

CHAPTER 3. GENERATION OF SPATIALLY DIVERSE WEATHER

3.1 Development of a statistical model for the creation of synthetic weather

Statistical modeling of the effect of urban features on resulting meso-climate delivers the engine for generation of synthetic weather data. The model is trained on observed weather data from many different parts of a city, consisting of suburbs and open areas.

Since the prediction is to be made on weather which has high diurnal and seasonal variability along-with the forces of nature that determine the climate of a specific location, it is desirable to have an algorithm which can grasp the following phenomenon (as depicted in Figure 15);

- ***Seasonality:*** The yearly data when fed to the algorithm, should be able to grasp the seasonal changes in weather variables like temperature, wind speed and humidity.
- ***Correlations between hourly values:*** Variables in each hour of a year are correlated in some form. For example, the temperature at a specific time is related to the hour before it.
- ***Local Winds:*** The pattern of weather between day and night is very specific to its location. In a city which is spread near a large water body, land and sea breezes affect this pattern. Distinct variations are also observed for hill and valley regions wherein air currents determine the variations between night and day.
- ***Correlations between weather variables:*** It is noteworthy that temperature, wind and humidity are all related to each other, as an increase in temperature increases

turbulence which increases the wind velocity. High temperatures and winds may either result in removal of humidity from still air or increase the humidity in air when dry air picks up the moisture from water bodies.

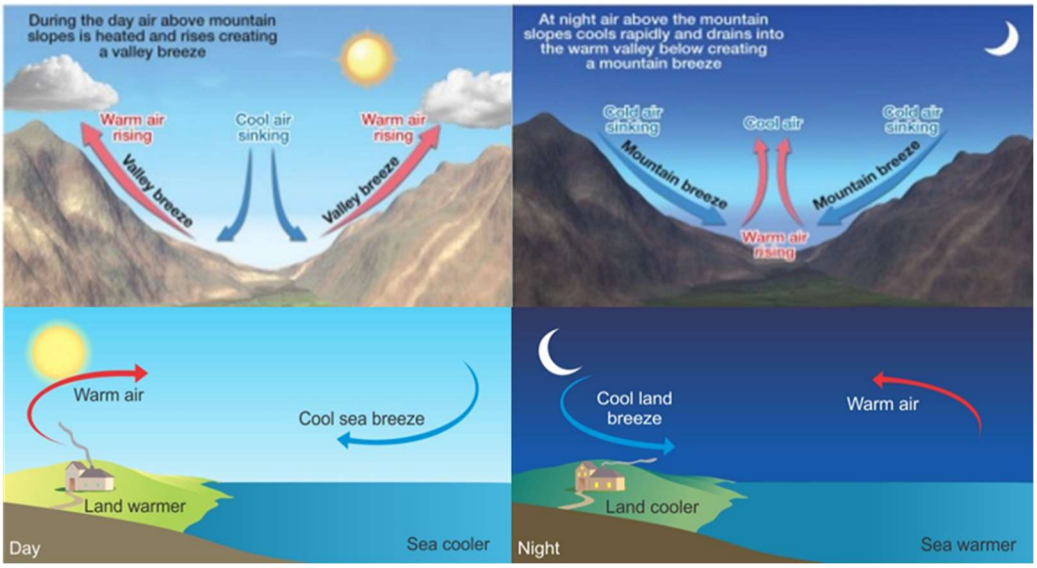

Figure 15 Local winds affecting diurnal patterns

- ***Relation to urban morphology:*** In addition to capturing above patterns, the model should be able to relate them to the urban features of a city without explicitly modeling the physical phenomena that govern these forces.

3.2 Urban morphology affecting local climate

In a bid to understand the role of urban morphology in altering weather, literature was sifted to identify prominent urban features that predominantly affect temperature, relative humidity and wind speed in urban spaces with built objects. (E.J.Plate, 1995) characterized the effect of structures in urban on wind forces as shown in Figure 16.

Configuration		Characteristics	Roof Shape	z_0	$\overline{H}$	$\sigma_H/\overline{H}$	$\overline{L}/\overline{B}$	$\overline{L}/\overline{H}$	λ_{ar}	λ_{fa}
1		New district, one family buildings 1 - 2 storeys	Mainly gable roofs, rarely flat roofs	0.1 - 0.3 (1.3)	8 - 10	~ 0	~ 1	~ 1.5	0.1 - 0.2	~ 0.1
2		Residential area 1 - 3 storeys	Mainly gable roofs, rarely flat roofs	0.1 - 0.3 (1.4)	8 - 12	< 0.2	~ 1	~ 1.5 - 2.5	0.15 - 0.25	~ 0.1
3		Residential blocks regularly aligned 3 - 5 storeys	Mainly gable roofs, rarely flat roofs	~ 0.3 (1.5)	12 - 20	< 0.2	< 0.5	~ 1 - 2	0.1 - 0.25	0.1 - 0.25
4		Residential area high-rise buildings and residential blocks 4 - 15 storeys	Gable roofs, flat roofs	> 0.5	> 15	0 - 0.5	< 0.5	~ 0.7 - 1.5	0.1 - 0.2	0.15 - 0.3
5		Cultural facilities churches, schools, etc.in residential areas	Gable roofs, flat roofs	0.3 - 1.5 (2.4)	> 8	> 0.5	0.5 - 2.0	~ 2 - 5	0.1 - 0.3	0.05 - 0.15
6		Block of buildings in City Centers 3 - 6 storeys	Mainly gable roofs, rarely flat roofs	~ 0.7 (2.1)	15 - 25	< 0.3	~ 1	~ 0.7 - 0.9	0.3 - 0.7	-
7		City Center areas including parks, ,high-rise buildings and public facilities	Gable roofs, flat roofs	0.3 - 0.7 (>2)	>15	< 0.4	~ 1	~ 1.5 - 2	< 0.5	0.1 - 0.2
8		Commercial and industrial area 2 - 5 storeys	Mainly flat roofs or gable roofs	~ 0.3 (0.6)	5 - 15	< 0.5	< 1	~ 2 - 5	0.3 - 0.4	0.05 - 0.2
9		Industrial plant with tanks	Mainly flat roof	~ 0.5 (1.6)	10 - 25	< 0.5	~ 1	~ 0.5 - 1.5	0.1 - 0.4	0.1 - 0.2
10		Industrial area 1 - 4 storeys	Mainly flat roofs, rarely gable roofs	0.3 - 0.5 (1.6)	5 - 15	0.3 - 0.5	~ 1	~ 2 - 7	0.2 - 0.4	0.05 - 0.2

z_0	Roughness height
$\overline{H}$	Mean Building Height
σ_H	Standard deviation in building height
λ_{ar}	Sum of all areas covered by buildings
λ_{fa}	Sum of average building areas normal to wind
$\overline{L}, \overline{B}$	Mean building length and width

Figure 16 Urban structures affecting wind speed

Similarly, a comprehensive literature review for temperature and relative humidity indicated that areas of vegetation, forests, water bodies and impervious surfaces have a significant impact on the temperature and humidity of a location, as shown in summarizes these findings and their corresponding literature.

Table 2 Studies pertaining to urban morphology and weather

Attributes	Studies
Pervious Surface	(Oleson et al., 2008)
Roof area	
Building surface area	
Vegetation cover	(Robitu, Musy, Inard, & Groleau, 2006)
Water cover	
Mean building height	(Plate, Kiefer, Vancouver, & 2004, n.d.)
Variation in building height – Std deviation	
Distance from reference station	(Liu et al., 2017)
Distance from large water body	(Chessa & Delitala, 1997)

Mean building height in surrounding grids	(Yuming Sun, Heo, et al., 2014)

3.3 Characterization of Urban Morphology for meso-climate

Meso-climate studies pertains to regions that are either at Super-fine resolution (3km x 3km radius) or ultrafine resolution (1km x 1km grids) (Takahashi et al., n.d.).

The intent of characterization is to study the influence of land cover on meso-climate of a region. If there is a lot of variability in the grid itself, the effect of each feature is hard to quantify. On the other hand, high variability between city grids helps to contrast and quantize these effects. Ultrafine resolution helps in capturing the variabilities of land use and land cover in a city landscape, keeping the individual grids homogenous.

The grid properties should convey all information about the land-use of the region it encompasses such that it can inform the weather alteration model with the inputs that are required to generate synthetic weather data. This information should ideally include all the features mentioned in section 3.2.

However, to be exhaustive, both superfine as well as ultrafine resolution has been taken as input features in the model.

3.4 Land Use data

The urban land form and land use information may either be represented in its raw form such as shape files for Geographic Information Systems or in pre-classified formats such as LCZ framework from the World Urban Database (WUDAPT).

Figure 17 LCZ framework by WUDAPT

The pre-classified data consists of land surface cover data, construction materials of built area and other details of urban morphology that are required for Weather Research and Forecasting (WRF) models. Each classification represents a type of land form/land use.

The raw data consists of land features represented as points, lines or polygons arranged in thematic layers such that each layer has only one kind of features. The three-dimensional information is projected on a two-dimensional representation to be viewed on screen or paper. The raw data is derived either from surveys or satellite imagery. Collection of data from surveys is calibrated and is now becoming obsolete. For this study, raw data is accessed from public data domains and conditioned for use in later stages of model building.

3.5 Conditioning of raw GIS data using ArcGIS Pro

ArcGIS is a powerful application from ESRI (Environmental Systems Research Institute) that may be used to store, map and analyze geographical information in 2D as well as 3D for any part of the world. The suite of integrated sub-applications includes ArcMap, ArcToolbox and ArcCatalogue to name a few.

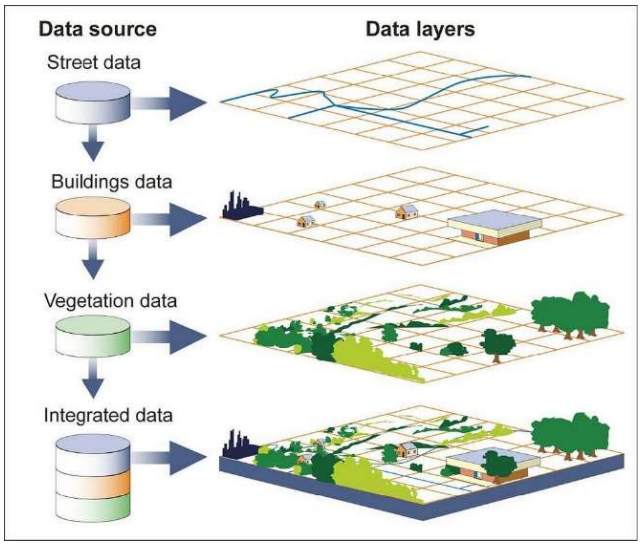

Figure 18 Layers of information in GIS (Source:GAO)

ArcGIS takes its input in two formats;

- ***Shapefiles:*** Shapefiles are 2D representations of urban features such that data attributes are linked to each shape in the file. In effect shapefiles with extension .shp are incomplete without its associated files that have extensions, .shx, .dbf. These additional files store information about the relative position of shapes in the files, metadata for the shapefile, their projections etc. A shapefile has only one feature class, i.e, if the shapefile represents airports as points, all the records in the shapefile would be points presumably showing airports.
- ***Geodatabase:*** a file-based database in which feature classes stored in one folder. These feature classes may be heterogenous implying that the geodatabase can have multiple feature classes representing lines, points as well as polygons. Geodatabases allow users to store data of different formats in the same folder. For example, a geodatabase for Atlanta may have feature classes that represents

highways as lines, polygon feature class may represent building footprints and lastly, a point feature class may represent schools in the city.

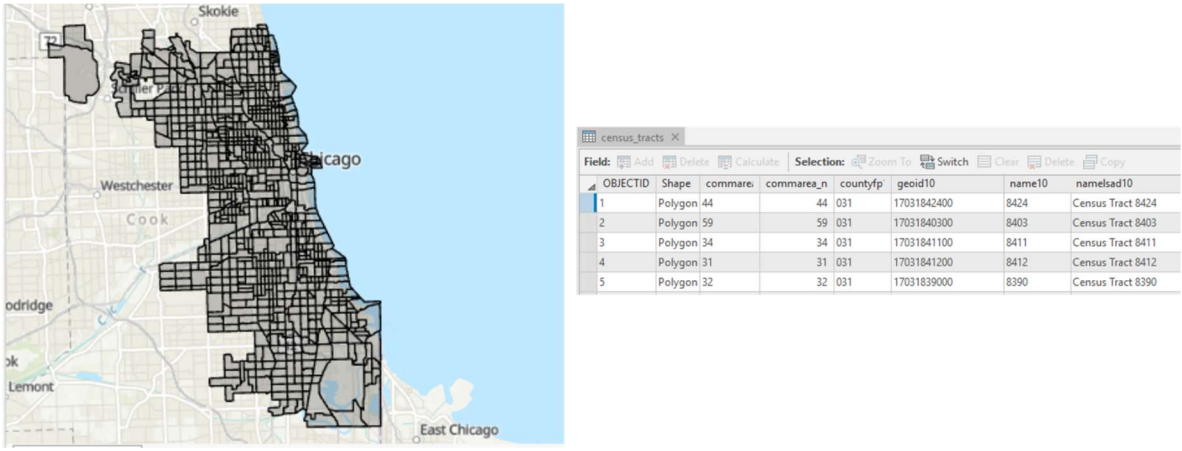

Figure 19 ArcGIS layer showing(a) census tracts as polygons (b) attribute table for census tract data

Both shapefiles as well as feature classes in ArcGIS have attribute tables that contain information about the geometric shapes that represent information about the city. In the example above, each polygon represents a census tract in the city of Chicago. Information about those tracts such as tract number, geoid, tract area etc. can be located in the attribute table. The metadata of each shapefile informs the user about methods of collecting data, agencies involved and limitations if any.

For this study limited to Chicago, geospatial data is drawn from the following sources;

- United Stated Environmental Protection Agency (US EPA)
- Data.gov
- City of Chicago open data portal
- cookcountyIL.gov
- Prairie research institute (University of Illinois at Urbana Champaign)
- OpenStreet maps

3.5.1 Datasets

To include all the urban morphology affecting meso-climate of the city as mentioned in section 3.2, the following datasets are searched and downloaded;

i. ***Building footprint data***: This data is sourced from the city of Chicago data portal with attributes for each building such as year of construction, number of stories, number of units in multi-family apartments, total footprint, address, direction of entrance, perimeter etc.
ii. ***Land use-vegetation***: A shapefile of all vegetation in the state of Illinois is obtained from US EPA. The attributes of each polygon included type of vegetation classified in the categories of park, grass, meadows, forests and nature reserves. Wherever possible, name of the record is displayed such as name of parks.
iii. ***Parking spaces***: Since complete information about paved surfaces is not available, data about parking spaces is drawn as a section of paved surfaces.
iv. ***Water bodies***: Geospatial information of all the waterbodies is obtained with attributes of location and area for each record.
v. ***Digital elevation***: Digital elevation files in raster format is obtained from Prairie research institute to find elevation at each point in the city.

The raw data thus obtained required formatting, sub-classification and conditioning to characterize urban morphology at meso-scale. The following sub sections show the steps that were followed to achieve the desired data quality.

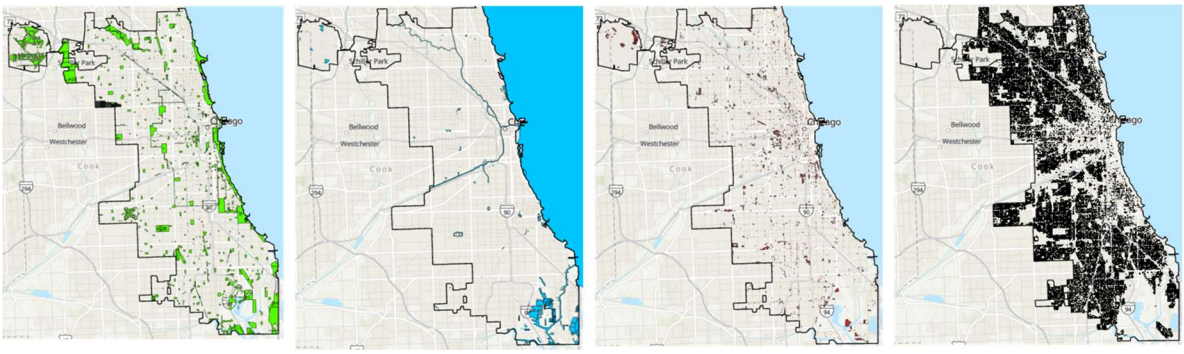

Figure 20 GIS datasets (a) Vegetation (b) Water bodies (c) Parking spaces (d) Building footprint

3.5.2 Projection of Shapefiles

The shapefiles obtained from data sources contain coordinate system information i.e, information about their location on earth as reported by satellites/ global positioning systems in spherical decimal coordinates. Since the surface of earth is not a smooth sphere but an obolid with different elevations at different locations, giving spatial reference to the shapefiles implies projecting the geographic coordinate system information to one that can be mapped on a 2D surface.

The units when projected coordinate system is absent is often shown in decimal degrees. However, when the geospatial data is projected, units are converted to standard units of length such as foot or meter. One should be mindful about the choice of pre-defined projection system as each system has spatial qualities that are well preserved in translation and some others that are not.

Since this study majorly deals with polygons and their areas, the state plane projection system "NAD 1983 UTM Zone 16N(Meters)" is used. All the data layers are projected to this projection system using the "*Define Projection*" tool of ArcGIS such that there is a

perfect overlap of all the layers and there is no anomaly while calculating geometry information (e.g. area and distances).

3.5.3 Clip tool

Since some of the layers that are obtained from federal resources cover the whole state of Illinois, layers of data need to be clipped to Cook county boundaries. Boundary shapefile was obtained from City of Chicago data portal and "*Clip*" tool of ArcGIS pro is used to bring uniformity of boundaries in all shapefiles.

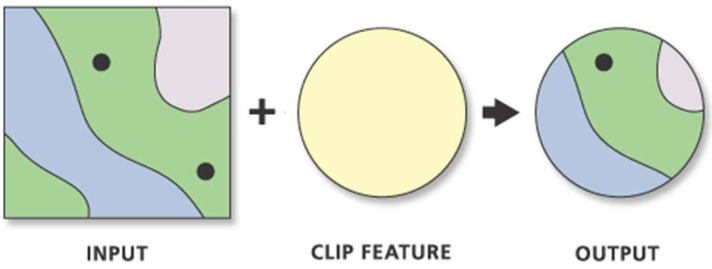

Figure 21 Clip tool (Source: arcgis.com)

3.5.4 Creating a fishnet grid

"*Create fishnet*" was used to construct a shapefile which would act as a stencil to divide the city in meso-scale blocks with homogenous urban features. The extent of the grid is same as the extent of city of Chicago and the grids which had area less than 0.9 km^2 were discarded as they were too small for the analysis.

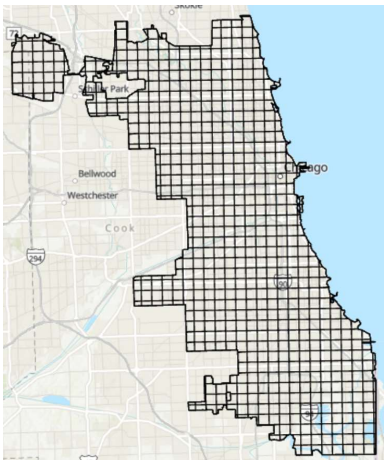

Figure 22 Building fishnet grids

3.5.5 Summarizing features within each grid

"*Summarize within*" of ArcGIS was used to calculate the total area of each urban feature within the fishnet grid. The tool works perfectly for water, parking and vegetation layers. However, due to large number of records in a building shapefile, simulation runs crash multiple times. The building shapefile records are then divided to create smaller shapefiles with a fraction of all records to complete the characterization.

3.5.6 Summarizing features within larger radius

There have been diverse studies to determine the influence of certain urban features on a location. They have found varying influence regions indicating that only features within the influence region have to be used to find the meso-climate of a location. (Gunawardena & Kershaw, n.d.) take a CFD domain of 2.1 km length to alter weather from airport to the building in question. (Tong, Chen, & Malkawi, 2016) suggest that although 3 building boxes around the target building suffice for the CFD simulation domain used for micro-

climate studies, a distance of up-to 15H is generally accepted in literature, H being the height of target building.

However, most of the studies are in context of micro-climate and CFD in urban simulations attempting to model changes in wind. Other urban features such as water bodies and forests too, have a profound effect on temperature, as well as humidity. In view of these facts, in urban weather modeling, a radius of 3km is taken to cover the expanse of meso-scale where all the urban features are summarized for the centroid of each grid cell.

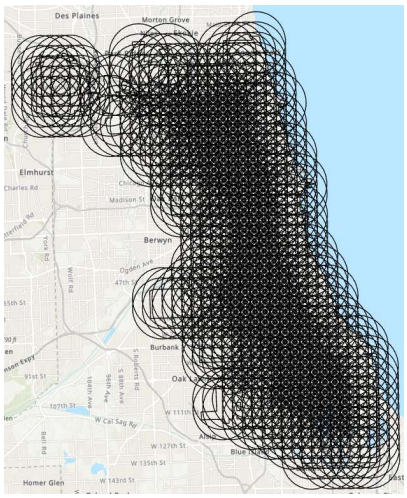

Figure 23 3km buffer around all grid centroids

3.5.7 Distance and angle from airport and Lake

As discussed in section 3.2, the distance from airport is expected to play a key role in alteration of wind from the recorded value at the airport. In addition to other urban features that surround individual grid cells, wind is affected by the distance that it covers from open spaces to densely built urban spaces or vice-versa. The relative angle between airport location and grid centroid is also computed to provide an input for the relative location of

the grid cell with respect to the point of observation. The "*Nearby*" geoprocessing tool is used for this exercise to find similar attributes for deriving proximity of grid to lake Michigan in our Chicago model.

3.5.8 Digital elevation for grids

The digital elevation model (DEM) is a raster file format which is used when geospatial information is continuous in nature such as land imagery, satellite derived surface temperatures and elevation surfaces to name a few. However, the information from DEM requires conversion to shapefile/geodatabase format to carry on the analysis. The "*Extract values to points*" tool from spatial analyst extension toolbox is run to assign elevation to centroids of each grid cell.

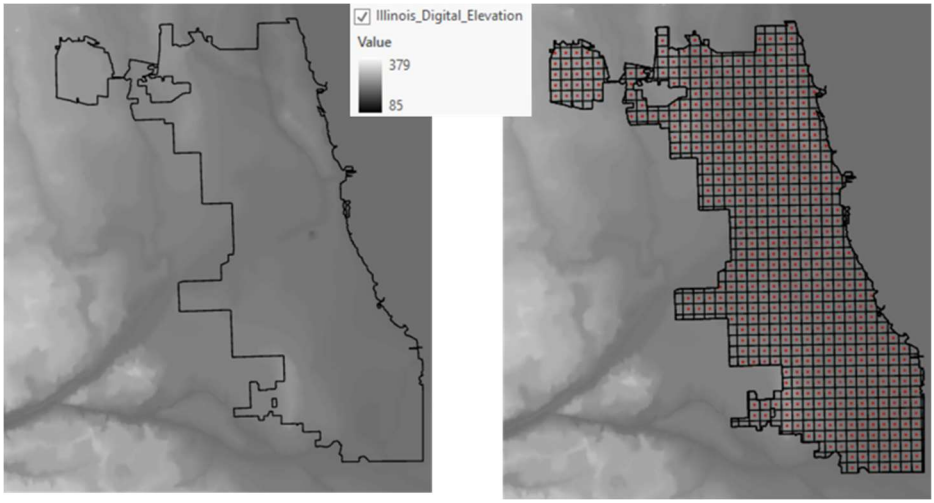

Figure 24 Elevation assignment to grid cells

3.6 Access to observed weather through weather API's

An API with 1million API calls was purchased from Weather-underground, a subsidiary of IBM with data from thousands of locations across the world. 55 weather stations in

Weather-underground's database were found to be inside the Cook county boundaries. Python coding was done as a medium to access and store the data from the cloud database. Information once received, was scrutinized to avoid absurd or missing data points.

3.7 Synthetic weather Modeling

Multi-variate regression techniques have been experimented with to predict the temperature variations in urban settings (Hjort, Suomi, & Käyhkö, n.d.) (Ninyerola, Pons, & Roure, 2000), mostly by regional planning disciplines, atmospheric sciences and geographical studies. Regression techniques are used as guiding pathways for interpolation techniques to take advantage of ancillary information from GIS that cloaks complex, non-linear spatially varying relationship with underlying land-use (Rigol, Jarvis, & Stuart, 2001).

Statistical methods have the potential to simplify climatological relationships provided there is enough data to run these algorithms covering all possibilities of explanatory variables on which they are regressed.

There is no dearth of literature in modeling different weather variables through a diverse set of modeling tools, however, there are very few that model the correlations of weather variables with each other as discussed in section 3.1. This study aspires to model not only a single variable like temperature but also its correlation with wind and humidity. Simple regression techniques could be based on running linear regression for every hour of the day on weather variables, but they run the risk of overfitting response data due to limited number of logger sites.

3.7.1 Tensors and Multiple Tensor on Tensor Regression

Tensors are represented as multi-dimensional arrays. More precisely, an "*N-th order tensor is an element of the tensor product of N vector spaces, each of which has its own coordinate system*" (Kolda & Bader, 2009).

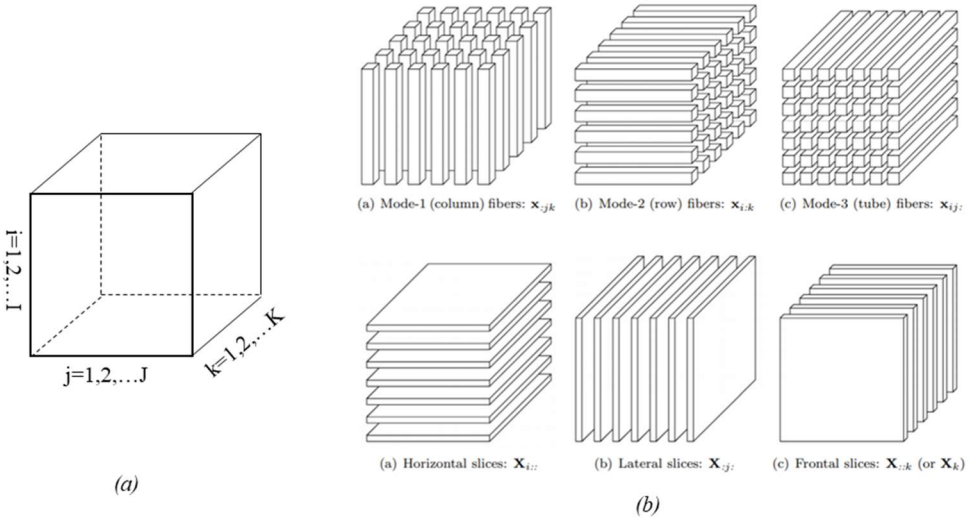

Figure 25. (a) A third order tensor $\mathcal{X} \in \mathbb{R}^{IXJXK}$(b) Fibers and Slices in Tensors

3.7.2 Basic Terminology related to Tensors

The order of tensor is the number of dimensions, also known as ways or modes. Fibers are data from a tensor when all the indices are kept constant except one. Similarly, slices are two dimensional sections of a tensor. These definitions help to realize functions on tensors that are then used in tensor decomposition (see section 3.7.3).

An N-mode tensor $\mathcal{X} \in \mathbb{R}^{I_1 \mathbf{x} I_2 \mathbf{x} \ldots I_N}$ is rank one if it can be written as an outer product of N vectors i.e.,

$$\mathcal{X} = a^{(1)} \circ a^{(2)} \circ \ldots \ldots a^{(N)}$$

Symbol ∘ represents the vector outer product which means that each element of the tensor is a product of corresponding vector elements.

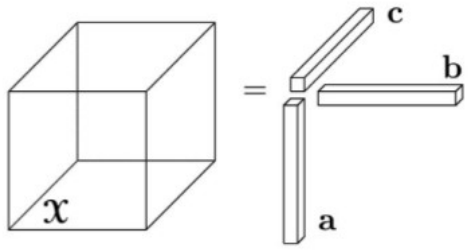

Figure 26. Rank one third order tensor, $\boldsymbol{\mathcal{X} = a \circ b \circ c}$

Matricization, also known as *unfolding* or *flattening* is the process of transforming a tensor to matrix by re-ordering the elements of an N-way array into matrix. For example, a 2x5x3 tensor can be arranged as 10x3 matrix or 5x6 matrix, and so on.

3.7.3 Tucker Decomposition

Tucker decomposition is a form of higher order PCA which breaks down a tensor in to a core tensor multiplied by matrix along each mode (Tucker, 1966). Thus, for a third order tensor $\mathcal{X} \in \mathbb{R}^{IxJxK}$

$$\mathcal{X} \approx \mathcal{G} x_1 A x_2 B x_3 C = \sum_{p=1}^{P} g_{pqr}\, a_p \circ b_q \circ c_r = [\![\mathcal{G}; A, B, C]\!]$$

Where, $A \in \mathbb{R}^{IxP}$, $B \in \mathbb{R}^{JxQ}$ and $C \in \mathbb{R}^{KxR}$ are the factor matrices that can be thought as principal components in each mode. If P, Q and R are smaller than I, J and K, the core tensor $\mathcal{G}$ can be assumed as a compact version of $\mathcal{X}$.

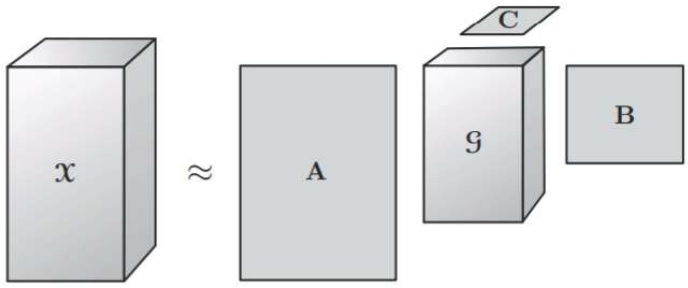

Figure 27. Tucker decomposition of a 3-way tensor

Weather variables extracted from API calls are Dry bulb temperature, wet bulb temperature, relative humidity and wind speed. Residues are calculated as the difference between Airport observation and local weather station observations. For example, dry bulb (DB in equation) residue at nth hour is calculated as;

$$T_{DB_n} = T_{DB-airpor\ _n} - T_{DB-weather\ station_n}$$

In this study, $\mathcal{Y} \in \mathbb{R}^{55x8760x4}$ represents a 3-way tensor with data from observed weather stations, where the modes represent logger sites, hours in a year and residues of weather variables that are taken into consideration as shown in Figure 28.

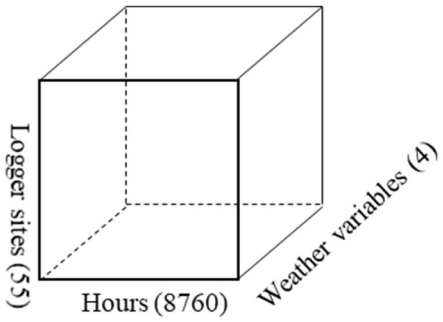

Figure 28. Weather data as tensor

3.7.4 Multiple Tensor on Tensor Regression

The linear regression method used in this study minimizes the least square loss function between input weather tensor and output weather tensor to estimate regression parameters. The model is coded in MATLAB and is based on the algorithms and libraries described in (Gahrooei, Yan, Paynabar, & Shi, 2018). The size of regression parameters is compressed using the Tucker decomposition as mentioned in section 3.7.3, such that interrelationships between modes are preserved in the process.

The methodology states that if the response tensor has the data size M, such that $\mathcal{Y}_i \in \mathbb{R}^{Q_1 \mathrm{x} Q_2 \mathrm{x} \ldots\ldots Q_d}$ (i=1,2,…M) and input tensor $\mathcal{X}_i \in \mathbb{R}^{P_{j1} \mathrm{x} P_{j2} \mathrm{x} \ldots\ldots P_{jl}}$ (i=1,…M;j=1,2,…p) where p is the number of inputs. The relationship between input tensors and response can be written as;

$$\mathcal{Y}_i = \sum_{j=1}^{P} \mathcal{X}_{ji} * \mathcal{B}_j + \mathcal{E}_i, i = 1, \ldots, M$$

For this application, response block $\mathcal{Y}$ is the tensor described in previous section, $\mathcal{X}$ is the matrix representing urban features of grids where each logger site is located as shown in Figure 29. It is assumed that parameter $\mathcal{B}_j$ can be represented as;

is assumed that parameter $\mathcal{B}_j$ can be represented as;

$$\mathcal{B}_j = \mathcal{C}_j \times_1 U_{j1} \times_2 U_{j2} \times_3 \ldots \times_{l_j} U_{jl_j} \times_{l_{j+1}} V_1 \times_{l_{j+2}} \ldots \times_{l_{j+d}} V_d$$

where, $\mathcal{C}_j$ is the core tensor and U_{ji} and V_i are basis matrices when $\mathcal{B}_j$ is decomposed using Tucker method. Figure 30 shows the stepwise estimation of $\mathcal{B}_j$ using MTOT.

Algorithm 1 Estimation procedure for multiple tensor-on-tensor regression

1: Initilize $\mathcal{C}_j$ for all j
2: Estimate U_{ji} using Tucker decomposition of $\mathcal{X}_j$ for all i and j
3: Initilize V_i for all i
4: Compute B_j for all j and set $w_0 = \left|\left|Y_{(1)} - \sum_{j=1}^{p} X_{j(1)} B_j\right|\right|_F^2$
5: **do**
6: Estimate $\mathcal{C}_j$ for all $j = 1 : p$
7: Estimate V_i for all $i = 1 : d$
8: Compute B_j for all j and set $w_k = \left|\left|Y_{(1)} - \sum_{j=1}^{p} X_{j(1)} B_j\right|\right|_F^2$
9: **while** $|w_{k+1} - w_k| > \epsilon$

Figure 29.Stepwise MTOT algorithm(Gahrooei et al., 2018)

3.8 Results from the weather model to generate synthetic weather data

Using the above methodology, data from 50 out of 55 weather stations (also referred to as logger sites) in Chicago was fed into the Tensor on Tensor regression model as a response tensor variable $\mathcal{Y}_i$ for the year 2018. The input tensor $\mathcal{X}_i$ represents urban morphology of the grid cell in which a respective weather station is located, calculated from available GIS data. These 50 weather stations were randomly chosen from the dataset. This segregates the available data in training dataset (50 weather stations) and test dataset (5 weather stations).

The model estimates the parameter tensor $\mathcal{B}_j$ in the form of core tensor and basis tensors along each mode of $\mathcal{Y}_i$. Thus, using the trained model, weather is predicted for the 5 weather stations that are in test dataset with $\mathcal{X}$ as grid properties calculated in section 3.5. The model is able to predict the weather in test datasets with a standardized mean square error of 0.04 implying that the model can explain approximately 96% of the variation in all weather variables.

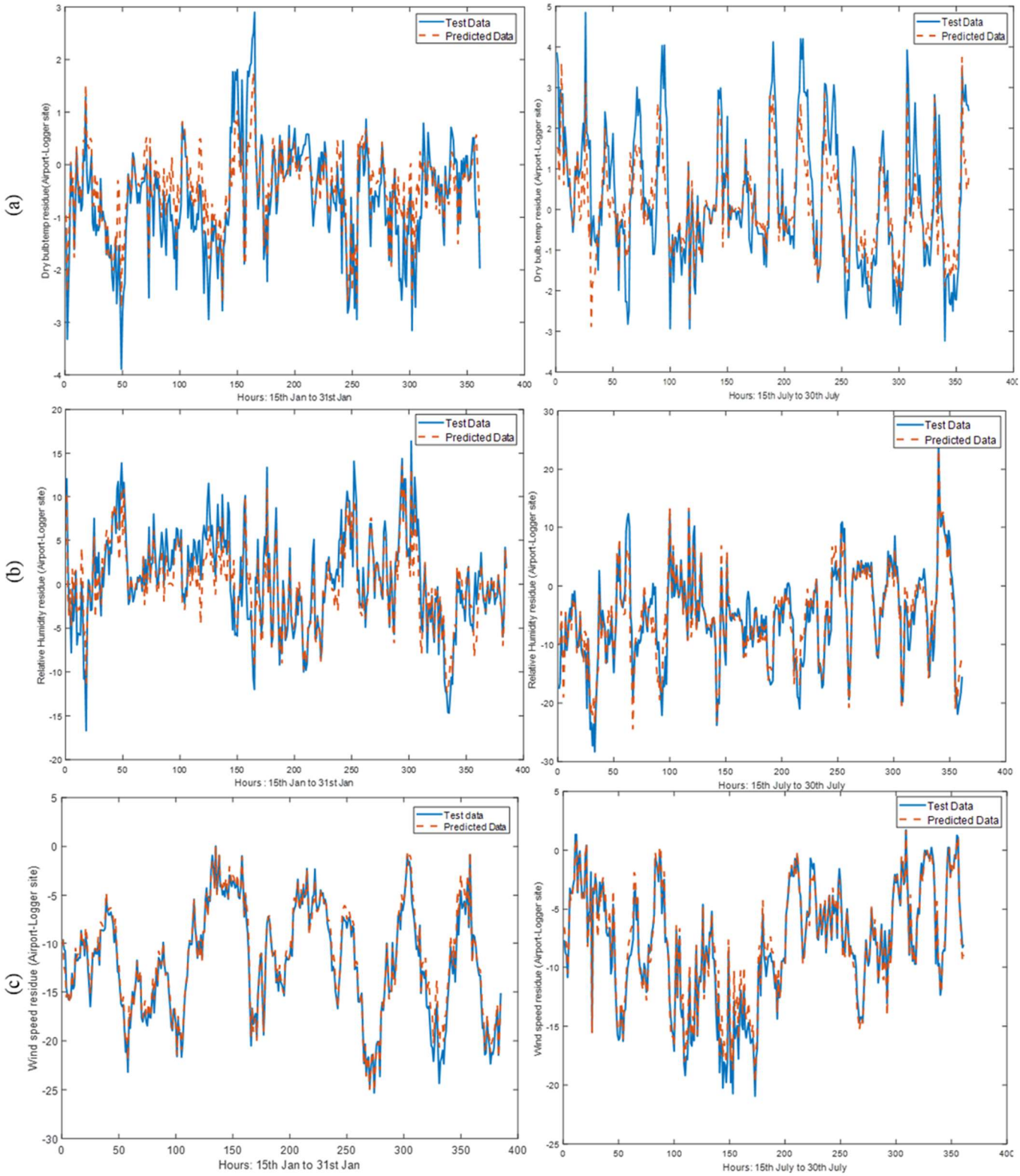

Figure 30 Plots of residues for Test data in comparison with predictions of (a) Dry bulb temperature (b) Relative Humidity (c) Wind Speed

Figure 30 shows the plots of test residue data from one of the 5 weather stations in comparison with predicted residue data from the statistical model for two weeks in peak summer and peak winter conditions.

By feeding the model with the urban morphology data of all 529 grids in Chicago the city-wide meso-scale weather data is generated. For some grids the generated weather shows absurd values for temperature and humidity; in some cases temperature is going up to 80 C.

After scrutinizing the statistical model for any inconsistencies, it proves that the grids with absurd predictions are the ones that have urban morphology parameters beyond the distribution on which the model is trained. This revelation highlights the importance of the source and "coverage" of training data and the variabilities that it must possess to allow reasonable weather predictions for all grid cells in question.

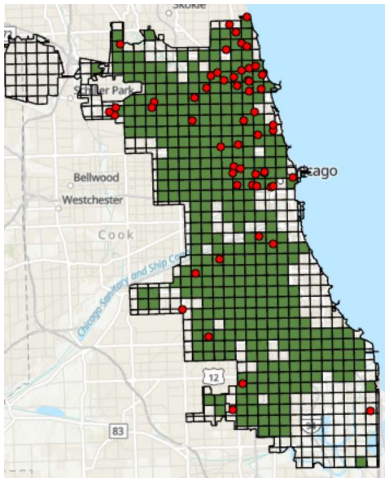

Figure 31 Viable grid cells for weather predictions in Chicago

The model is able to generate 375 meso-scale weather files for grid cells that were within the distribution range of the training dataset, leaving out 154 grid cells out of total 529 grid

cells across the city. Figure 31 represents the cells for which weather data could be generated, the red dots represent location of logger sites. It can be deduced from the GIS map that due to scarcity of logging sites in southern parts of Chicago, the training dataset is heavy on morphology types encountered in the northern parts of the city. To generate a complete coverage of city, spatial interpolation techniques may be used to fill in the missing data. Alternatively, more weather stations could be installed (or data acquired from existing ones) in the southern parts of Chicago to provide coverage for all ranges of grid properties.

3.8.1 Importance of urban characteristics in synthetic weather generation

The urban characteristics described in the literature are fragmented based on the weather variable that is being modelled. For example, literature on formation of urban heat islands focusses primarily on the impervious fraction and vegetation in the area under study. Similarly, studies on the effect of urbanization on wind are based on the resistance offered to the flow of wind by urban structures such as high rise buildings.

In an attempt to cover all the factors that affect weather variables being modelled, the characterization includes all possible urban features mentioned in studies that model weather in different parts of the world. However, since each city is unique in the way its meso-climate is affected by the urban layout, it makes an interesting case to observe the urban characteristics that affect the meso-climate of Chicago.

To identify the impact of each urban feature, an MTOT model was run with stepwise variable elimination in the original model that contained all the variables (19 urban characteristics) needed to predict the weather. With elimination of each characteristic, the

model is run and $\mathcal{B}_j$ can be estimated. The newly trained model then predicts the weather for randomly selected five weather stations. The impact on standardized mean square error was noted for predicted values. Model prediction accuracy is the percentage of variation in predicted values that are explained by the MTOT model, computed as follows:

Model Prediction Accuracy= 1-Standardized Mean Square Error (SMSE)

Loss of accuracy as the name suggests is an indication of reduced ability of the model to predict the weather grid cells when one of the variables is eliminated from the training dataset.

Loss of Accuracy=Model Prediction Accuracy (with all characteristics)- Model Prediction Accuracy (after elimination of one variable)

Table 3 Loss of accuracy after elimination of individual urban characteristic

X	Urban Characterstic	SMSE	Model Prediction Accuracy	Loss of Accuracy
All	All	0.0434	0.9566	
1	Elevation	0.0490	0.9510	0.0056
2	Average height- Grid	0.0421	0.9579	-0.0013
3	Variance in building height- Grid	0.0428	0.9572	-0.0006
4	Park- Grid	0.0445	0.9555	0.0011
5	Forest- Grid	0.0436	0.9564	0.0002
6	Grass- Grid	0.0450	0.9550	0.0016
7	Parking- Grid	0.0446	0.9554	0.0012
8	Distance from Airport- Grid	0.0440	0.9560	0.0006
9	Building Footprint- Grid	0.0452	0.9548	0.0018
10	Water- Grid	0.0434	0.9566	0.0000
11	Building Footprint -Radius	0.0434	0.9566	0.0000
12	Parking-Radius	0.0434	0.9566	0.0000
13	Forest-Radius	0.0434	0.9566	0.0000
14	Grass-Radius	0.0437	0.9563	0.0003
15	Park-Radius	0.0435	0.9565	0.0001
16	Angle to Airport-Radius	0.0436	0.9564	0.0002
17	Water-Radius	0.0412	0.9588	-0.0022
18	Average height-Radius	0.0433	0.9567	-0.0001
19	Distance to lake-Radius	0.0436	0.9564	0.0002

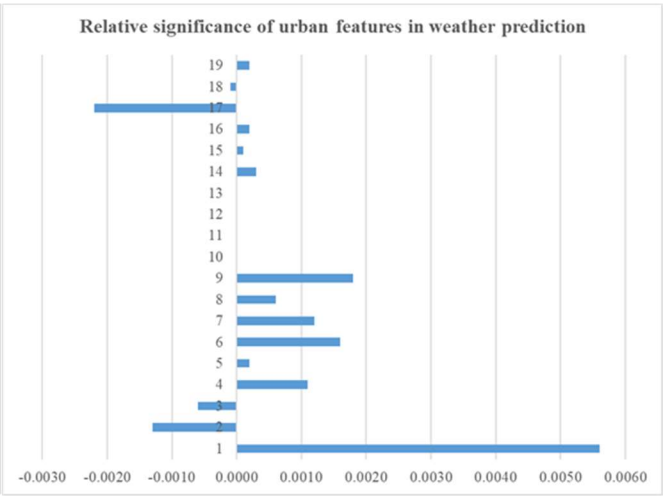

It should be noted that the modelling and calculation of SMSE is done on the block dataset of three weather variables, namely, temperature, wind speed and relative humidity as we also want the capture the correlations between the weather variables themselves. For

example, relative humidity would be impacted by both temperature and wind speed. Therefore, the importance of each urban characteristic is computed for the complete weather model and not individual variables.

It can be seen from that for Chicago, elevation of a grid cell is of utmost importance in determining the meso-climate of that part of city followed by grid properties of urban features. Counterintuitively, characteristics related to height of buildings and presence of water had either no or negative influence on the model's ability to predict the local climate in Chicago. One possible explanation is that building footprint, distance and angle to centroid of grid is able to compute variation in wind speed and height of buildings is a redundant characteristic that introduces noise in the prediction of temperature and relative humidity. Additionally, superfine resolution, i.e, characteristics at 3 km x 3 km resolution are not contributing towards improvement of the model.

The explored behaviour of the statistical model warrants further research with multiple cities and larger datasets. This is however beyond the scope of this thesis. Our main objective is to use the generated weather at meso scale as input in simulation studies of various types and practical uses and compare the outcomes to those obtained with one and the same weather in all grid cells. This objective is well served by the weather model as developed above.

CHAPTER 4. IMPORTANCE OF MESO-SCALE WEATHER FOR THE ACCURACY OF BUILDING SIMULATION OUTCOMES

For buildings that are in the early stages of design, building simulation models predict quantifiable measures of functionalities expected from them. For example, the stakeholders of a yet to be built project may require it to be well daylit for increased productivity in addition to being energy efficient. The expected performance can be expressed as a set of criteria, where each criterion is quantified using an agreed measure (Augenbroe, 2011), sometimes referred to as performance indicators. In this example, the criteria we target are daylighting and energy efficiency, which can be expressed by a range of alternative performance indicators. Here we choose cumulative hours of daylight autonomy and energy use intensity (EUI) of the building, to be computed, or rather simulated, through a well-constructed virtual experiment by the modeler. It is most common that experiments in the form of building simulations produce the quantified measures for the criteria that are formulated upfront to aid the design decisions aimed at accomplishing a set of final goal(s).

However, when such analysis is done with deterministic inputs, indicating that the modeler has perfect information about building envelope as well as the scenarios in which the building will operate, the outcomes of the performance indicators are deterministic quantities which do not account for uncertainties as discussed in Chapter 2. Similarly, for retrofit decisions in existing buildings, even though there is in theory complete knowledge about construction properties of the house, unobservable defects such as cracks and low maintenance of air conditioning units may lead to erroneous assumptions about building

fabric as well as systems. It should be recognized that even for existing buildings, many of the "idealized" parameters in their corresponding building models are only partly observable and at best only indirectly measurable. These recognitions have led to many recent research efforts that aim to quantify the modeler's lack of knowledge due to realization uncertainty (in design studies) and incomplete observability (for existing studies), and consequently propagate the quantified uncertainties into predicted outcomes. The study in this chapter follows in these footsteps, adding one more element of uncertainty (or properly stated, variability) to the mix and gauge its effect on predicted outcomes (De Wit, 2001). We adopt the terminology established in the cited works, in distinguishing three types of uncertainty: (1) in model parameters, (2) in the scenarios that the building is subjected to, and (3) uncertainties in the model itself, usually referred to a s model discrepancy or model form uncertainty. More details will be discussed below.

Every building design decision comes with its own settings, criteria, stakeholders and scope of design. Establishing the role of uncertainties in a particular decision is therefore inherently case based, albeit that the expectation is that for certain type of decisions the role of uncertainties can be universally established. For this thesis, three types of real-life cases are considered. Simply stated they deal with Quantities of Interest (QoI) in three broad categories; energy consumption, yield of building integrated photovoltaics, and natural cooling potential. For each category the starting point of the investigation is a reference building model ("QuickStart | EnergyPlus," n.d.) in EnergyPlus. This model is then used for a comparative analysis following three incremental steps, i.e;

Approach (a): The EnergyPlus models are subjected to only parameter and scenario uncertainties that have already been established and quantified by the academic community

as will be described in section 4.1.1. In this approach, TMY3 is used as the base weather input for all simulations.

Approach (b): EnergyPlus models are simulated with all sources of uncertainty that are considered in approach (a) along with equal probability sampling of synthetic weather files created by the statistical weather model (see Chapter 3) developed for the city of Chicago at meso-scale. For case III, since the building is located in Atlanta, recorded weather from different parts of Atlanta is utilized as an approximation of meso-scale weather uncertainty. The parameter sensitivity of the selected QoI in each of the cases is ranked to analyze the importance of higher resolution weather in building simulation in comparison with the standard sources of uncertainty considered in approach (a). The comparison of (a) and (b) will reveal the relative influence of the weather spatial variability.

Approach (c): To nudge the difference between weather scales at meso vs micro level, samples are drawn for variation in wind pressure coefficients in addition to uncertain inputs considered in approach (b). The method of computing the sampling space for wind pressure coefficients is described in section 4.1.3. This approach is introduced to conduct the comparative analysis when the influence of local weather is amplified, as is indeed the case in ventilation studies which are primarily driven by local wind speed.

4.1 Types of Uncertainties

4.1.1 Parameter and "Internal" Scenario Uncertainty

For buildings that are yet to be built and are in the design stage, simulation engineers typically use standard thermal properties of the materials that are specified in the

construction documents. These properties are at best idealizations of reality. They have been obtained through experimentation in controlled conditions in a scientific laboratory. In effect, however, the material properties are not deterministic values, rather, they are probabilistic distributions due to change in properties of materials in uncontrolled (or real-world use) or imperfections during construction process. For example, the conductance of insulation material in practical circumstances will depend on workmanship related issues that can only be predicted within a margin of uncertainty (this can relate to the secure assembly of building components, protection against water penetration, and the presence of thermal bridges around edges and joints).

The second major reason for uncertainty is the inherent lack of knowledge about how the building is going to be occupied and operated. A scenario of use is typically represented in simulation models as schedules in the form of time series with hourly values, e.g. for occupancy, lighting, plug load. HVAC control schedules are treated similarly, with a specification of causal logic for its operation. Both are within the boundary of the building and are hence categorized as "internal" scenarios. The estimates for these schedules are derived either from interviews or surveys or informed assumptions from the literature and engineering manuals. There are new developments that represent these scenarios with stochastic generators rather than fixed values.

For this thesis, assumptions regarding parameter and scenario uncertainties are primarily derived from (J. Chen, 2018a; YM Sun, 2014). The air leakage in residential buildings are guided by study published by (Chan, Nazaroff, Price, Sohn, & Gadgil, 2005) whereas in commercial buildings, air leakage assumptions are gleaned from (Belleri, Lollini, Environment, & 2014, n.d.).

4.1.2 Weather as "External" Scenario Uncertainty

In addition to sources of error mentioned in section 4.1.1, there are "external" scenario uncertainties with weather being the most immediate manifestation of those. They are represented as an external (hourly) time series based on published data as discussed in section 4.1. However, the hourly values only represent one possible realization of the actual weather. In reality, there is considerable variation, of a stochastic nature and possibly with a superimposed long-term trend which evolves over the building's lifetime, e.g. based on a climate change model. Nevertheless, current deterministic simulations use only one (TMY) time series for their prediction. Based on the way the TMY is constructed, this may have been justified for certain types of studies (such as for aggregated energy consumption), but for other applications (peak power occurrence, or more generally, power duration curve) one statistically average TMY does not do the job as the spatial variation of weather as well as occurrence of extreme weather events is not well enough represented in current TMY scenarios. Different remedies are available to incorporate the temporal variation and extreme weather events in building simulation, i.e. by generating multiple weather time series with a stochastic generator, or by using a large number of actual historical years. However, it should be noted that the uncertainty in the weather scenario has both a spatial and a temporal dimension. This makes its characterization complex. Since the primary aim of this thesis is to recognize the impact of spatial variability of weather on building simulation outcomes, an uncertainty and sensitivity analysis can be done with either spatially recorded data or with the meso-scale weather generated by MTOT model described in Chapter 3.

4.1.3 The translation from meso weather to micro climate

There is no generally accepted way to translate the weather information from meso scale to the boundary conditions that govern the heat and air exchange phenomena at the external surfaces of the building. These hyperlocal phenomena are addressed by the term micro climate as indeed they can be understood as the conditions in the immediate (micro)vicinity of the building. It is generally a safe assumption that micro scale variations of air temperatures are small enough to ignore. This is not true for the local air movement at the surface and the way that long and shortwave exchange takes place with the sun, external surfaces and sky dome. At the micro scale, these external conditions are impacted by the form and thermal properties of the skin as well as the physical objects in the immediate surroundings of the building in question. The effect of the surroundings is driven primarily by two phenomena, namely, thermal radiation exchange with surrounding buildings and alteration of wind speed as well as its flow patterns owing to the presence of one or more obstructions in the surrounding and their relative placement.

Recent advances have made it possible to model long wave radiation exchange in EnergyPlus from the building being modelled to the surrounding building and land features such as water bodies and green areas (Hong & Luo, 2018). Just as in the case of shading from surrounding trees and buildings, it is now up-to the discretion of the building modeler to include the nearby structures for long wave thermal exchange with the building and it may no longer be considered an uncertainty which should be propagated into simulation outcomes. This reflects the truism that higher resolution modelling diminishes the magnitude of uncertainty.

On the other hand, modelling of variations in wind speed and its flow patterns and pressure require detailed computational fluid dynamics modelling to get a view of the full impact of

surroundings on building performance. (Costola, Blocken, environment, & 2009, n.d.) present an exhaustive overview of methods used to calculate wind pressure coefficients (Cp) in building energy simulation emphasizing that the largest difference in assumed values of Cp comes from the modelling of flow-impacting buildings.

For this thesis, a repository of wind pressure coefficient data is generated using the regression model devised by (Yuming Sun et al., n.d.) which alters the wind pressure coefficients calculated by Swami and Chandra model (Swami, transactions, & 1988, n.d.) for different attack angles of wind. Training data for this regression model is obtained from TNO's Cp generator (Knoll, Phaff, & Gids, 1995), which, in turn is fed from 81 scenarios where eight adjacent buildings are parameterized in Community Land Model over four variables, namely, Canyon Height (H), canyon ration (H/W), building height to length ratio (H/B_L) and building width to length ratio (B_W/B_L).

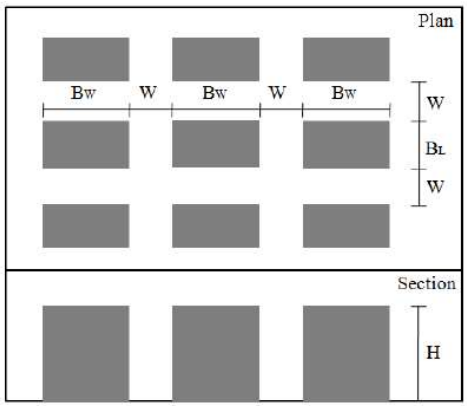

Figure 32 Urban Parameterization scheme in Community Land Model (Yuming Sun et al., n.d.)

A set of Cp values for angles ranging from 0 to 180 degrees, graduating at 30 degrees is sampled from this repository with equal probability and populated in building model to represent the uncertainty in wind pressure due to surrounding buildings.

4.2 Experiment Set Up

The assessment of the importance of spatially diverse weather is divided into two parts;

- Uncertainty Quantification: This represents the probability distribution of a Quantity of Interest when simulated over a large number samples with inputs drawn from their respective uncertainty distribution. If this results in a wide distribution of the resulting QoI, it suggests that the modeler is rather unsure or ignorant about the inputs that affect this particular QoI. The distribution of a QoI may be so wide that the prediction becomes non informative which means that the conducted uncertainty quantification can only be regarded as the first step and needs to be followed by an incrementally refined analysis with the aim to improve the modeler's prior knowledge and thus narrow the distributions of the input parameters.
- Sensitivity Analysis: A building performance model can have hundreds of inputs that are required for its simulation but there are only a few that have a pronounced effect on a selected QoI. These critical inputs, if not estimated within a narrow range, result in wide distribution of building performance measure as mentioned in the previous point. Hence, these inputs must be identified, and an endeavour should be made by the modeler to have better information about the plausible ranges for these variables. A sensitivity analysis entails regressing the variance of QoI results with the variance in the uncertain inputs leads to a ranking from most to least influential source responsible for QoI uncertainty.

Our approach discussed in the beginning of this chapter aims to inspect the level of scenario uncertainty, when we are ignorant about the location of a building in the city with respect to its local (meso scale) weather. Additionally, this study also attempts to examine (as approach c) whether the contribution of high fidelity meso scale weather fades relative to micro scale weather uncertainties manifested mostly as variation in wind pressure coefficients.

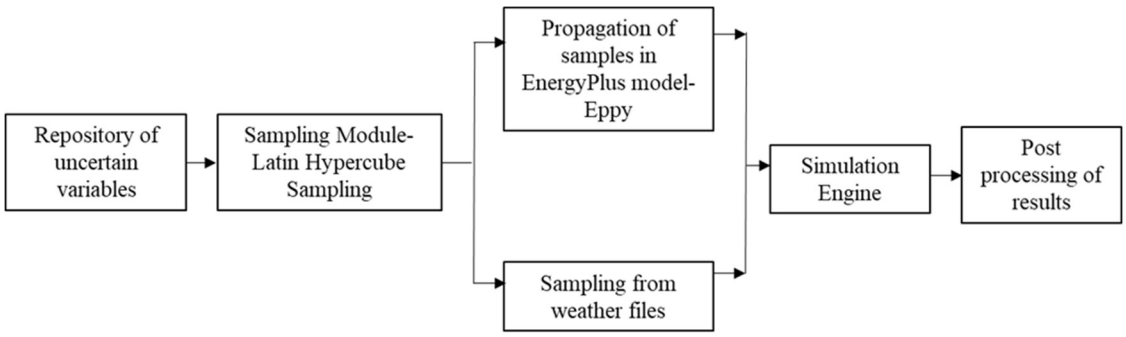

Figure 33 Experimental setup for UQ Analysis

Samples are drawn over probability distributions of uncertain variables using Latin Hypercube Sampling (LHS) with the SciPy library of python. These samples are then propagated through the EnergyPlus model of the building in question for each case by using the scripting language *Eppy* in Python.

4.2.1 Eppy

Eppy is a python scripting language that takes advantage of the Object Oriented Programming (OOP) structure of the EnergyPlus building simulation software. By using idioms and data structure defined for eppy, bulk modifications can be made in Energy Plus objects and the altered file can be saved and run from the Python console itself. The results

are returned from the EnergyPlus engine after the run is complete and collated for post processing.

4.2.2 Sensitivity Analysis using MARS

As discussed briefly in section 4.2, a sensitivity analysis (hereby abbreviated as SA), finds the input variables which have the largest impact on a QoI obtained with a specific building model. A large sample space and consecutive outputs from building simulation are statistically processed to rank the uncertain input variables.

For non-linear single value input samples, relatively simple regression methods such as multivariate linear regression may be used with along with ANOVA to analyse the sensitivity of a QoI to an input parameter. However, in this study, weather acts as a non-linear time series which cannot be treated like an additional parameter. Performing an SA that deals with a hybrid mix of parameters and time series is an interesting challenge dealt with in statistics (J. Chen, 2018b; Yuming Sun, 2014). A pragmatic approach which has been proven to give adequate results is based on the introduction of a categorical variable for weather, which is given a binary value 0 or 1 depending whether the scenario sample contains meso scale weather or weather from the airport with the latter de facto representing city-wide uniform weather. The sampling randomly assigns one of the two weather scenarios to a parameter sample. The influence of weather is now ranked through its categorical variable in the SA routine described below.

Multivariate Adaptive Regression Spline (MARS) method developed by (Friedman & Roosen, 1995) is used for regression in the post processing phase for which implementation is appropriated from (J. Chen, 2018b). MARS takes the form as follows;

$$\hat{f}(x) = \sum_{i=0}^{k} \beta_i B_i(x)$$

Where $x = x_{1,\ldots\ldots,}x_n$ are n dimensional inputs, B_i is the basis function, which could be a constant value 1, a hinge function max (0, $x_i - const$) or a product of multiple hinge functions and β_i are corresponding coefficients. The model progresses in forward phase by building basis functions which typically overfits the data, in backward phase the model is simplified by deleting at least one basis function. After both the phases, the model with lowest General Cross Validation (GCV), an estimator for prediction Mean Square Error, is selected as the final one.

$$GCV = MSE_{train} \,/\, \left(1 - \frac{enp}{n}\right)^2$$

Where MSE_{train} is Mean Square Error of model on training data, n is the number of observations and enp is effective number of parameters.

The relative importance of variables is calculated as (J. Chen, 2018b);

$$\frac{\sum_{t=1}^{k} Decrease\ of\ RSS\ of\ Sub - Models\ with\ variable\ j}{\sum_{t=1}^{n} Decrease\ of\ RSS\ of\ all\ the\ Sub - Models}$$

The relative importance of one variable j is calculated by dividing the sum of residual Sum of Squares (RSS) decrease for all the sub models containing variable j, by the total sum of RSS decrease for all the sub models combined in the variable selection process.

4.3 Discussion of the three application cases

The three selected application cases are chosen as representative of the large set of building simulation settings, varying in type of building, usage scenario and type of inspection, i.e. QoI. The objective is to find in each case what the relative importance is of the use of meso weather for the fidelity of the QoI. This is done with and without the recognition that the translation to micro scale introduces an additional uncertainty (in wind pressure) that may have a compounding influence. This is the reason for approach (c) in the investigation.

4.3.1 Case I: Energy; EUI of a House

This case aims to take an in depth look at the role of meso scale weather in retrofit decisions for an existing dwelling in the city of Chicago. Weatherization of old houses like the one considered in this case study, requires investment in building structural and system properties that are primary drivers of energy consumption. Information about building properties that when improved, give the best return on investment by the homeowners or may be utilized by energy policy makers to make informed recommendations to weatherization programs.

Building construction properties are drawn from Residential Energy Consumption Survey (RECS) for houses built before year 1990. Their geometry is based on Department of Energy (DOE) reference buildings published by Pacific Northwest National Laboratories (PNNL).

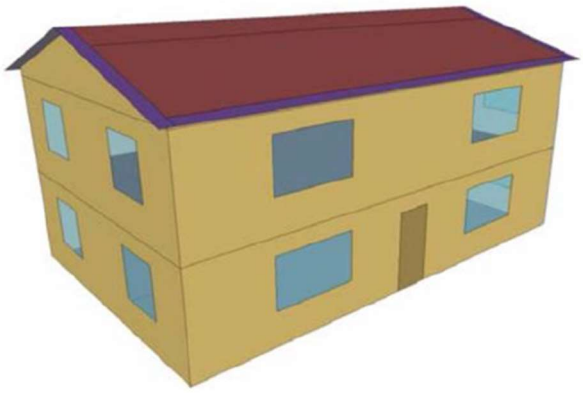

Building Property	Values
Floor area (m2)	111.4
#Stories	2
Exterior Wall Insulation	7
Ceiling Insulation	11
Floor Insulation	0
Windows (U value, SI units)	2.95 (W/m^2K), SHGC-0.66
Heating system	Gas Furnace
Heating COP	0.78
Cooling COP	3.97

Figure 34 Residential prototype geometry and properties

Table 4 Applicable uncertainties for Case I, their distribution and references

Uncertain Variable	Distribution	σ/LB	μ/UB	UB	Ref
Cooling COP	NormalRelative	0.05			(YM Sun, 2014)
Fan Efficiency	NormalRelative	0.05			(YM Sun, 2014)
Burner Efficiency	NormalRelative	0.05			(YM Sun, 2014)
Wall Conduction	NormalRelative	0.05			(J. Chen, 2018a)
Wall Solar Absorptance	NormalRelative	0.1			(J. Chen, 2018a)
Roof Conductivity	NormalRelative	0.05			(J. Chen, 2018a)
Roof Solar Absorptance	NormalRelative	0.1			(J. Chen, 2018a)
Window Conduction	NormalRelative	0.1			(J. Chen, 2018a)
Window Transmittance	NormalRelative	0.05			(J. Chen, 2018a)
Electrical Equipment	UniformRelative	0.7	1.3		(J. Chen, 2018a)
Electrical Equipment	UniformRelative	0.7	1.3		(J. Chen, 2018a)
Lights	UniformRelative	0.7	1.3		(J. Chen, 2018a)
Occupancy	UniformRelative	0.7	1.3		(J. Chen, 2018a)
ELA (cm^2/m^2)	NormalAbsolute	2.4	10		(Chan et al., 2005)
Outside surface convective coefficient $h_c=aV_z+b$	Bivariate Normal [a,b]~ N(μ,Σ)				(J. Chen, 2018a)
Weather	Random				
Wind Pressure Coefficient	Random				(YM Sun, 2014)

A total of 250 samples are drawn from published uncertainty distributions of certain model parameters using LHS sampling from SciPy library in Python and the EnergyPlus model

is populated with drawn samples. Following the creation of EnergyPlus files, the three approaches described in the beginning of this chapter are executed one after another.

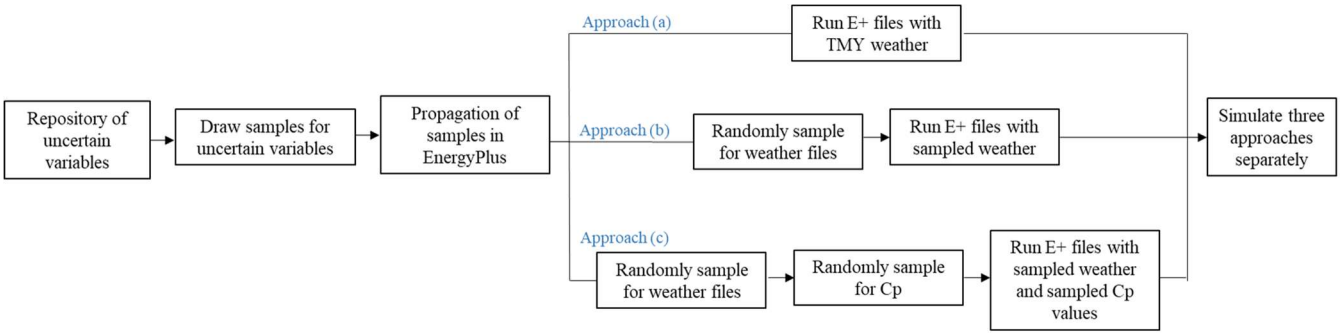

Figure 35 Simulation procedure for the cases

Once the runs are complete, data from EnergyPlus output files is read, collated and passed on to MATLAB for UA and SA using MARS.

4.3.1.1 Case I: Approach (a): Propagation of uncertainties with Airport 2018 weather

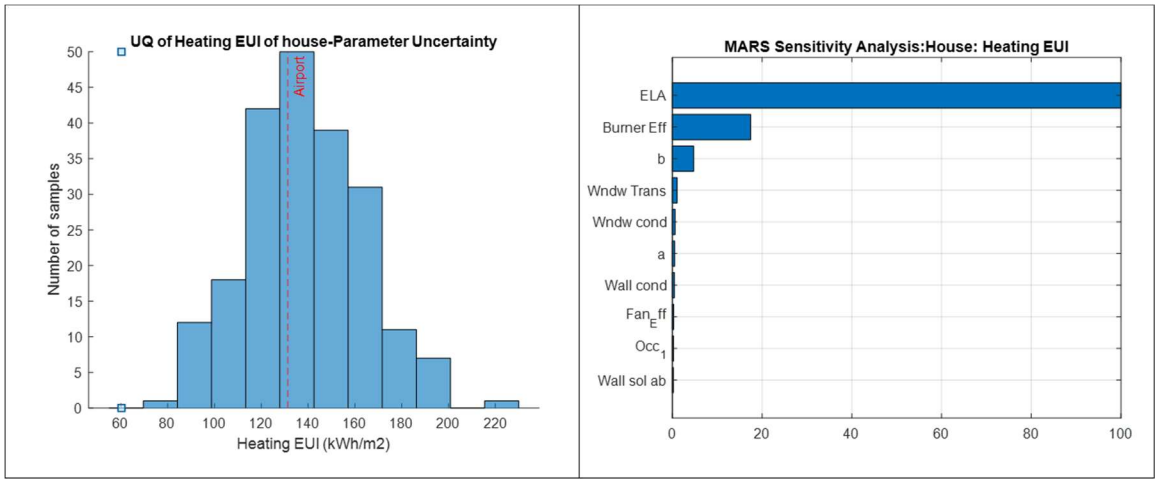

Figure 36 Case I, Approach (a): UQ and SA

With the customary set of parameter uncertainties in approach (a), the UA plot for heating EUI in the considered residential prototype building has a considerably wide spread around

the value obtained with a deterministic simulation using uniform weather based on recorded airport data. The deterministic value (shown as the red dotted line) is in fact close to the mean of the EUI distribution. This is not surprising as the deterministic inputs for the uncertain variables for this simulation are taken as the mean of the distributions as listed in Table 4. It should be noted that this is typically not the case in practice as modelers tend to show bias in their choice of input values. This gives the confidence that TMY3 weather derived from an open space like the nearby airport may be a reasonable choice for run of the mill simulations. They seem indeed low risk as the used weather represents the "mean" weather for the city of Chicago. The SA on this QoI shows that ELA outranks other sources of uncertainty by a large margin followed by the efficiency of the natural gas burner. This is followed by coefficients of surface convective heat transfer coefficients (h_c) and thermal properties of the window. With these results, a homeowner can decide to prioritize the weatherization of residential buildings that were built before year 1990 in Chicago, i.e. sealing cracks in the building by caulking and/or installing high efficiency heating equipment. However, these results are based on the presumption that it does not matter where the building is located in the city, therefore a proposed intervention such as 15% increase in burner efficiency would promise identical energy savings for a home anywhere in Chicago.

4.3.1.2 Case I: Approach (b): Propagation of uncertainties with spatially diverse weather

From the results of approach (b) one observes that although there is no significant difference in the resulting heating EUI distribution, the sensitivity to weather ranks in the

top three factors that affect heating EUI of the house in addition to ELA and burner efficiency as already seen in approach (a).

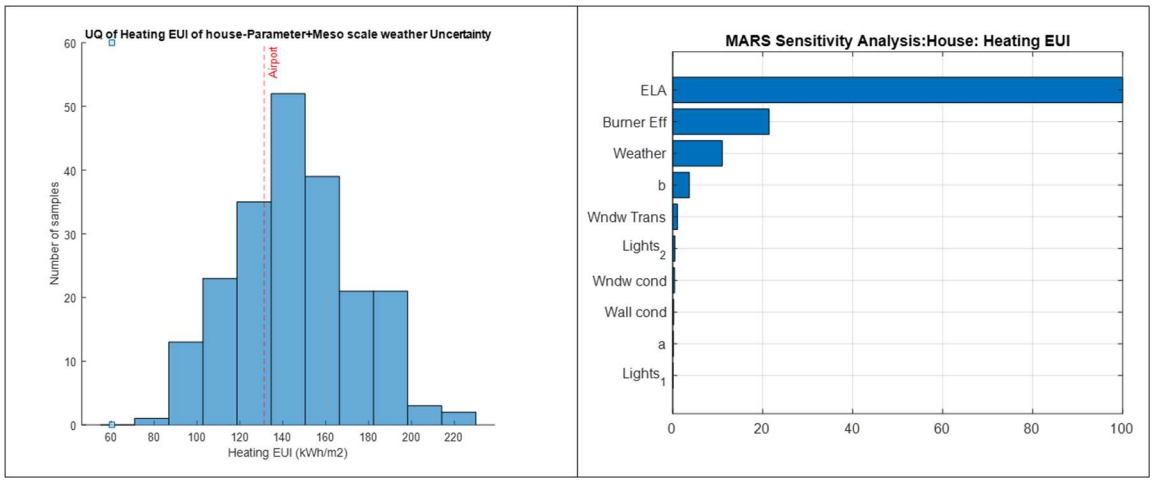

Figure 37 Case I, Approach (b): UQ and SA

This result implies that over the population of locations, in residential buildings of Chicago, there is some (exhibited by SA) but not a large influence of weather (based on the QoI distribution). This means that for prioritizing a technology for retrofit as a general measure, the use of uniform weather is justified. This does however not imply that the investment decision for an individual building is not impacted if based on meso diverse rather than on uniform weather. It is to be expected that a housing retrofit is slightly more effective in reducing heating energy consumption in a colder part of the city. This avenue can be pursued by comparing the QoI pre-retrofit and post retrofit. The comparison between the two outcomes should reveal how the meso scale weather changes the tails of the distribution. An investor is interested in risk avoidance so it is most telling to inspect the tail of the energy saving at the low end of the distribution which would be part of the future work. In fact, many such investment studies are currently carried out based on deterministic predictions. In that case the question is justified whether such deterministic studies need to

be diversified per locality. This is exactly the question that will be answered in Chapter 5. There, application case II deals with the same building and it is shown that observation of meso scale weather leads to maximum difference of approximately $146 in energy bills between the warmest and coldest part of the city. A tentative conclusion at this point is that although local does not constitute a major contributor to the uncertainty in our predictions, it tends to be an important factor in location specific decision making if we base those on deterministic predictions.

4.3.1.3 Case I: Approach (c): Propagation of uncertainties with spatially diverse weather and uncertainty in wind pressure coefficients

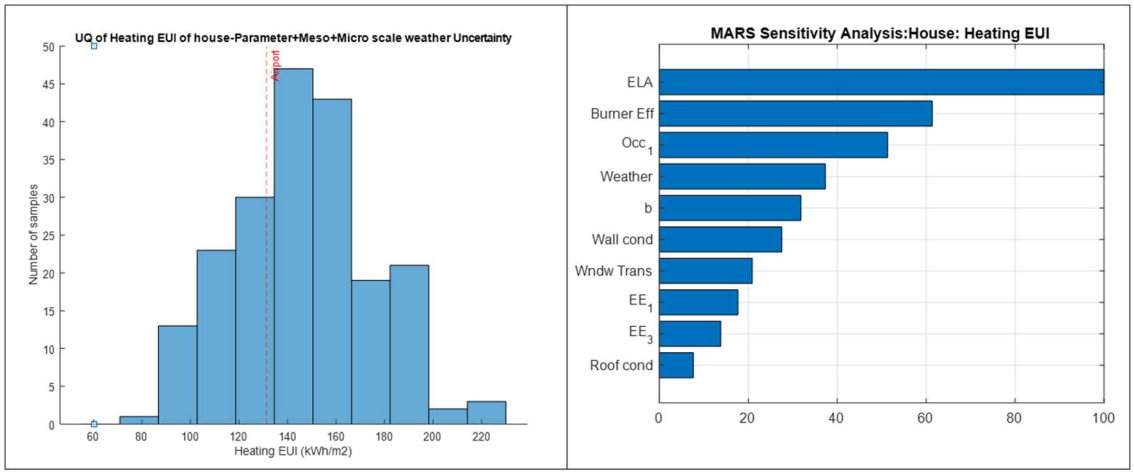

Figure 38 Case I, Approach (c), UQ and SA

Figure 38 illustrates that the distribution of heating EUI does not change much with introduction of uncertain wind pressure coefficients nor is the model sensitive to them. This result may be attributed to the fact that in a leaky building, the infiltration is so high that it is barely affected by changes in wind pressure coefficients. More so in winters when the difference between outdoor and indoor temperature is quite high, driving the thermally

induced infiltration through the cracks. The fact that ELA remains the dominant source of uncertainty is another confirmation of above finding.

4.3.2 Case II: Natural cooling potential; Hybrid cooling in an office building

This choice of this case is inspired by recent studies into the use of natural cooling in commercial buildings. The building model used in this example is a modified EnergyPlus example file EMSAirflowNetworkOpeningControlByHumidity,idf taken from the repository published by US DOE. It is a single-story office building divided into 3 interior conditioned zones and 1 unconditioned zone with details listed in Fig 8 and Table 2.

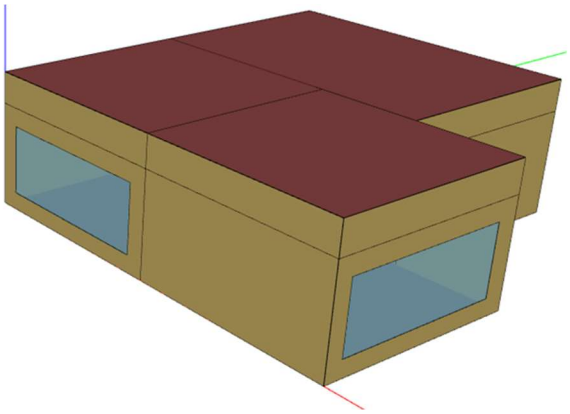

Building Property	Values
Floor area (m2)	130
#Stories	1
Exterior Wall Insulation	5
Ceiling Insulation	11
Floor Insulation	0
Windows U-factor	2.62 (W/m^2K), SHGC-0.71
Heating system	Gas Furnace
Heating COP	0.78
Cooling COP	3

Figure 39 Small office geometry and properties

The Energy Management System (EMS) is designed such that windows are opened when outdoor relative humidity is in the range 20%-75% and outdoor temperature is between 22°C-26°C (the zonal cooling set point is 26°C) to take advantage of the natural cooling potential of weather. Cooling EUI is obviously the QoI for this analysis since the aim is to observe the impact of spatially diverse weather on cooling when a building has automated controls for operative windows to benefit from natural cooling whenever appropriate.

Table 5 Applicable uncertainties for Case II, their distribution and references

Uncertain Variable	Distribution	σ/LB	μ/UB	UB	Reference
Cooling COP	NormalRelative	0.05			(YM Sun, 2014)
Fan Efficiency	NormalRelative	0.05			(YM Sun, 2014)
Burner Efficiency	NormalRelative	0.05			(YM Sun, 2014)
Wall Conduction	NormalRelative	0.05			(J. Chen, 2018a)
Wall Density	NormalRelative	0.1			(J. Chen, 2018a)
Wall Specific Heat	NormalRelative	0.1			(J. Chen, 2018a)
Wall Solar Absorptance	NormalRelative	0.1			(J. Chen, 2018a)
Roof Conductivity	NormalRelative	0.05			(J. Chen, 2018a)
Roof Density	NormalRelative	0.1			(J. Chen, 2018a)
Roof Specific Heat	NormalRelative	0.1			(J. Chen, 2018a)
Roof Solar Absorptance	NormalRelative	0.1			(J. Chen, 2018a)
Window Conduction	NormalRelative	0.1			(J. Chen, 2018a)
Window Transmittance	NormalRelative	0.05			(J. Chen, 2018a)
Electrical Equipment	UniformRelative	0.7	1.3		(J. Chen, 2018a)
Lights	UniformRelative	0.7	1.3		(J. Chen, 2018a)
Occupancy	UniformRelative	0.7	1.3		(J. Chen, 2018a)
Discharge Coefficient	TriangleAbsolute	0.4	0.65	0.75	(Parys, Breesch, Hens, & Saelens, 2012)
ELA	TriangleAbsolute	0.4	4.1	7.8	(Belleri et al., n.d.)
a	Bivariate Normal [a,b]~ N(μ,Σ)				(J. Chen, 2018a)
b					
Weather	Random				
Wind Pressure Coefficient	Random				(YM Sun, 2014)

4.3.2.1 Case II: Approach (a): Propagation of uncertainties with TMY

Figure 40 shows the distribution of space cooling EUI for the office building in consideration and it may be noticed that it is very wide in its range spanning from 14 kWh/m^2 to 22 kWh/m^2 with output from a deterministic simulation right near the mean with 16.71 kWh/m^2. This output is consistent with Case I where it was deduced that weather at the airport is indeed the mean representative of weather for the whole city.

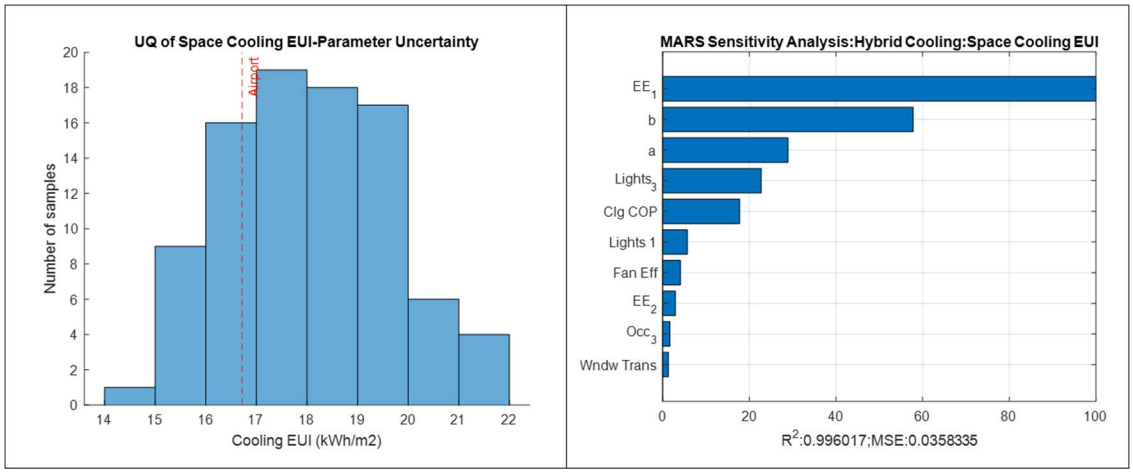

Figure 40 Case II, Approach (a), UQ and SA

The SA results shown on the right reflect that QOI is sensitive to heat emitted by appliances and occupant metabolic rate. Amongst building systems, cooling COP and fan efficiency affect the space cooling significantly. This approach, however, does not take into account whether these system specifications are affected by meso scale weather at the building location and assumes that the system sizing based on these results would be equally effective throughout the city.

4.3.2.2 Case II: Approach (b): Propagation of uncertainties with spatially diverse weather

A nuanced observation may be made from the UA plot for approach (b) shown in Figure 41, i.e., if the mean is considered 18 kWh/m^2 on the basis of plots in approach (a) and (b), there are more samples that fall below this mean with spatially diverse weather. This indicates that some areas of the city are colder or less humid than other areas resulting in more time when the windows are being operated resulting in lower cooling EUI. This fact

is also apparent from the SA plot where weather ranks in the top three variables that affect the cooling EUI of the office building.

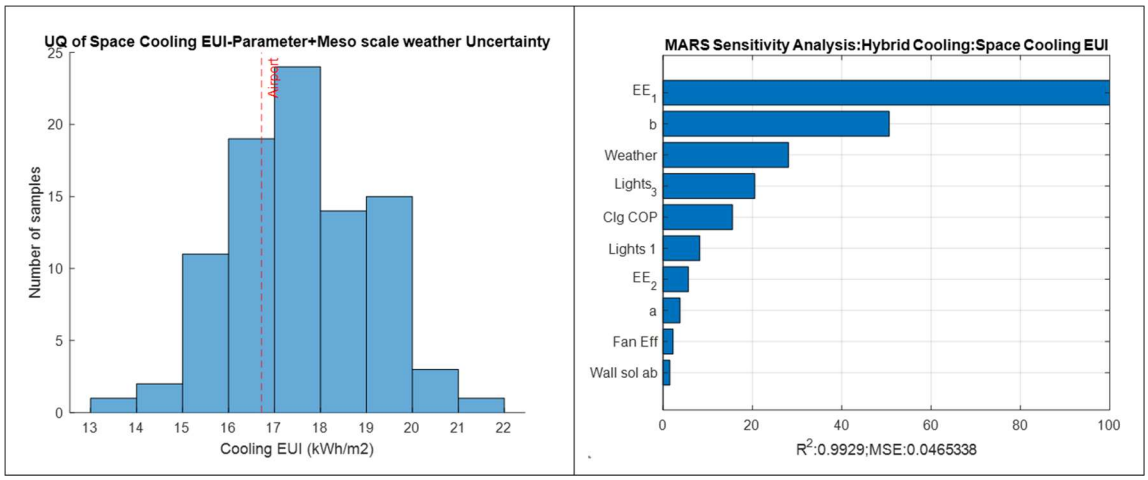

Figure 41 Case II, Approach (b), UQ and SA

Overall the conclusion is warranted that the meso scale weather leads to only a small upward shift in the distribution of EUI. This means that the natural cooling analysis without regard of local weather leads to a slight overestimation of the cooling potential for overall Chicago.

4.3.2.3 Case II: Approach (c): Propagation of uncertainties with spatially diverse weather and uncertain wind pressure coefficients

Figure 42 shows that there is no significant impact of introducing uncertain wind pressure coefficients on the distribution of Cooling EUI as well as on results of the SA. This can be expected since the reference building has large operable windows (10 m^2 each) and once they are opened, the impact of wind pressure on ventilation is minimal. This effect is well represented in the Airflow Network of EnergyPlus used in this study.

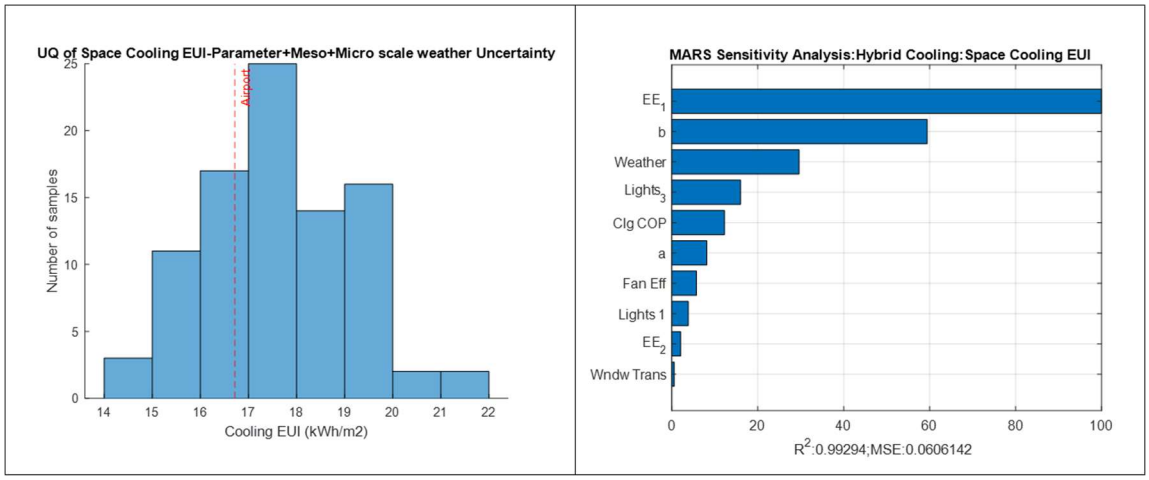

Figure 42 Case II, Approach (c), UQ and SA

It allows incoming wind to dissipate in adjoining zones causing low resistance to the incoming wind. This explains that extra force from higher wind in certain locals has relatively small influence.

4.3.3 Case III: Net Zero Building; Kendeda Building at Georgia Tech

This case is inspired by the increasing number of studies into the performance of ultra efficient buildings, many of which have to prove over their lifetime that strict efficiency targets defined at the outset are met. The Kendeda building at Georgia Tech (Atlanta) is a state of art educational and research facility which is constructed to qualify for the Living Building Challenge (LBC). One of the requirements of certification is that the building should generate 105% of its energy needs on-site using renewable energy systems without any combustion on the building site for a minimum of 12 months post occupancy. To fulfil this requirement, the envelope is designed to have very high efficiency in addition to architectural design choices, that must result in low energy footprint of the facility. The entire roof of the building is used for installation of PV systems that supply the energy for building operations.

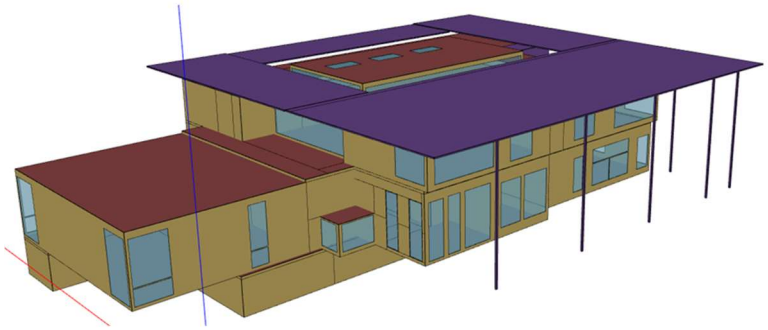

Building Property	Values
Floor area (m2)	2945
#Stories	2
Exterior Wall Insulation	20
Ceiling Insulation	31
Floor Insulation	25
Windows U-factor	0.701 (W/m^2K), SHGC-0.211
Heating system	Gas Furnace
Boiler η (Radiative heating)	0.89
Cooling COP	4.5
PV Efficiency	19%

Figure 43 Kendeda building geometry and properties

The QoI for this study is the percentage of annual energy consumption supplied by the on-site photovoltaic system and the model has been modified to replace district chilled and hot water (steam) supply by a chiller and boiler, the efficiency of which is modelled based on expert judgment.

Since the MTOT weather generator was used only to create weather for Chicago, it cannot be used for this case. For this reason, the spatially diverse weather for Atlanta is sourced from IBM's The Weather Channel. The coverage is sparse because only data from only 15 weather stations across Atlanta could be acquired since many other stations and sources had missing hourly data in their databases.

The yield from photovoltaic systems depends heavily on factors such as temperature, variation in solar insolation, accumulation of dirt and cloud cover. The range for this source of uncertainty of the panel efficiency is determined after consultation with industry experts.

Table 6 Applicable uncertainties for Case III, their distribution and references

Uncertain Variable	Distribution	σ/LB	μ/UB	UB	Reference
Fan Efficiency	NormalRelative	0.05			(YM Sun, 2014)
Wall Conduction	NormalRelative	0.05			(J. Chen, 2018a)
Wall Density	NormalRelative	0.1			(J. Chen, 2018a)
Wall Specific Heat	NormalRelative	0.1			(J. Chen, 2018a)
Wall Solar Absorptance	NormalRelative	0.1			(J. Chen, 2018a)
Roof Conductivity	NormalRelative	0.05	1.3		(J. Chen, 2018a)
Roof Density	NormalRelative	0.1	1.3		(J. Chen, 2018a)
Roof Specific Heat	NormalRelative	0.1	1.3		(J. Chen, 2018a)
Roof Solar Absorptance	NormalRelative	0.1	1.3		(J. Chen, 2018a)
Window Conduction	NormalRelative	0.1	1.3		(J. Chen, 2018a)
Window Transmittance	NormalRelative	0.05	0.4	0.35	(J. Chen, 2018a)
Electrical Equipment	UniformRelative	0.7	1.3		(J. Chen, 2018a)
Lights	UniformRelative	0.7	1.3		(J. Chen, 2018a)
Occupancy	UniformRelative	0.7	1.3		(J. Chen, 2018a)
Chiller COP	NormalRelative	0.05			(YM Sun, 2014)
PV Efficiency	TriangleAbsolute	0.18	0.2	0.2	Expert opinion
Boiler Efficiency	NormalRelative	0.05			(YM Sun, 2014)
a	Bivariate Normal [a,b]~ N(μ,Σ)				(J. Chen, 2018a)
b					
Weather	Random				
Wind Pressure Coefficient	Random				(YM Sun, 2014)

4.3.3.1 Case III: Approach (a): Propagation of uncertainties with TMY

Figure 44 shows the results of the UA, i.e. distribution for the percentage of energy supplied by the on-site PV plant. It should be noted that the PV system is not supposed to cover all of the energy consumption. The building uses an ingenious way to cover its winter heating need by heat-pumps that use the chilled water loop of the campus district cooling system. The amount of energy saved this way is irrelevant for our investigation and hence not accounted for.

The target of this case investigation is to find the percentage of coverage that the PV system can supply. With our modeling assumptions and embedded uncertainties it becomes

obvious that the installed system is by itself not sufficient to power the building for its annual energy requirement. This is indeed expected based on the availability of the other indirect energy source explained above.

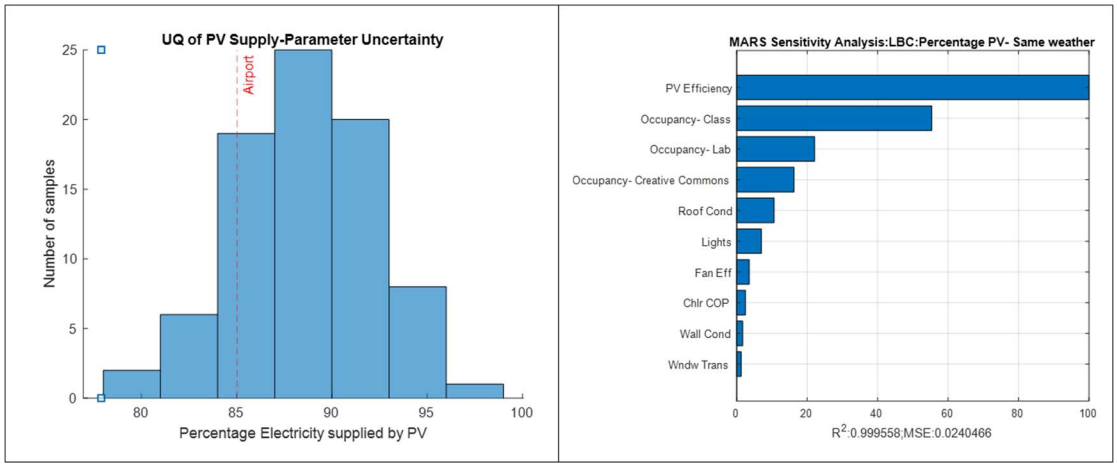

Figure 44 Case III, Approach (a), UQ and SA

The deterministic simulation result showing that PV would be able to fulfill 85% of the building energy demand, is again located near the mean of the distribution, albeit on the lower end representing a somewhat pessimistic outcome. With these results, a risk averse building energy modeler would look for ways to reduce the likelihood of not being able to meet the energy requirement of certification. A sensitivity analysis on the chosen QoI confirms that the efficiency of the PV system is the most impactful variable. Other than the renewable energy system, occupancy emerges as the predominant uncertain variable. In an educational facility, it is difficult to estimate the occupancy of students through the day during an academic session. This leads to a high level of uncertainty in the schedules of occupancy which influences lighting and appliance use. This is indeed reflected in the high ranking of occupancies in different zones in the SA. Since this study does not account for change in yield of PV due to temperature, and insolation across Atlanta is assumed

constant, only the variability in heating and cooling demand of the building is the reason for the QoI variability.

4.3.3.2 Case III: Approach (b): Propagation of uncertainties with spatially diverse weather

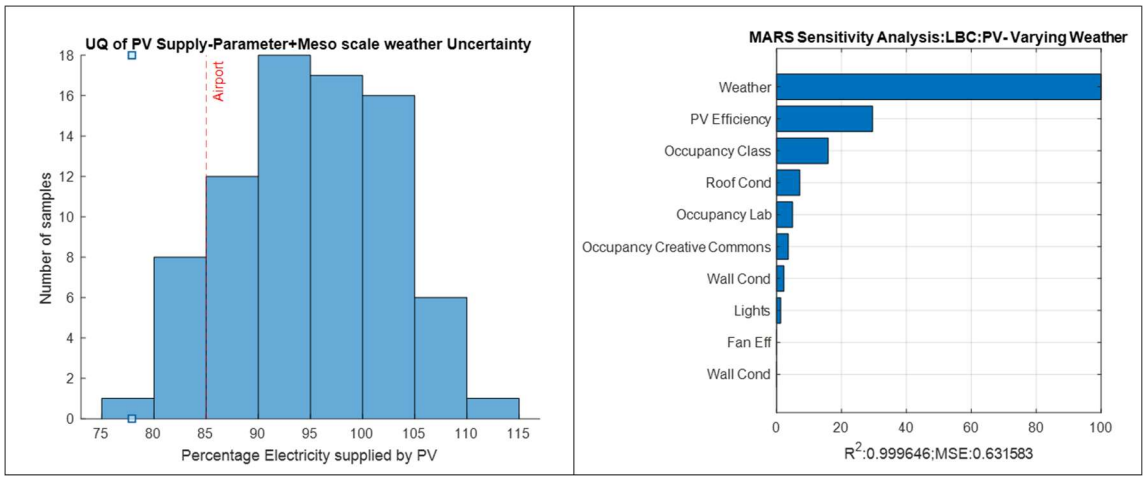

Figure 45 Case III, Approach (b), UQ and SA

Given the fact that the actual Kendeda building is in one specific location, we conduct the thought experiment that the assessment is performed for the building without specifying a location except that it is in Atlanta. Under that assumption meso variability can be viewed as an uncertainty similar to the previous two cases. Addition of local weather as an uncertainty increases the tail ends of the QoI distribution considerably, suggesting that location-related uncertainty, resulting from meso weather variability across the city, adds significantly to the uncertainty in air conditioning load. Strikingly, weather ranks even higher than the PV efficiency in the sensitivity of our QoI. This conclusion could however be strongly influenced by the fact that the weather information is spatially sparse which opens the possibility of a strong bias in the weather. This indicates the importance of high-

fidelity weather data for projects that stand the risk of failing compliance with imposed energy usage thresholds.

4.3.3.3 Case III: Approach (c): Propagation of uncertainties with spatially diverse weather and uncertain wind pressure coefficients

Figure 46 shows that the distribution of QOI when wind pressure coefficients are introduced remains virtually unchanged.

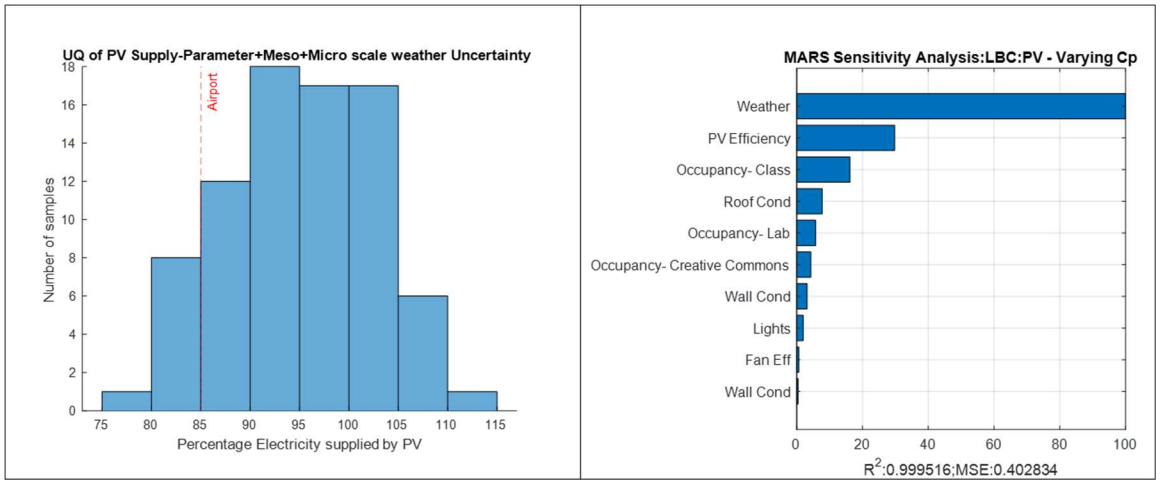

Figure 46 Case III, Approach (c), UQ and SA

The building envelope in this case study is already very tight and has a high resistance value to prevent any unwanted infiltration and transmission thereby reducing the role of surface convective heat coefficient h_c and wind pressure coefficients C_p in heat transfer across it. Hence the QoI distribution as well as the SA plot shows little difference with case (b).

4.4 Summary of the findings in this chapter

This chapter tests the relevance of using meso scale weather information as compared to city wide reference weather in three common applications of single building performance assessments relying on building simulation. To start from a common basis for the comparison we use recorded 2018 weather for the airport from National Oceanic and Atmospheric Administration) as the city-wide uniform weather. It can be regarded as the "low fidelity" weather data in our investigation. We then apply our statistical model to generate the meso scale local weather for 2018 (recall that the statistical model was developed based on 2018 recording at dispersed weather stations), leading de facto to "high fidelity" weather data. To arrive at an objective determination of the effect of using high fidelity versus low fidelity weather data, the effect of using one variant versus the other variant is ranked against the effect of other sources of variability in a simulation. These other sources are directly linked to sources of uncertainty, i.e. imprecise physical knowledge of model parameters and partly unknown processes (scenarios) in the building. For each considered case we inspect the resulting distribution of a chosen QoI as well as the ranking of all contributors to variability. This leads to some general conclusions:

- By comparing the results obtained with the low and high fidelity weather, it is found that generally there is an effect that is not dominant for buildings that have model parameters that exhibit rather large uncertainty such as in this case ELA, because the leakiness of the older buildings studied is typically large and has a large variability across the housing stock.. In such cases, although high fidelity weather impacts the QoI distribution, it does not alter its tail ends which means that a large influence in a risk-based decision is unlikely. To arrive at a definitive conclusion

the analysis should be repeated with different levels of uncertainty. In the ultimate case that we rule out any uncertainty (i.e. a deterministic simulation) we are able to isolate the role of meso weather variability in different decision settings. This is the subject of the next chapter.

It can be expected that the translation of meso weather to micro climate conditions could amplify the effect of the weather variability. This is especially true for the role of wind speed and hence wind pressure which is the major factor in the micro climate conditions. Its possible effect is therefore tested separately leading to the following observations:

- In the first two cases located in Chicago, the windy city, local wind is indeed found to amplify the effect of the high fidelity weather. It impacts winter infiltration in the house and promotes natural ventilation for summer cooling in the office building. In general it can be said that as wind varies with locality it is not surprising that the influence of meso scale weather becomes more relevant when wind driven phenomena are studied, i.e. infiltration and ventilation. Natural cooling which is indirectly wind driven, on the other hand is much less sensitive because opening large windows achieves the necessary cooling, in whatever wind condition. In the last case (Kendeda), wind does not have significant impact (a) because Atlanta has on average a benign wind conditions and (b) because the building is rather airtight. Note that this case ignores the impact of weather on PV yield. Future work could take that into account, even though there are enough studies that have shown that wind and air temperature have only a secondary effect on the efficiency of a solar panel.

- Even for the building as thermally insulated as Kendeda, variation in weather stretches the tail ends of the UA distribution for percentage of energy supplied by on-site PV systems which is supported by SA highlighting that weather impacts this QoI. Since only air conditioning load is dependent on weather, it may be gathered that there are locations with high contrast in weather that induces these long tails., which is significant as even a small increase in energy supplied by PV may make the project meet its strict energy goals.

This Chapter gives meaningful insights for three very specific cases which lead to some general findings. Some caution should be exercised in generalizing them to the full extent of building simulation practice without further examination of different building types, QoI with shorter intervals, different cities and multiple levels of uncertainty and or modeler's bias. If the risks of not meeting a performance target are high, especially if the QoI is a critical or extreme outcome, it seems advisable to invest extra effort in sourcing and using high fidelity weather data. For a QoI with long interval aggregation (such as yearly energy consumption) this advice is not sustained by the results of this chapter.

CHAPTER 5. IMPACT OF LOCAL WEATHER IN URBAN BUILDING SIMULATION STUDIES

In the previous chapter the outcomes of a building simulation were investigated for a specific building in an unspecified location in the city. In this Chapter, three case studies are discussed that use performance measures of buildings at specific locations, or more precisely in specific grid cells across a city, with the aim to make location specific decisions. The case studies compare hypothetical decision scenarios for stakeholders such as urban planners and policy makers when these building simulations are done with local weather data versus when they use uniform weather data from a nearby location such as the airport. The key question is then whether the use of local weather will lead to different location specific measures compared to a city wide measure based on uniform weather data. The ultimate objective is to test if it is worth the additional effort to create and use high fidelity weather data for urban decision scenarios. This chapter tests this for three typical urban decision scenarios, encountered in recent application studies.

5.1 Typical Applications of USim models

Urban Building Simulation study (referred to as USim in this document) is the growing field where building simulation is performed on a "shadow" version of the true urban scene. The composition and setting of the buildings constitute a synthetic, virtual city or neighbourhood depending on scale. The USim model is developed through aggregation of individual building models where some form of physical interaction between buildings and surroundings is also added (Quan, Li, Augenbroe, Brown, & Yang, 2015a) . The thus

composed USim model can serve to study large-scale building construction and energy interventions as part of social, economic and technological policymaking. A few examples of these scenarios include getting a qualitative insight in areas of city where dwellers are most vulnerable to overheating in built spaces, finding neighbourhoods that are prone to suffer from energy inequality/poverty, or determine which neighbourhoods have the highest potential to benefit from distributed energy generation or have the highest potential to reduce GHG emissions (Shimoda et al., 2010)(Quan et al., 2015a). The simulation outcomes inform decision making at different levels of aggregation, for instance by looking at city scale outcomes as determined by the "attributes" for Multi Attribute Value Model that policymakers use to frame policy interventions. Multi Attribute Decision Models (MADM) are decision analysis models based on multi attribute utility theory and are a subset of Multi Criteria Decision Making (MCDM). For example, (Jones, Hope, & Hughes, 1990) demonstrates the use of MCDM in drawing up the energy policy for UK with multiple attributes considered by the stakeholders.

Attribute	Indicator	Best	Worst	Rating
Security of supply	Hrs of supply disruption/person/yr	0	50	100
Competitiveness	Ratio UK:world fuel prices in 2010	0.33	3	90
Employment	'000 jobs created by 2010 due to policy	500	−1500	70
Nuclear waste	% change in activity not disposed by 2010	−20	20	60
Cost	£bn total cost of supply/yr	25	100	60
Greenhouse effect	% change in CO_2 emitted by 2010	−20	20	50
Low energy prices	% change in energy prices by 2010	−50	50	50
Balance	% supplied from largest fuel in 2010	20	90	40
Conservation	% change in demand by 2010	−75	50	40
Diversity	Number of fuels supplying >10% in 2010	5	1	40
Acid rain	% change in SO_2 emitted by 2010	−70	20	40
Radioactivity	% change in dose per person by 2010	−20	10	40
Decentralization	Number of energy suppliers in 2010	50	4	30
Capital requirement	Max. energy investment (% of total inv.)	8	20	30

Figure 47 Attributes, their domain range and stakeholder rankings (Jones et al., 1990)

Figure 47 shows the shortlisted attributes from above study that decide the preference for the type of energy generation technologies in UK. According to the preference of

stakeholders, rankings or importance is attached to each attribute which acts as a weight in final computation of aggregated numerical measures that helps policymakers arrive to a decision.

Generally speaking, every decision scenario depends on the preferences of stakeholders in selecting the attributes that they deem to be important to arrive to a decision in a well-defined scenario. There may be a case where stakeholders from different organizations and backgrounds have conflicting views of the importance of attributes affecting their weightage. In above example, a stakeholder from the social policy group may view affordability as the highest-ranking attribute whereas a representative from hazards and safety group may consider radioactivity as the attribute with highest weightage. This conflict is avoided by having limited number of members on board and resolving conflicts by dialogue. Finally, the composition of decision-making panel decides the attributes, their weightages and final numerical measure that informs their decision and is unique for every scenario. The numerical measures may be calculated by using a number of algorithms as described in the overview by (Pohekar & Ramachandran, 2004). For the hypothetical decision scenarios in this thesis, simplistic numerical measures are formulated and the weighted sum method (WSM) is used to calculate them.

5.2 Urban Building Simulation: Status Quo

It is important to acknowledge at the outset that USim is a domain which is heavily dependent on the quality and resolution of data that is used for models of neighbourhoods or entire cities. These models, though grounded in real data, still present only a virtual test bed that is deemed good enough to answer pertinent “what if” questions without claiming

to be a digital twin mirroring the on-ground reality. In fact, how to create a good enough synthetic representation for a given inquiry is an unresolved question that is a core challenge of the emerging USim discipline. This thesis adds one additional dimension to the synthetic composition in the sense that it investigates the role of local weather at the granularity of grid cells.

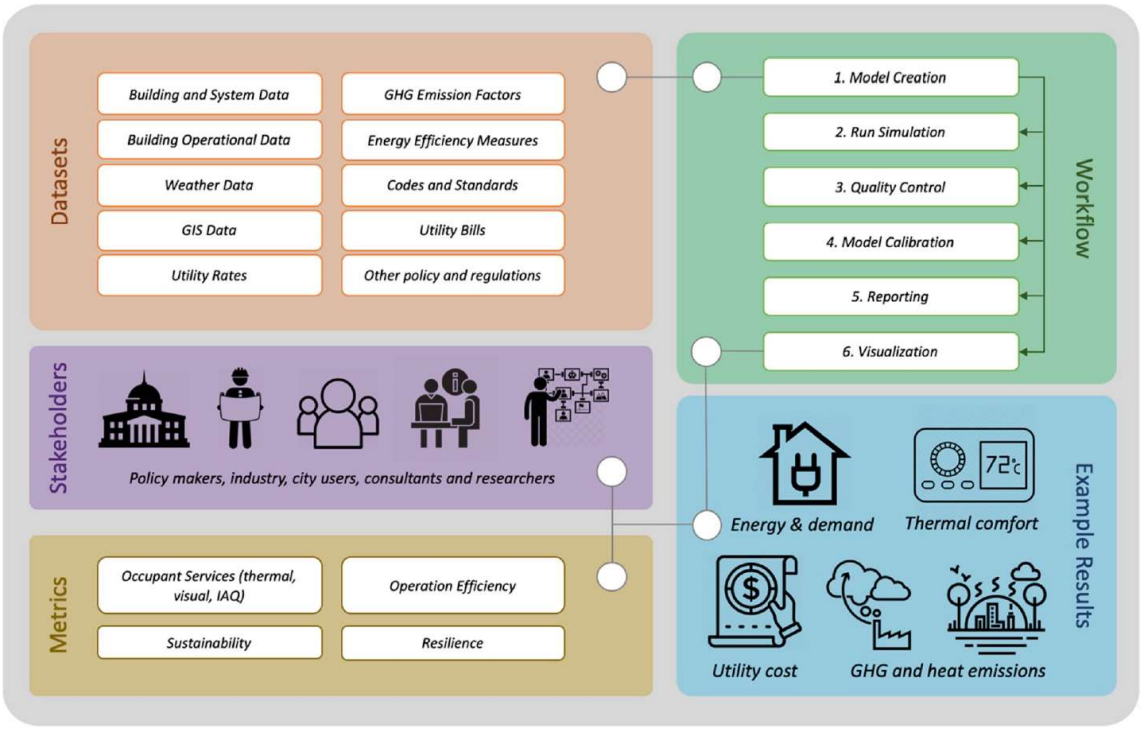

Figure 48 Overview of Urban Building Energy Models (Hong, Chen, Luo, Luo, & Lee, 2020)

There are currently two approaches to build urban models in the thermal/energy domain;

i. **Top Down approach**: Resulting models are generally referred to as black box models, derived from data that are collected by the utilities, census agencies and urban planning agencies. The data collected by these organizations is curated by statistical methods of clustering and regression to generate building types and their

behaviours in different parts of the city. For example, with datasets of housing characteristics and actual natural gas consumption, a regression model may be created which can predict energy consumption based on housing characteristics (Bednar, Reames, & Keoleian, 2017). This approach is best suited to understand the properties of existing building stock; however, it cannot be used to predict the outcomes if one wishes to see the impact of policy interventions or adaptations to changes in building regulations.

ii. **Bottom up approach:** Resulting models are physics-based and generally referred to as white box models. Inputs from datasets like AHS, RECS and GIS information help in the creation of housing stocks of a city which is categorized in vintage (year built) and types (e.g., single family detached, multi family etc.) of buildings. Using well-established categorization by building type, an archetype is chosen for every type. Building simulation models are created for each archetype. They can be detailed models created in high fidelity simulation tools such as Energy Plus. Recent examples of this approach are UMI (Reinhart et al., n.d.) and CityBES (Y. Chen, Hong, & Piette, 2017). Other studies use reduced order models such as EPC (Quan, Li, Augenbroe, Brown, & Yang, 2015b). Every white box USim model requires detailed inputs at the building level such as occupant behaviour, window to wall ratio, infiltration, equipment and lighting schedules etc some of which are nearly impossible to determine based on standard information or calibrate even if high resolution energy consumption data is available from the utility. The lack of sufficient knowledge of this detailed information adds one additional layer to the artificiality to USim models. Not surprisingly, therefore, any USim model is in

some sense synthetic and can only be considered a reflection of city's housing stock that should at least be able to mimic the basic behavioural responses and trends.

5.3 Use and scale of local weather in USim studies

Under ideal conditions, weather that applies to the building locations should be used in USim models. However, collecting site data can be both expensive as well as time consuming and carries the risk that weather data recorded for a limited period may be an outlier year. (Oke, 2006) identified very early on, the need for weather data for relatively homogenous regions of city for application in urban design, building energy consumption, air quality and health. He published this study to guide meteorologists for setting up representative weather stations in urban sites for complete coverage in variation of weather across a city.

The role of Urban Heat Island (UHI) in the variability of building simulation outcomes is well established, i.e. influencing energy use, peak loads and thermal comfort (Chung et al., n.d.; Mavrogianni DipArch et al., n.d.). MIT's Urban weather generator (UWG) quantizes UHI for an urban area relative to a rural weather station based on a set of 42 parameterized inputs and can be used to generate weather files for use in USim. However, besides having the shortcoming of having a large number of input parameters, it only computes variation in temperature and humidity and misses on the wind aspect of urban weather.

Another popular method of obtaining local weather for USim is downscaling Weather Research and Forecasting (WRF) weather to smaller resolution. Recent advances in this domain are trying to couple WRF model with Energy Plus models for large scale urban simulation (Jain, Luo, Sever, Hong, & Catlett, 2020), however, computational time to

generate WRF data is still a big hurdle in its widespread adoption. Lastly, fast Computational Fluid Dynamics (CFD) techniques known as CityFFD are being used to couple CFD with urban simulation models (Katal, Mortezazadeh, & Wang, 2019).

For the case studies in this chapter, meso-scale weather created from the "in-house" MTOT statistical model is used as the high-fidelity weather data. As explained, the objective is to inspect the importance of using local weather in certain USim application cases. The first step towards this is the creation of a synthetic version of the Chicago building stock as the core of the USim model. Our approach follows the simplified approach from earlier cited examples where the synthetic city model is a straightforward aggregation over individual buildings.

5.4 Creating the virtual city of Chicago- Datasets and Building stock

The starting point of developing a mirror city of Chicago is identifying building prototypes following the workflow similar to National Energy Modeling System (NEMS) which is used by the Energy Information Administration (EIA) for aggregated energy systems in their macroeconomic model. Building prototypes that are generated by Pacific Northwest National Laboratory (PNNL) on behalf of US Department of Energy (DOE), are borrowed as generalizable dwelling geometry information.

Building modelling parameters are added to the PNNL prototype models. At the higher level, buildings are categorized in vintages that relate certain building parameters to the building footprint data obtained from City of Chicago data-portal, ASHRAE guidelines and Residential Energy Consumption Survey (RECS). These parameters include thermal properties for building fabric, schedules, plug loads and air-conditioning systems.

RECS provide a comprehensive dataset for the type of materials and insulation properties being used in the US for residential construction from the year 1979 to date. The data is aggregated based on four regions of the US, namely, Northeast, Midwest, South and West. From this data, assumptions for Chicago are taken from Midwest part of report.

The city of Chicago data-portal allows public access to GIS dataset for building footprints of the city with access to the attributes shown in Table 7.

Table 7 Attributes from Building footprint data

Attributes	Explanation
Building ID	Internal Use for City planning
Building square footage	Building footprint
Year built	Year of construction
Building status	Active/Proposed/Demolished
Number of Units	Number of residential units in the building
Stories	Number of stories in the building
Pre Dir	Orientation of house

Based on data obtained from above sources, the workflow shown in Figure 49 is followed for creating building simulation models that reflect the current building stock of the city.

This chapter only considers residential buildings in Chicago due to missing information about commercial buildings in the GIS data. The three application cases are selected in decision scenarios that are directly relevant to communities of residential buildings.

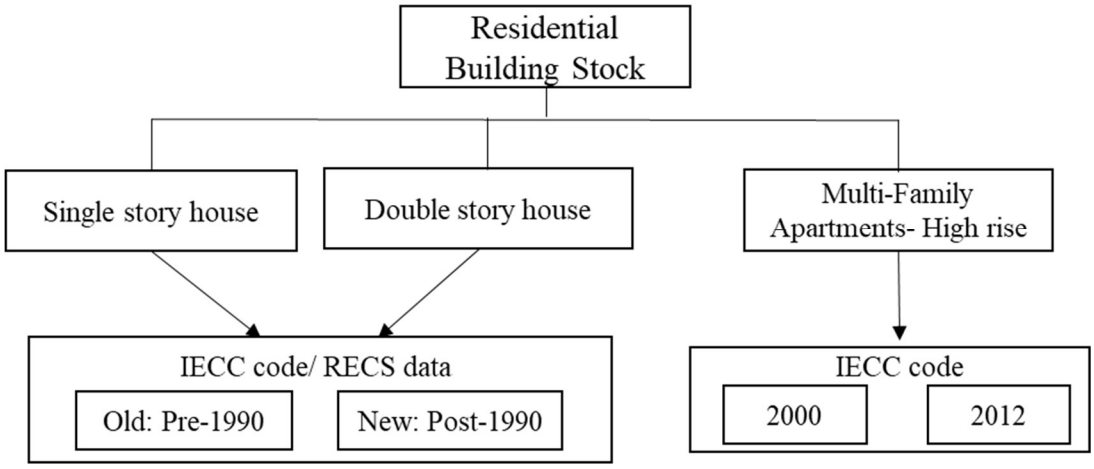

Figure 49 Building prototypes in Chicago for Urban Simulation

5.4.1 Application case I- Heat Vulnerability

The subject of heat vulnerability due to overheating in buildings is gaining steady momentum spurred on by increasing ambient temperatures as a result of climate change. Most often, heat vulnerability indices (HVI) are proposed that provide a qualitative assessment of areas of the city where significant population is at the risk of health impacts due to high temperatures. As discussed in section 5.1, these vulnerability indices are a function of attributes that stakeholders deem important for designing policy interventions. These attributes can include social indicators such as income, race, education, health status etc or demographic indicators such as age and sex ratio to name a few and reflect the three aspects of sensitivity, exposure and adaptive capacity of population in general for calculation of HVI's.

The vulnerability is heightened when it is a compound event wherein heat waves are accompanied by a power outage in the same period such as those seen in New York during the 2003 heat wave (Anderson & Bell, 2012).

Sensitivity	Exposure	Adaptive Capacity
Diabetes Prevalence	Land Surface Temperature	Living Below Poverty Line
Living Alone		Less than High School Education
Over Age 65		No AC Access
Over Age 65 and Living Alone		No Full AC Access
NonWhite		

Figure 50 Computation of typical HVI's (Mallen, 2019)

During a heat wave, power systems operations are impacted due to high peak cooling loads which when sustained over a long duration, increase the stress on distribution systems as high temperatures impact electrical load bearing capacity of power lines making the power grids more susceptible to failure (Ke, Wu, Rice, Kintner-Meyer, & Lu, 2016).

For this study, HVI has been computed to assess the areas of Chicago where an elderly population (age>65 years) is vulnerable to high temperatures in a concurrent event of power loss due to grid failure with a heatwave. Therefore, two attributes that form the numerical measure of HVI are age demographics and mean exposure temperature during heat wave in a power outage situation.

To inspect the use of spatially diverse weather in this case study, a contrast is drawn between the heat impact shown as heat index across the city of Chicago during the heat wave between June 16th to June 18th 2018 (US Department of Commerce, n.d.).

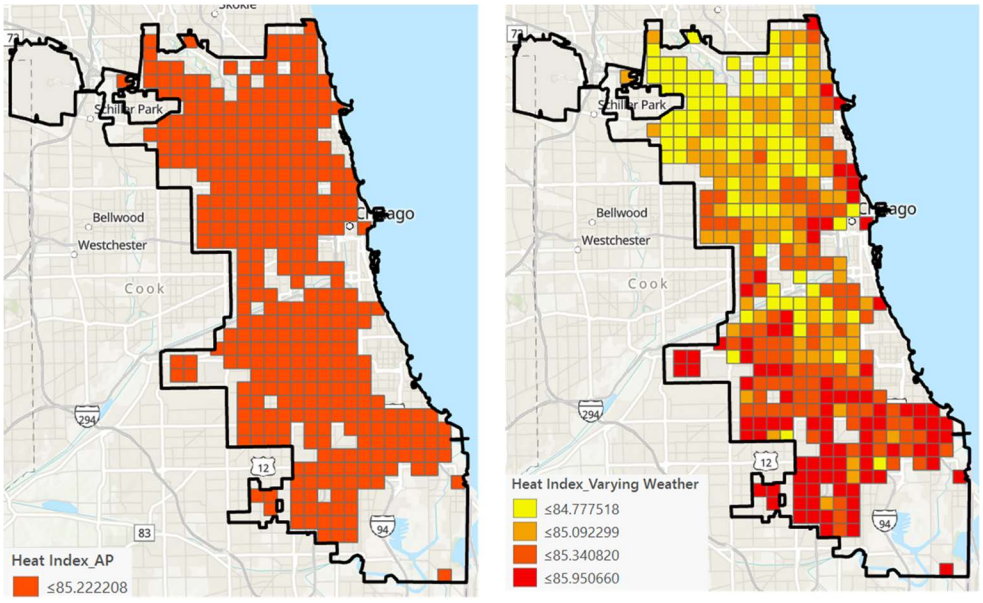

(a) (b)

Figure 51 Heat Index comparison during June heatwave between (a) Airport and (b) Meso-scale weather

Heat Index (Rothfusz, Worth, National, & 1990, n.d.) is used by National Weather Service to issue a warning in the event of a heat wave and is calculated as follows;

$$\text{Heat Index} = -42.38 + 2.049T + 10.14RH - (0.2248T * RH) - 0.006838T^2 - 0.05482RH^2 + (0.001229T^2 * RH) + (0.0008528T * RH^2) - (0.00000199T^2 * RH^2)$$

Where, T = Ambient temperature in °F

RH = Relative Humidity

Figure 51 illustrates the difference of up to 2°F in heat index based on airport weather (uniform value across the city) and spatially diverse weather for Chicago, giving a preliminary indication of the importance of using meso-scale weather for such studies.

For this thesis, the exposure is computed with the mean indoor temperature inside each prototype (see Figure 52) for each grid cell from June 16th to June 18th which was the worst heatwave in Chicago for 2018. It is assumed that the mechanical cooling is unavailable due to loss of power and residents operate the window when indoor temperature is higher than outdoor temperature.

The "exposure temperature" (ET) for each grid cell is an overlay of average indoor temperature during the heatwave with building footprint data and calculated as follows;

$$ET_{grid\ i} = \sum_{Prototype\ 1}^{6} T_{mean-prototype} * \frac{Total\ square\ footage\ of\ prototype}{Total\ built\ up\ area\ in\ the\ grid}$$

The ET thus calculated depends on the weather for the grid cell and represents the building stock in the grid cell.

	A	C	E	G	I
1	Grid No	SF_Old_Mean	SF_New_Mean	SF2_Old_Mean	SF2_New_Mean
2	183	27.46163227	27.19353742	28.9649401	28.90854975
3	272	27.41442308	27.14452579	28.84636436	28.79036231
4	115	27.39542354	27.12546803	28.89702739	28.84261864
5	396	26.75139515	26.48788927	28.72397723	28.66841857
6	153	27.44724464	27.17897453	28.90342814	28.84814303
7	248	27.51817925	27.24805561	28.96150661	28.90528893

Temperature in prototypes w/o AC for each grid

	A	B	C	D	E
1	Grid No	SF_Old	SF_New	SF2_Old	SF2_New
2	183	0.17755	0.02244	0.78246	0.01755
3	272	0.16009	0.01511	0.32537	0.06902
4	115	0.29724	0.04153	0.54612	0.03539
5	396	0.07446	0.21997	0.47336	0.23221
6	153	0.25938	0.02032	0.70028	0.02002
7	248	0.18395	0.12881	0.67244	0.0148

Percentage of built area of each prototype in a grid

Figure 52 Calculation of ET for each grid cell

This process is repeated with average indoor temperatures calculated from recorded weather from the airport and mapped over the whole city for the representative building stock in each grid cell.

The community data for elderly population in Chicago is obtained from EnviroAtlas tool of US Environmental Protection Agency (EPA) as percentage of senior citizens in every

census tract of the city. Each grid cell is then assigned this attribute depending on the census tract that covers the maximum area in that grid cell.

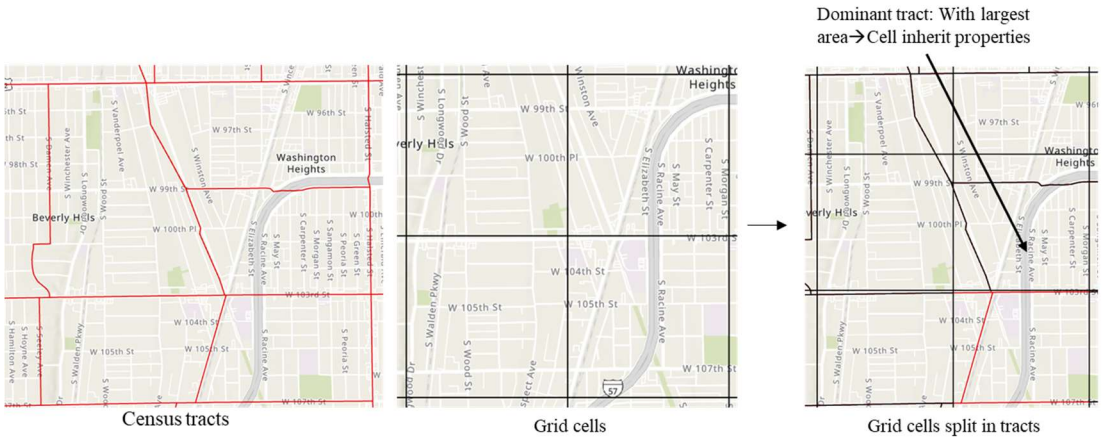

Figure 53 Assignment of demographic properties to grid cells

Figure 54 shows the methodology to converge the datasets of demographics and ET for calculation of HVI, where each dataset is divided in four quartiles and a category of 1 through 4 is assigned to each quartile, where 1 represents Q1 and 4 represents Q4. This is done because these datasets have different units and any measure involving linear addition may not be intuitively insightful for a policy maker. For example, ET of 28°C represents Q1 whereas ET of 31°C represents Q4. HVI for each grid cell is calculated as follows;

HVI=Percentile categorization (ET)+ Percentile categorization (Percentage senior citizens)

In this way, if a grid cell has large population of senior citizens and high ET, they will both fall in Q4 with HVI, a sum of 8 (the highest value).

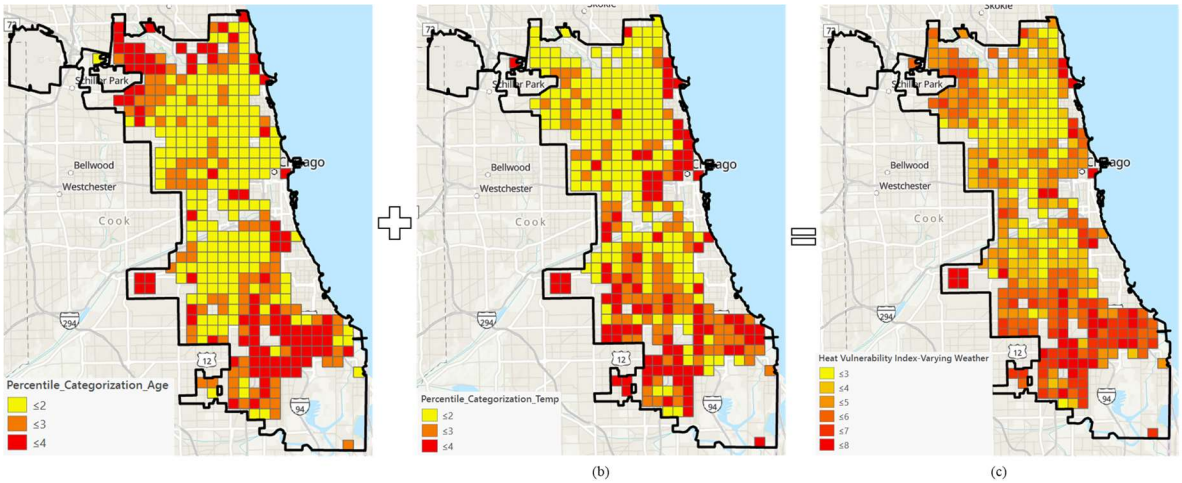

Figure 54 Percentile calculation and HVI (a) Percentile categorization of Age (b) Percentile categorization of exposure temperature (c) HVI with meso weather

The Quartile limits calculated based on ET calculated by meso-scale weather is also applied to airport weather data to preserve the homogeneity of categorization.

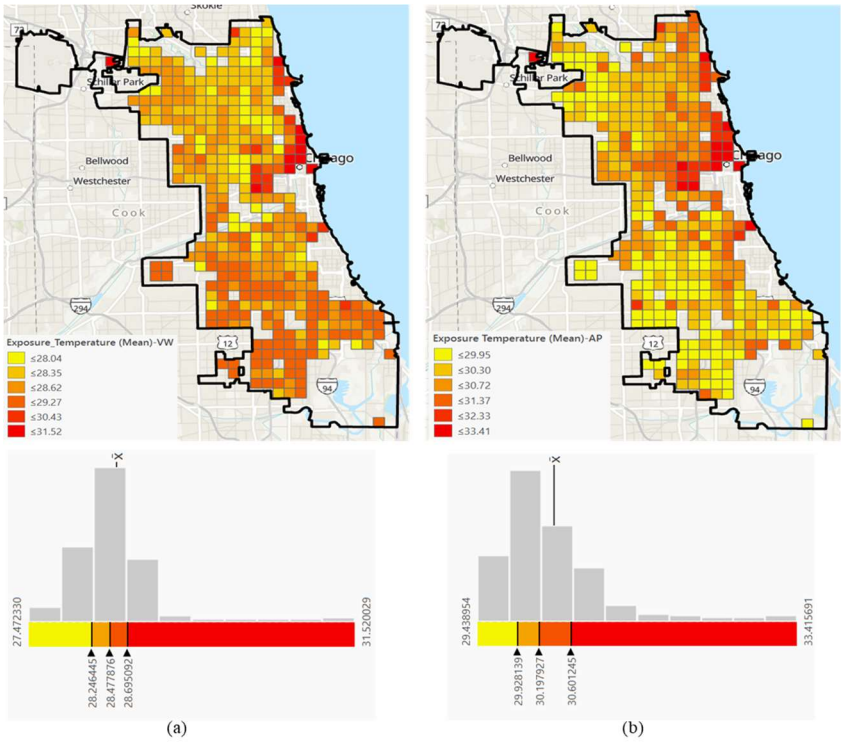

Figure 55 ET with (a) Meso-scale weather (b) Airport weather

It may be noticed from that ET based on airport weather data always falls in Q4 of the categorization indicating that the temperature at the airport is on the higher side of the ET distribution as compared to rest of the city for the 2 days of heatwave.

A comparison is drawn between the areas rendered as vulnerable by the HVI (maximum value of 8) for uniform vs spatial weather data. For any other value of HVI, i.e. less than 8, it cannot be said with confidence, whether the grid cell is vulnerable because of higher number of elderly population or due to higher ET making it difficult to choose between policies related to public health or urban planning.

Figure 56 shows the that the number of areas vulnerable to heat are significantly higher when weather from the airport is uniformly applied.

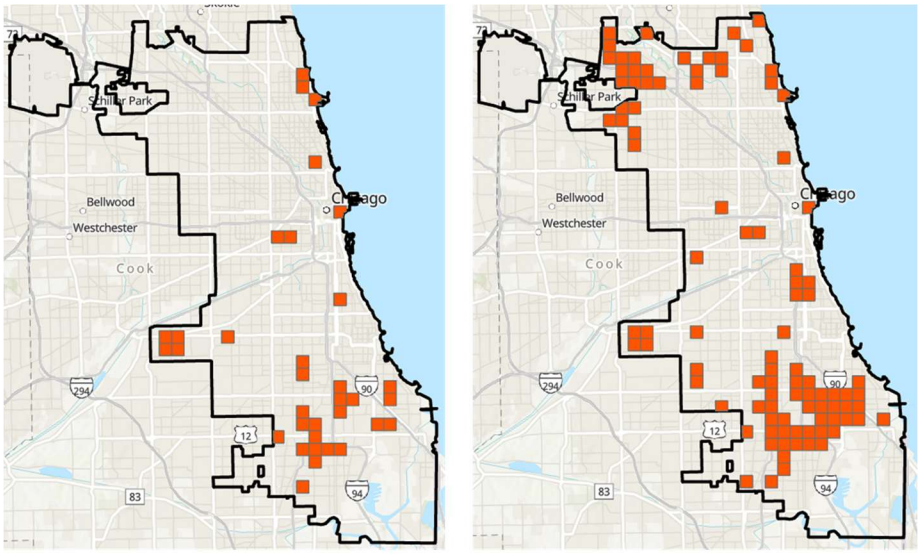

Figure 56 Vulnerable grids with (a) Meso scale weather (b)Airport weather

The number grids with high heat vulnerability is 34 when spatial weather data is used whereas 96 grids show up on the map when uniform weather data based on airport data is

used. Since each grid is approximately 1km^2, any intervention such as increasing greenery in vulnerable areas or encouraging reflective roofs that are planned on the basis of airport weather would cover three times more area and hence significantly higher planning and investment to reduce the vulnerability of elderly population to heat.

5.4.2 Application case II- Energy Poverty

The definition of energy poverty derived from Great Britain's Warm Homes and Energy Conservation Act states the following (Murkowski & Scott, 2014);

Energy insecurity is defined to include both fuel poverty, the inability to pay for heating or cooling required to maintain a home at a reasonable temperature, and the loss of electricity through cessation of service due to non-payment or other factors.

According to RECS report in 2015, approximately 30% of the American households reported challenges in paying their energy bills for heating and cooling their homes.

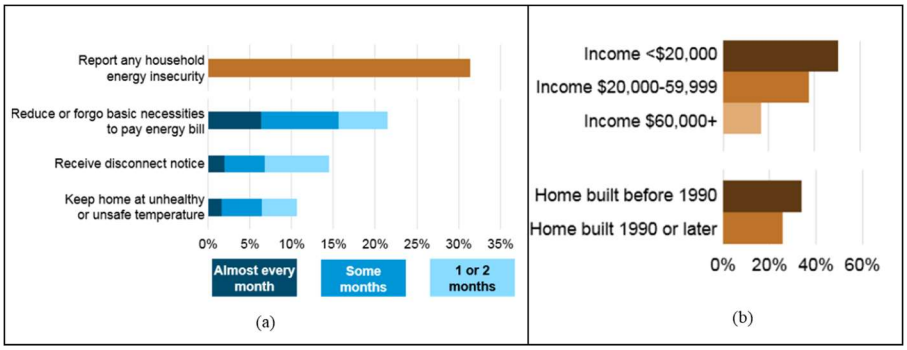

Figure 57 US Energy Information Administration, Residential Energy Consumption Survey 2015 (a) Households experiencing energy insecurity in the US (b) Energy insecurity housing characteristics

Households that face energy insecurity end up having unhealthy thermal environments as they try to use less energy, have reduced productivity and/or get into debt to pay for energy

services. Therefore, federal programs like Low Income Home Energy Programs (LIHEAP) and US DOE's Weatherization Assistance Programs (WAP) targets these households and helps them with either financial assistance to pay for their energy bills or start weatherization programs for dilapidated dwellings.

(Bednar et al., 2017) attempt to identify areas in Detroit that are prone to energy poverty based on income and heating EUI's of houses based on RECS and American Housing Survey (AHS) data. EUI for houses are computed based on a regression model built on housing characteristics such as year in which the house was built, unit type, income level etc. EUI is used as an attribute for the weatherization assessment instead of energy consumption data as it was observed that low income households had relatively high consumption due to high EUI of houses owing to the age and ill maintenance of building.

Taking inspiration from the above literature, this application case tries to find the difference between number of houses that would be targeted for weatherization programs when meso-scale weather data is used vs when uniform weather based on airport data is used. To limit the otherwise large scope of the problem statement, only single-family homes of vintage pre-1990 are considered for demonstration. Note that a similar approach can be used for all housing types. This vintage was used as the report from US DOE (Spanier, Scheu, Brand, & Yang, 2012) found that most of the houses built in Chicago (see Figure 58) are old and also because the RECS report from EIA (Berry, n.d.) mentioned above reflect that houses built prior to 1990 are more prone to energy insecurity.

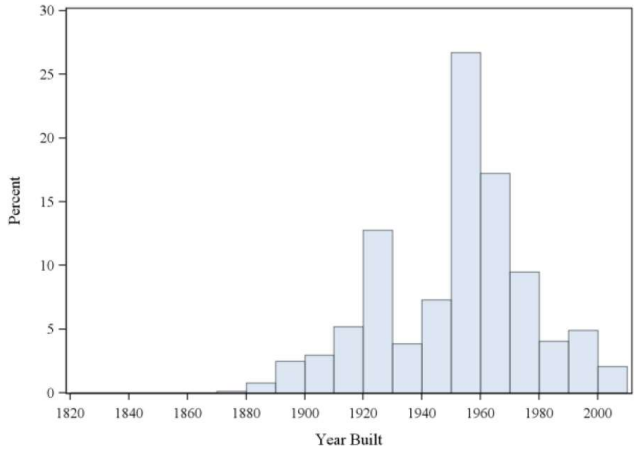

Figure 58 Distribution of single-family homes by year in which they were constructed (Spanier, Scheu, Brand, & Yang, 2012)

The housing characteristics are also taken from the same report and are used to create an Energy Plus model of the archetypical house. The model is simulated with both airport as well as meso-scale weather data to find the heating EUI in each grid cell respectively. The focus is on heating since Chicago is in a heating dominated region.

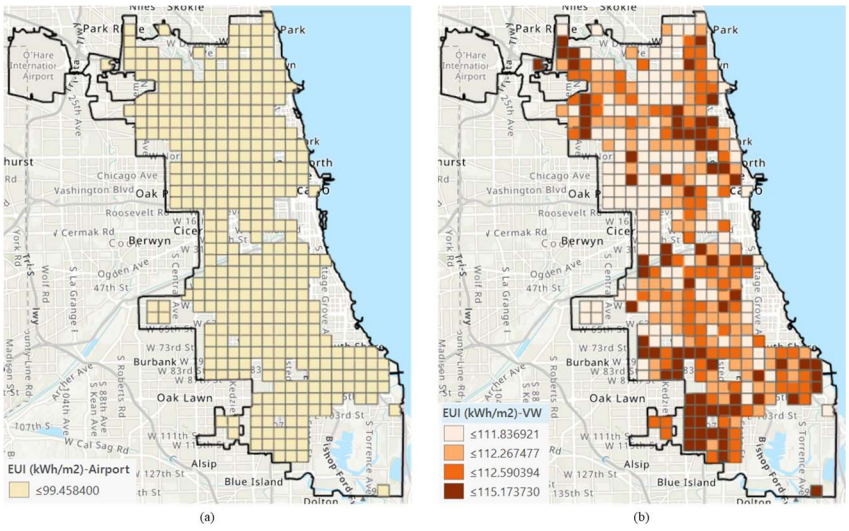

Figure 59 Comparison of heating EUI for Chicago (a) Using only airport weather (b) Using high fidelity weather data

From Figure 59 one may observe a large variation of approximately 15 kWh/m^2 in EUI between airport and some parts of Chicago. For the housing prototype considered in this case study, having 334 m^2 conditioned floor area, this difference roughly amounts to following dollar value;

Difference in annual energy consumption= 15 * 334= 5010 kWh=171 Therms

With an average rate of $0.853/therm in Chicago (Bureau of Labor Statistics, 2020),

the difference in heating energy bill will amount to 171*0.853 or $146.

The methodology to collate household income data with heating EUI follows the same approach as discussed in the first application case in section 5.4.1 with the difference that Q4 for income is assigned a value of 1, denoting low importance when looking for areas with low income and high EUI. For example, if a grid cell has low income (Q1), the percentile categorization would be numeric value 4. EUI on the other hand will have a numeric categorization 1 if it falls in Q1 as shown inFigure 59.

Energy Poverty Index (EPI)=Percentile categorization (EUI)+ Percentile categorization (Income)

Figure 60 illustrates the methodology to overlay the attributes of income and EUI to find the areas with population most susceptible to energy poverty (EPI=8) and should be prioritized for weatherization programs.

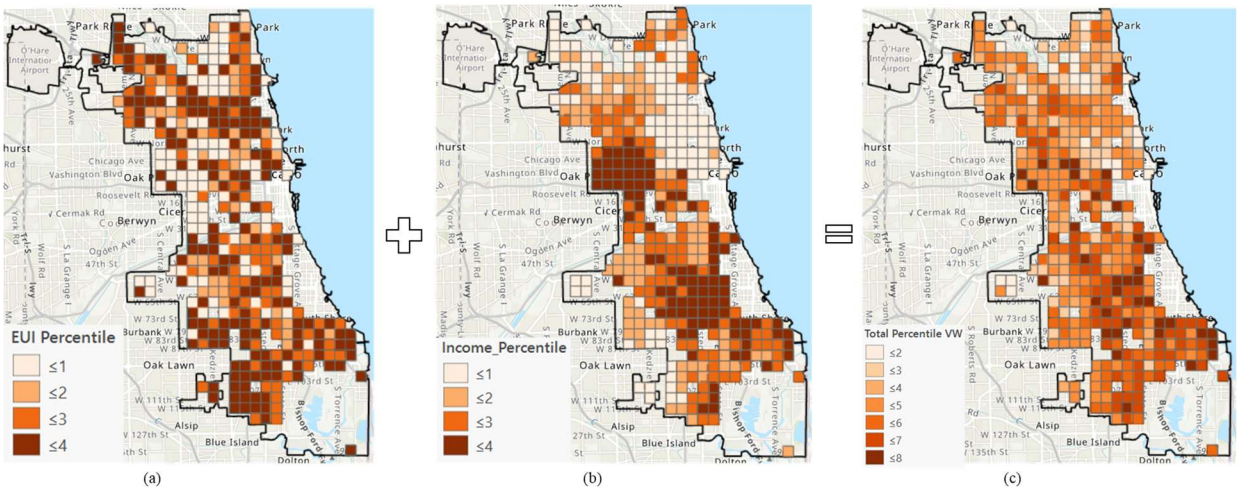

Figure 60 Methodology to identify energy poor areas based on income and EUI (a) Percentile categorization of EUI (b) Percentile categorization of Income (c) EPI as a sum of EUI and Income percentile categories

Since the heating EUI from the Energy Plus model simulated with airport weather lies in Q1 of distribution, a percentile categorization of 1 is combined with data for income. This yields the highest value of 5 for our EPI (as compared to 8 found with spatial weather data) and solely dependent on income inequality. Therefore, obviously, grid cells with a value of 5 would be considered ones that would require priority for weatherization programs.

The grid cells with high EPI for both these cases are filtered and combined with the number of single family housing units that in these grid cells found from the building footprint data described in section 5.4.

As seen in Figure 61, there are many grid cells that have high EPI and hence a large number of houses that would need weatherization if airport weather is uniformly applied. When meso-scale weather is used, policy makers can zoom in on areas that are colder owing to their location as well as fall into the low-income census tracts.

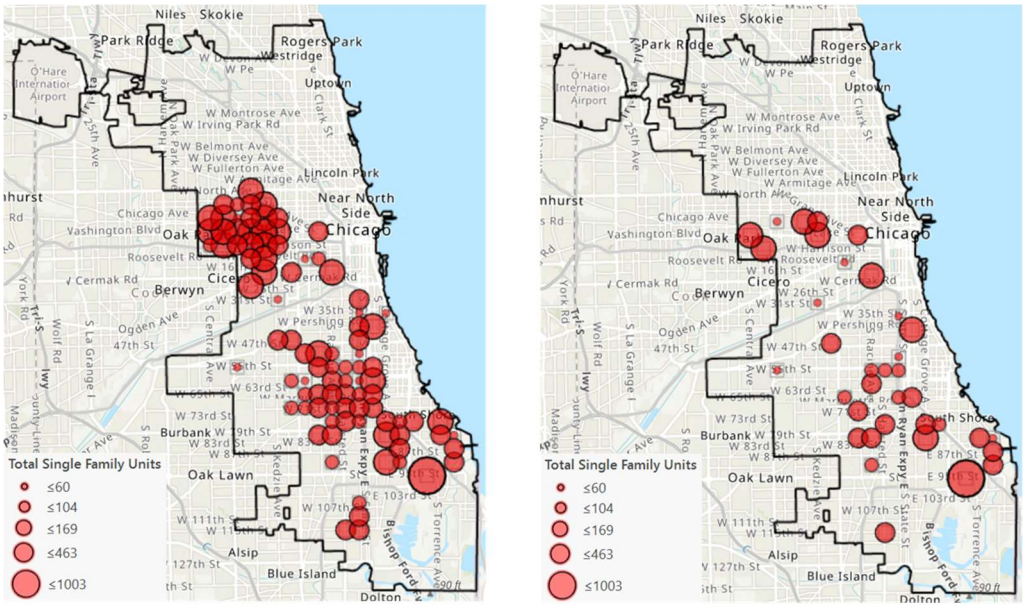

Figure 61 Number of single-family housing units in grids with high EPI (a) Airport weather (b) Meso scale weather

From the building footprint data, total number of houses in high EPI grid cells are calculated for each of the two comparison cases. According to this application case, the number of houses that need weatherization is highly inflated when weather from the airport is uniformly applied.

Table 8 Total number of houses that need weatherization

	Airport weather	**High fidelity weather**
Maximum EPI	5	8
Number of grids with max EPI	94	36
Number of housing units for weatherization	14427	5972

5.4.3 Application case III- Financial assessment of PV systems in Urban simulation

The state law in Illinois states that 25% of its electric power should come from renewable sources such as solar and wind energy by 2025, but, up until Q3 of year 2019, renewables make up only 4% of the energy mix in the state (MCCOPPIN, n.d.). Also, Chicago has committed to fulfil 100% of its energy requirements by renewable sources by 2035 with the *Resilient Chicago plan* formulated in 2017 ("Urban Resilience + 100 Resilient Cities Partnership | Resilient Chicago," n.d.). To accelerate the amount of solar PV installation by distributed generation, *Solar Chicago* program has been initiated by the Mayor's office streamlining the solar rooftop application process, reducing application fee and increasing the affordability of residential rooftop projects for homeowners.

The key metrics for financial models of rooftop projects include cost, revenues, net present values (NPV), Internal Rate of Return (IRR) and Return on Investment (ROI) for 25 year period (City of Chicago, 2018).

This application case examines the role of spatial weather data in load projections of the building stock of Chicago with an assumed blanket adoption of solar PV for all the residential buildings that are suited for rooftop solar owing to their orientation towards South direction. In this hypothetical case, each grid cell will independently form a community rooftop solar alliance, where the yield from the (within a grid cell) aggregated PV system is intended to shave off loads for the aggregated demand generated within the grid cell. The final test is whether key metrics such as NPV for solar financial model are affected by using applying weather that is derived from the airport.

Table 9 Datasets used for Application case III

Dataset	Use
ComEd	Hourly utility rates
Building Footprint	Total area of South facing roofs in each grid cell, building stock information
PVWatts	Hourly energy yield from PV (AC kWh/DC kW installed)
2020 Annual Technology Baseline (NREL)	CAPEX ($/kW DC)

The case study utilizes *Time of Use* (TOU) hourly energy prices from ComEd which is the dominant electricity provider for Chicago residences. The composition of housing stock has been limited to detached houses as most of the high-rise buildings are not strictly residential and have hybrid use, with some floors being used purely for commercial purposes.

The PVWatts simulation tool from National Renewable Energy Laboratory (NREL) is used to get hourly energy yield (kWh) from a 1 kW (DC) system so that it may be scaled for the total projected installed capacity of each grid cell. It should be noted that the yield from PV systems is calculated on the basis of TMY3 solar data to limit the scope of this work. However, in future work, more detailed simulation models may be used to calculate this yield which would differ with meso scale weather for each grid cell. It should be noted though that the PV yield is dominated by available direct and diffuse solar irradiation. Solar data is mostly independent from urban morphology and the meso scale solar data only differs marginally from airport solar data.

For financial metric data of overnight capital expenditure per kW (DC) installation, the Annual Technology Baseline sheet from NREL is referenced.

The residential buildings primarily facing South direction (see Table 7) are selected from the building footprint data and total available rooftop area is summarized for each grid cell using GIS. With the rule of thumb that each kW (DC) installation requires about 10 m^2 area, potential installation capacity for each grid cell is calculated. The available area for PV installation per grid cell does not take into account the shading from obstacles near the building itself.

All the calculations are done on per hour basis for 8760 hours of the year for each grid cell since utility TOU rates are available in the hourly resolution. From the information and datasets mentioned above, the annual hourly PV energy yield is calculated as follows;

$$P_{Gen}\ (kWh)_{hou\ \ i}^{grid\ j} = Installed\ PV^{grid\ j} * PVWatts\ output_{hou\ \ i}$$

For calculation of hourly demand from buildings for each grid cell, the building prototypes are simulated with meso-scale weather data for each grid cell. Prototypes are also simulated for recorded weather data from airport.

The peak load for each hour is then normalized to get peak power demand per unit area (P_D) for each hour for each prototype. To get total load for all the prototypes in the grid cell, each prototype is multiplied by the area that its footprint covers in the grid cell (obtained from building footprint GIS data described in section 5.4). For example, for single family, single story homes (abbreviated as SF_Old for brevity) with pre-1990 construction,

$$\left(P_{D-SF\_Old}\right)_{hour\ i}^{grid\ j} = \left(\frac{Power\ Demand_{hou\ \ i}}{Total\ Building\ Area_{SF\_Old}}\right) * Total\ Footprint_{SF\_Old}{}^{grid\ j}$$

Similarly, for each grid cell, total hourly demand for each prototype is calculated and added to obtain a final hourly peak load for each grid cell.

$$(P_{D-Total})_{hour\ i}^{grid\ j} = \sum_{prototype\ 1}^{prototype\ k} (P_{D-k})_{hour\ i}^{grid\ j}$$

This process is repeated to obtain hourly load profiles for each grid with airport data. A comparative GIS map for difference between summer (June 2018) and annual energy consumption between meso scale weather and airport weather is shown in Figure 62.

It is interesting to note that Annual consumption shows a much larger difference in energy consumption as compared to June. This is because in winters, the electrical energy consumption is low for most homes that are heated by natural gas. Therefore, due to net metering, in colder months, rooftop PV exports more power to the grid than in summer months when more electrical energy is needed for air conditioning.

The difference between energy consumption and energy bills are calculated as;

Difference (Energy Consumption) = Energy consumption with Meso-scale weather- Energy consumption with uniform airport weather

Difference (Energy Bill)=Energy bill with Meso-scale weather- Energy bill with uniform airport weather

It is also worthwhile to mention that in June, the difference between consumption is high and negative with areas for low heat index (see Figure 51) suggesting that the weather at

airport is hotter than in the rest of the city. This has been observed in the other application cases.

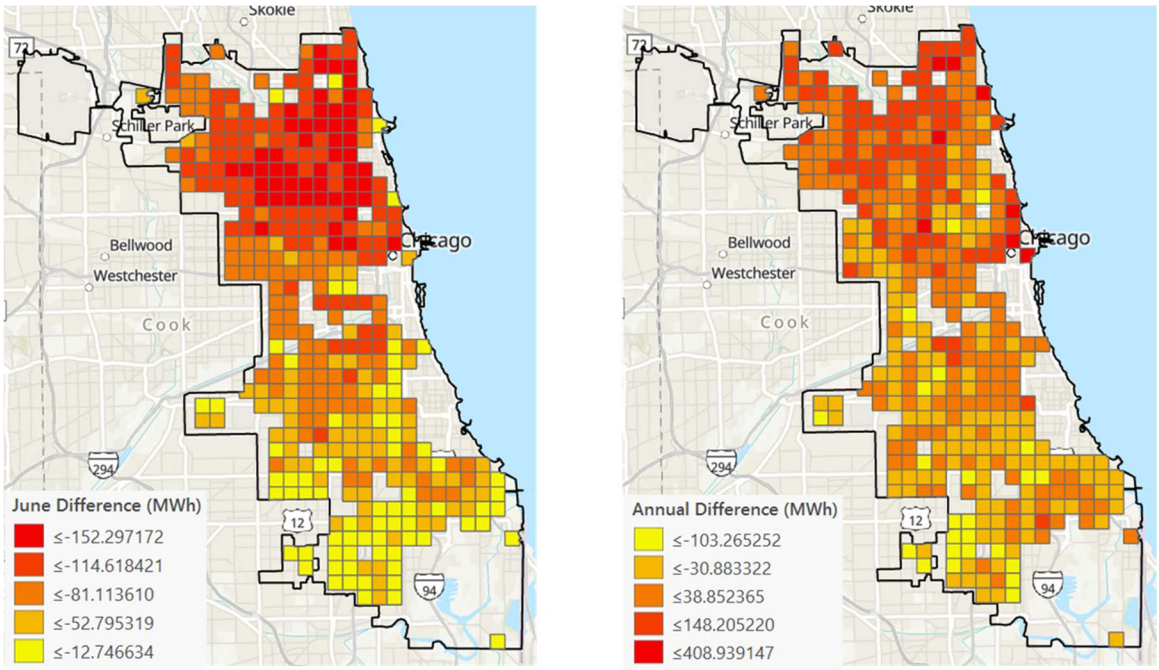

(a) (b)

Figure 62 Difference in energy consumption (Meso scale-Airport weather) (a) June 2018 (b) Annual 2018

Once hourly generation and demand have been ascertained for each grid cell, the energy bill for each hour is calculated inclusive of saving from load shaving due to PV generation,

$$Energy\ Bill\ (\$)_{hour\ i}^{grid\ j} = \left[\left((P_{D-Total})_{hour\ i}^{grid\ j}\ \right) - \left(P_{Gen}\ (kWh)_{hour\ i}^{grid\ j}\right)\right] * TOU_{hour\ i}$$

The hourly energy bill calculated is summed for every hour of the year for each grid cell. Similarly, energy bill with uniformly applied airport weather is computed hourly and then annually.

Figure 63 illustrates the difference between energy bills computed when meso scale weather is used vs when weather data from the airport is used.

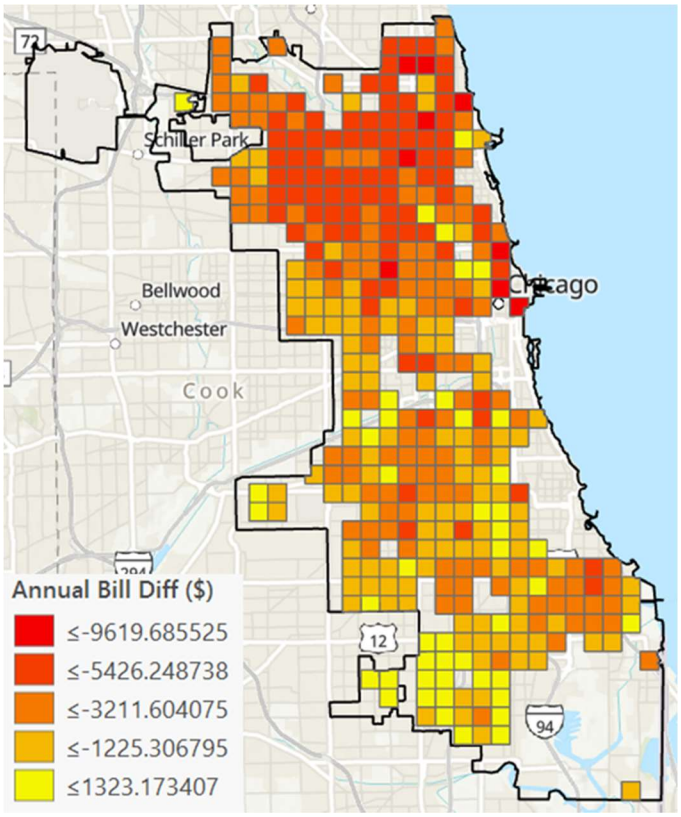

Figure 63 Difference in Annual Energy bill (Meso scale-Airport weather)

The difference in energy bills so computed are solely due to difference in assumption of weather for building simulation in the same grid since other factors such as footprint for each prototype, PV potential, utility rates etc are same. Again, grids in the Northern part of the city have large negative amounts suggesting that bills are lower when local weather is used as compared to weather from airport. This result is in line with the energy consumption results also suggesting that air conditioning during summer is the dominant factor in the variation of energy bills.

Figure 64 shows the difference in annual energy bill as a percentage of CAPEX that needs to be invested in each grid to install PV systems for its complete potential. Since the investment in each grid depends on total area of rooftops facing South, this percentage is smaller where there is lower rooftop potential as systems are smaller and require less initial investment.

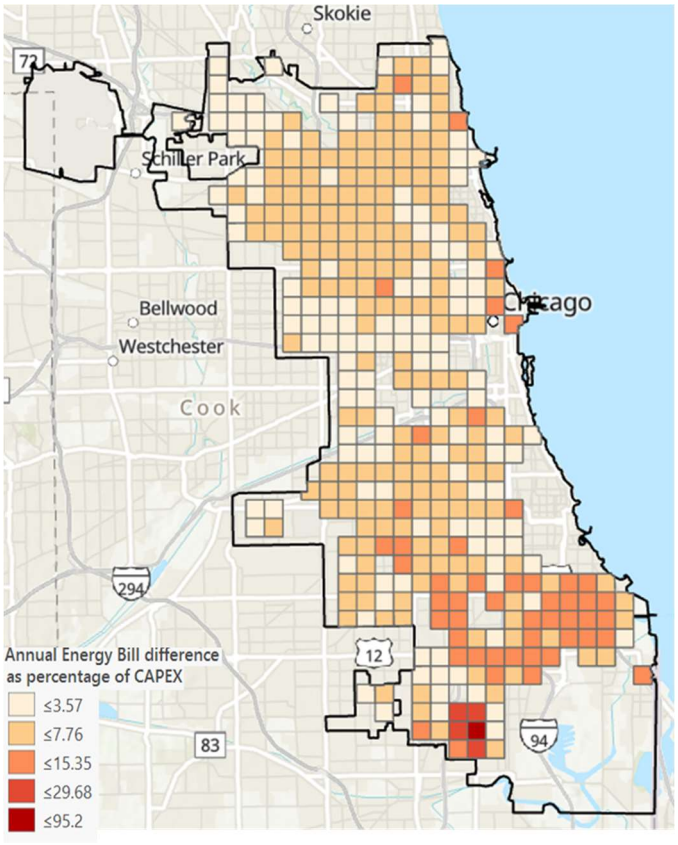

Figure 64 Energy bill difference as a percentage of CAPEX required for each grid

Thus, during the planning stage of large distributed solar projects like this hypothetical case suggests, even a 3% variation in capital investment accumulated over 25 years is likely to affect the interest rate on loans taken from financial institutions. This highlights the significance of using high fidelity weather data in the assessment of project viability of large distributed PV projects in the planning stage.

5.5 Concluding remarks

This chapter focuses on location sensitive decision scenarios following established USim approaches abased on deterministic simulations. It turns out that the use of local weather makes a significant difference in the assessment of three widely used indicators.

This conclusion is based on the grids for which synthetic weather could be created by the MTOT algorithm. This however represents only a subset of all the areas in Cook county of Chicago. Therefore, as discussed in section 3.8, to get a complete coverage of a city for making decisions such as HVI based on urban simulation, more and spread out weather monitoring stations should be set up. Alternatively, more elaborate technologies such as WRF may be used.

Although the outcomes of Chapter 4 and 5 seem in some sense contradictory, recall that the investigations in Chapter 4 focused on a single building simulation in an unspecified location in the city. Not knowing for what location the simulation is performed raises no issues when uniform airport weather is used, but when spatially diverse weather applies, location does obviously matter. To inspect how much it matters, we regard the spatial variability as an additional source of uncertainty and gauge its relevance among other sources of uncertainty. It turns out that the influence is rather minor for QoI that are long interval aggregates of simulation outcomes.

In this chapter we take another angle and ask the question whether location sensitive decisions are affected by using meso scale weather. When this is done in a traditional deterministic sense, it is found that the influence is significant. But as seen in Chapter 4, if there is a lack of information or if there is large uncertainty in some important (read

sensitive) building simulation inputs, it is difficult to skim out the impact of high resolution weather data amongst the noise created by the variance caused by other sources of variability. Nonetheless, urban decisions that aim to identify areas of high impact in the city can benefit from higher resolution data in deterministic bottom up approach of USim.

In a future follow-up step, the USim models should be subjected to an uncertainty analysis which would bring the two angles in harmony, leading to an understanding about impact of aggregated building level uncertainties in urban decision scenarios.

CHAPTER 6. CONCLUSIONS AND FUTURE WORK

Building Simulation practice has been traditionally reliant on the typical meteorological years (TMY) for decades now albeit with the cognizance that the methodology for creation of these files was originally designed for solar energy conversion systems. Their inclusion in the National Solar Radiation database involved attaching more weight to the solar radiation elements of the weather (Wilcox & Marion, 2008). But, in the absence of any other credible method that could provide the typical weather for a location, TMY3 remains the preferred "boundary condition" for building simulation models.

There has been a consistent interest in the scientific community to examine the variation in simulation outcomes when the weather is not typical, i.e., when a building is subjected to an extreme year (temporally), or when large scale UHI or the immediate surroundings of a building (spatially) modify the weather. These temporal and spatial modifications affect some performance measures more than others. The extent of this effect is furthermore unique to the building in question.

This thesis focuses on the effect of spatial variability of weather across a city. It is studied at the scale of individual buildings and at neighbourhood scale but sporadically at meso-scale. As meso scale weather does generally not exist for a whole city, the research starts off by developing a methodology that can alter the weather data collected from open spaces to reflect the urban features of a city in different locations. A collection of synthetic weather files that cover the expanse of variance in weather due to local urban morphology

across the city of Chicago is generated. This repository paves the way for the ensuing study of the relevance of meso scale weather information.

The investigation of its importance is then conducted from two different angles, namely;

- The effect on building simulation outcomes is tested in three cases where spatial diversity of weather is ranked in comparison with other sources of ignorance/incomplete information about simulation inputs. The results suggest that weather does not significantly change the shape of the UQ distribution for buildings where uncertainty in other parameters is dominant, such as is the case in old residential houses. For buildings that are new and constructed to stricter codes, model parameter uncertainty is generally much reduced. In that case the spatial variability of weather becomes more important and may stretch the tail ends of the QoI distribution. This effect has not been researched in detail, but the expectation is that the effect is minor.
- In the context of decisions at the urban scale it was found that using weather that is local to the buildings can affect local decision outcomes significantly.

  In Application case I, it was observed that the regions that were most vulnerable to heat exposure increased almost three times in area when uniform weather from the airport was used for the analysis. Similarly, in Application case II, the number of low-income households that are projected to be vulnerable to energy poverty are significantly higher when weather from the airport is used. In Application case III, the energy requirements and hence energy bills for grid cells in various parts of the city are shown to have remarkable difference when meso-scale weather is used. The threshold at which differences in the urban simulation indicators compel the

stakeholders to use meso-scale weather is highly case specific in the real world, and a comprehensive cost-benefit analysis can extend the dialogue on this issue, which is out of scope of this work.

It should be recognized that this finding is based on established deterministic simulations which are routinely used for these assessments.

6.1 Future Work

- Chicago was selected as the test region due to availability of good quality recorded weather and GIS data. Also, all the experiments are done with weather data from the year 2018.Treating this thesis as starting point, more cities in different climate zones should be tested using the methodology described in this thesis to make any generic conclusion about importance of spatially diverse weather on building simulation.
- The test cases for UQ can be expanded to include more scenarios of buildings and different QoI to reach a thorough understanding of weather that can be generally applied based on type of building, chosen QoI and decision context.

REFERENCES

Ahmet, G. (2014). Micro-siting of wind turbines using navier-stokes solutions coupled with a numerical weather prediction model a thesis submitted to the graduate school of natural and applied sciences of middle east technical university. Retrieved from http://etd.lib.metu.edu.tr/upload/12617818/index.pdf

Anderson, G. B., & Bell, M. L. (2012). Lights out: Impact of the August 2003 power outage on mortality in New York, NY. *Epidemiology*, *23*(2), 189–193. https://doi.org/10.1097/EDE.0b013e318245c61c

Augenbroe, G. (2011). The role of simulation in performance based design. *Building Performance Simulation for Design and Operation (Hensen JLM and Lamberts R, Editors). Spon Press. ISBN13*, 970–978.

Bednar, D. J., Reames, T. G., & Keoleian, G. A. (2017). The intersection of energy and justice: Modeling the spatial, racial/ethnic and socioeconomic patterns of urban residential heating consumption and efficiency in Detroit, Michigan. *Energy and Buildings*, *143*, 25–34. https://doi.org/10.1016/j.enbuild.2017.03.028

Belleri, A., Lollini, R., Environment, S. D.-B. and, & 2014, undefined. (n.d.). Natural ventilation design: An analysis of predicted and measured performance. *Elsevier*. Retrieved from https://www.sciencedirect.com/science/article/pii/S0360132314001954

Berry, C. (n.d.). RECS: One in three U.S. households faced challenges in paying energy

bills in 2015. Retrieved November 8, 2020, from Energy Information Administration, Residential Energy Consumption Survey Data 2015 website: https://www.eia.gov/consumption/residential/reports/2015/energybills/

Bruse, M. (2004). *ENVI-met 3.0: Updated Model Overview*. Retrieved from www.envi-met.com

Bueno, B., Norford, L., Hidalgo, J., & Pigeon, G. (2013). The urban weather generator. *Journal of Building Performance Simulation*, *6*(4), 269–281. https://doi.org/10.1080/19401493.2012.718797

Chan, W. R., Nazaroff, W. W., Price, P. N., Sohn, M. D., & Gadgil, A. J. (2005). Analyzing a database of residential air leakage in the United States. *Atmospheric Environment*, *39*(19), 3445–3455. https://doi.org/10.1016/j.atmosenv.2005.01.062

Chen, J. (2018a). Investigation of hybrid ventilation potential of commercial buildings in us.

Chen, J. (2018b). Investigation of hybrid ventilation potential of commercial buildings in us. Retrieved from https://smartech.gatech.edu/handle/1853/61662

Chen, Y., Hong, T., & Piette, M. A. (2017). Automatic generation and simulation of urban building energy models based on city datasets for city-scale building retrofit analysis. *Applied Energy*, *205*, 323–335. https://doi.org/10.1016/j.apenergy.2017.07.128

Chessa, P. A., & Delitala, A. M. S. (1997). Objective analysis of daily extreme temperatures of Sardinia (Italy) using distance from the sea as independent variable.

International Journal of Climatology, *17*(13), 1467–1485. https://doi.org/10.1002/(sici)1097-0088(19971115)17:13<1467::aid-joc200>3.3.co;2-a

Chinazzo, G., Rastogi, P., & Andersen, M. (2015). Assessing robustness regarding weather uncertainties for energy-efficiency-driven building refurbishments. *Energy Procedia*, *78*, 931–936. https://doi.org/10.1016/j.egypro.2015.11.021

Chung, W. J., Cecinati, F., Liu, C., Rajasekar, E., Coley, D., & Natarajan, S. (n.d.). *The Impact of Weather Spatial Variations on Thermal Mass Design in India*.

Costola, D., Blocken, B., environment, J. H.-B. and, & 2009, undefined. (n.d.). Overview of pressure coefficient data in building energy simulation and airflow network programs. *Elsevier*. Retrieved from https://www.sciencedirect.com/science/article/pii/S0360132309000444

De Wit, M. S. (2001). *Uncertainty in predictions of thermal comfort in buildings*. Retrieved from https://repository.tudelft.nl/islandora/object/uuid:a231bca8-ec81-4e22-8b34-4bafc062950e?collection=research

Domínguez-Muñoz, F., Cejudo-López, J. M., & Carrillo-Andrés, A. (2010). Uncertainty in peak cooling load calculations. *Energy and Buildings*, *42*(7), 1010–1018. https://doi.org/10.1016/J.ENBUILD.2010.01.013

Dorer, V., Allegrini, J., Orehounig, K., Moonen, P., Upadhyay, G., Kämpf, J., & Carmeliet, J. (n.d.). Modelling the urban microclimate and its impact on the energy demand of buildings and building clusters.

Friedman, J. H., & Roosen, C. B. (1995). An introduction to multivariate adaptive regression splines. *Statistical Methods in Medical Research*, *4*(3), 197–217. https://doi.org/10.1177/096228029500400303

Fujita, T., Newstein, H., & Tepper, M. (1956). *Mesoanalysis: An important scale in the analysis of weather data*. Retrieved from https://books.google.com/books?hl=en&lr=&id=Yw8hL7pQvDsC&oi=fnd&pg=PA1&dq=Mesoanalysis:+An+Important+Scale+in+the+Analysis+of+Weather+Data&ots=64iU1zaiUG&sig=ZYjkyeLWX_H6oi3r8OgMfuQ_Hwk

Futcher, J. A., Kershaw, T., & Mills, G. (2013). Urban form and function as building performance parameters. *Building and Environment*, *62*, 112–123. https://doi.org/10.1016/j.buildenv.2013.01.021

Gahrooei, M. R., Yan, H., Paynabar, K., & Shi, J. (2018). *A novel approach for fusion of heterogeneous sources of data*. Retrieved from http://arxiv.org/abs/1803.00138

Gunawardena, K. R., & Kershaw, T. (n.d.). *URBANCEQ-2017 International Conference on Urban Comfort and Environmental Quality Urban climate influence on building energy use*.

Hjort, J., Suomi, J., & Käyhkö, J. (n.d.). *Spatial prediction of urban-rural temperatures using statistical methods*. https://doi.org/10.1007/s00704-011-0425-9

Hong, T., Chen, Y., Luo, X., Luo, N., & Lee, S. H. (2020). Ten questions on urban building energy modeling. *Building and Environment*, *168*, 106508. https://doi.org/10.1016/j.buildenv.2019.106508

Hong, T., Chou, S. K., & Bong, T. Y. (1999). A design day for building load and energy estimation. *Building and Environment*, *34*(4), 469–477. https://doi.org/10.1016/S0360-1323(98)00035-3

Hong, T., & Luo, X. (2018). *Modeling building energy performance in urban context Passive technologies for reducing building cooling needs: evaporative cooling. View project Machine learning for buildings research View project*. Retrieved from https://www.researchgate.net/publication/326682222

Jain, R., Luo, X., Sever, G., Hong, T., & Catlett, C. (2020). Representation and evolution of urban weather boundary conditions in downtown Chicago. *Journal of Building Performance Simulation*, *13*(2), 182–194. https://doi.org/10.1080/19401493.2018.1534275

Jentsch, M. F., James, P. A. B., Bourikas, L., & Bahaj, A. B. S. (2013). Transforming existing weather data for worldwide locations to enable energy and building performance simulation under future climates. *Renewable Energy*, *55*, 514–524. https://doi.org/10.1016/j.renene.2012.12.049

Jones, M., Hope, C., & Hughes, R. (1990). A multi-attribute value model for the study of uk energy policy. *Journal of the Operational Research Society*, *41*(10), 919–929. https://doi.org/10.1057/jors.1990.144

Katal, A., Mortezazadeh, M., & Wang, L. (Leon). (2019). Modeling building resilience against extreme weather by integrated CityFFD and CityBEM simulations. *Applied Energy*, *250*, 1402–1417. https://doi.org/10.1016/j.apenergy.2019.04.192

Ke, X., Wu, D., Rice, J., Kintner-Meyer, M., & Lu, N. (2016). Quantifying impacts of heat waves on power grid operation. *Applied Energy*, *183*, 504–512. https://doi.org/10.1016/j.apenergy.2016.08.188

Knoll, B., Phaff, J., & Gids, W. De. (1995). *Pressure simulation program*. Retrieved from https://www.narcis.nl/publication/RecordID/oai:tudelft.nl:uuid%3Ae1d7f901-a9af-4b19-8942-7ae62999204e

Kolda, T. G., & Bader, B. W. (2009). Tensor decompositions and applications. *SIAM Review*, Vol. 51, pp. 455–500. https://doi.org/10.1137/07070111X

Lee, B. D., Sun, Y., Hu, H., Augenbroe, G., & Paredis, C. J. (n.d.). A framework for generating stochastic meteorological years for risk-conscious design of buildings. In *ibpsa-usa.org*. Retrieved from http://ibpsa-usa.org/index.php/ibpusa/article/view/449

Liu, S., Pan, W., Zhang, H., Cheng, X., Long, Z., & Chen, Q. (2017). CFD simulations of wind distribution in an urban community with a full-scale geometrical model. *Building and Environment*, *117*, 11–23. https://doi.org/10.1016/J.BUILDENV.2017.02.021

Mallen, E. S. (2019). *A Methodological Assessment of Extreme Heat Mortality Modeling and Heat Vulnerability Mapping in Atlanta, Detroit, and Phoenix*. Georgia Institute of Technology.

Masson, V., Grimmond, C. S. B., & Oke, T. R. (2002). Evaluation of the Town Energy Balance (TEB) Scheme with Direct Measurements from Dry Districts in Two Cities. *Journal of Applied Meteorology*, *41*(10), 1011–1026. https://doi.org/10.1175/1520-

0450(2002)041<1011:EOTTEB>2.0.CO;2

Mavrogianni DipArch, A., Davies, M., Batty FBA FRS, M. B., Belcher FRMetS, S. M., Bohnenstengel, S., Carruthers, D., … Ye BEng, Z. (n.d.). *The comfort, energy and health implications of London's urban heat island*. https://doi.org/10.1177/0143624410394530

MCCOPPIN, R. (n.d.). Solar power popularity growing in Illinois, despite obstacles - Chicago Tribune. Retrieved November 7, 2020, from https://www.chicagotribune.com/news/breaking/ct-solar-power-boom-in-illinois-20190906-hzn4psuv7jd2dond35zkrtxx6y-story.html

Meehl, G., Stocker, T., Collins, W., & Friedlingstein, P. (2007). *Global climate projections*. Retrieved from https://publications.csiro.au/rpr/pub?list=BRO&pid=procite:1452cb7a-9f93-44ea-9ac4-fd9f6fd80a07

Memon, R. A., Leung, D. Y. C., & Liu, C. H. (2010). Effects of building aspect ratio and wind speed on air temperatures in urban-like street canyons. *Building and Environment*, *45*(1), 176–188. https://doi.org/10.1016/j.buildenv.2009.05.015

Mirsadeghi, M., Cóstola, D., Blocken, B., & Hensen, J. L. M. (2013). Review of external convective heat transfer coefficient models in building energy simulation programs: Implementation and uncertainty. *Applied Thermal Engineering*, Vol. 56, pp. 134–151. https://doi.org/10.1016/j.applthermaleng.2013.03.003

Murkowski, L., & Scott, T. (2014). *Plenty at Stake: Indicators of American Energy*

Insecurity. Retrieved from https://www.energy.senate.gov/services/files/075f393e-3789-4ffe-ab76-025976ef4954

Ninyerola, M., Pons, X., & Roure, J. M. (2000). A methodological approach of climatological modelling of air temperature and precipitation through GIS techniques. *International Journal of Climatology*, *20*(14), 1823–1841. https://doi.org/10.1002/1097-0088(20001130)20:14<1823::AID-JOC566>3.0.CO;2-B

Nor&n, J., Westberg, K., Jernberg, P., Haagenrud, S. E., & Sjiistriim, C. (n.d.). *Service life prediction of buildings and the need for environmental characterisation and mapping*.

Oke, T. R. (2006). INSTRUMENTS AND OBSERVING METHODS REPORT No. 81. In *ww.instesre.org*. Retrieved from http://ww.instesre.org/GCCE/UrbanMeteorologicalObservations.pdf

Oleson, K. W., Bonan, G. B., Feddema, J., Vertenstein, M., & Grimmond, C. S. B. (2008). *An Urban Parameterization for a Global Climate Model. Part I: Formulation and Evaluation for Two Cities*. https://doi.org/10.1175/2007JAMC1597.1

Parys, W., Breesch, H., Hens, H., & Saelens, D. (2012). Feasibility assessment of passive cooling for office buildings in a temperate climate through uncertainty analysis. *Building and Environment*, *56*, 95–107. https://doi.org/10.1016/j.buildenv.2012.02.018

Pernigotto, G., Prada, A., & Gasparella, A. (2019). Extreme reference years for building energy performance simulation. *Journal of Building Performance Simulation*, 1–17.

https://doi.org/10.1080/19401493.2019.1585477

Plate, E., Kiefer, H., Vancouver, J. W.-F. C. on U. E., & 2004, undefined. (n.d.). *Wind and urban climates*.

Pohekar, S. D., & Ramachandran, M. (2004, August 1). Application of multi-criteria decision making to sustainable energy planning - A review. *Renewable and Sustainable Energy Reviews*, Vol. 8, pp. 365–381. https://doi.org/10.1016/j.rser.2003.12.007

Quan, S. J., Li, Q., Augenbroe, G., Brown, J., & Yang, P. P. J. (2015a). Urban data and building energy modeling: A GIS-based urban building energy modeling system using the urban-EPC engine. *Lecture Notes in Geoinformation and Cartography*, *213*, 447–469. https://doi.org/10.1007/978-3-319-18368-8_24

Quan, S. J., Li, Q., Augenbroe, G., Brown, J., & Yang, P. P. J. (2015b). Urban data and building energy modeling: A GIS-based urban building energy modeling system using the urban-EPC engine. *Lecture Notes in Geoinformation and Cartography*, *213*, 447–469. https://doi.org/10.1007/978-3-319-18368-8_24

QuickStart | EnergyPlus. (n.d.). Retrieved November 10, 2020, from https://energyplus.net/quickstart

Rastogi, P. (2016). *On the sensitivity of buildings to climate: the interaction of weather and building envelopes in determining future building energy consumption*. *6881*(August). https://doi.org/10.5075/epfl-thesis-6881

Reinhart, C. F., Dogan, T., Jakubiec, A., Rakha, T., & Sang, A. (n.d.). UMI-an urban simulation environment for building energy use, daylighting and walkability .

Rigol, J. P., Jarvis, C. H., & Stuart, N. (2001). *International Journal of Geographical Information Science Artificial neural networks as a tool for spatial interpolation Arti cial neural networks as a tool for spatial interpolation*. https://doi.org/10.1080/13658810110038951

Robitu, M., Musy, M., Inard, C., & Groleau, D. (2006). Modeling the influence of vegetation and water pond on urban microclimate. *Solar Energy*, *80*(4), 435–447. https://doi.org/10.1016/J.SOLENER.2005.06.015

Rothfusz, L., Worth, N. H.-F., National, T., & 1990, undefined. (n.d.). The heat index equation (or, more than you ever wanted to know about heat index). *204.227.127.200*. Retrieved from http://204.227.127.200/images/oun/wxsafety/summerwx/heatindex.pdf

Shahmohamadi, P., Che-Ani, A. I., Maulud, K. N. A., Tawil, N. M., & Abdullah, N. A. G. (2011). The Impact of Anthropogenic Heat on Formation of Urban Heat Island and Energy Consumption Balance. *Urban Studies Research*, *2011*. https://doi.org/10.1155/2011/497524

Shimoda, Y., Okamura, T., Yamaguchi, Y., Yamaguchi, Y., Taniguchi, A., & Morikawa, T. (2010). City-level energy and CO2 reduction effect by introducing new residential water heaters. *Energy*, *35*(12), 4880–4891. https://doi.org/10.1016/j.energy.2010.08.043

Spanier, J., Scheu, R., Brand, L., & Yang, J. (2012). *Chicagoland Single-Family Housing Characterization*. https://doi.org/10.2172/1219715

Stone, B., Vargo, J., Liu, P., Habeeb, D., Delucia, A., Trail, M., … Russell, A. (n.d.). *Avoided Heat-Related Mortality through Climate Adaptation Strategies in Three US Cities*. https://doi.org/10.1371/journal.pone.0100852

Sun, YM. (2014). *Closing the Building Energy Performance Gap by Improving Our Predictions (Doctoral Dissertation)*.

Sun, Yuming. (2014). *Closing the building energy performance gap by improving our predictions*. Georgia Institute of Technology.

Sun, Yuming, Gu, L., Wu, C. F. J., & Augenbroe, G. (2014). Exploring HVAC system sizing under uncertainty. *Energy and Buildings*, *81*, 243–252. https://doi.org/10.1016/J.ENBUILD.2014.06.026

Sun, Yuming, Heo, Y., Tan, M., Xie, H., Jeff Wu, C. F., & Augenbroe, G. (2014). Uncertainty quantification of microclimate variables in building energy models. *Journal of Building Performance Simulation*, *7*(1), 17–32. https://doi.org/10.1080/19401493.2012.757368

Sun, Yuming, Heo, Y., Xie, H., Tan, M., Wu, J., & Augenbroe, G. (n.d.). *Uncertainty quantification of microclimate variables in building energy simulation*.

Swami, M., transactions, S. C.-A., & 1988, undefined. (n.d.). Correlations for pressure distribution on buildings and calculation of natural-ventilation airflow. *Pascal-*

Francis.Inist.Fr. Retrieved from https://pascal-francis.inist.fr/vibad/index.php?action=getRecordDetail&idt=7369168

Takahashi, K., Mochida, A., Yoshino, H., Mitamura, T., Miyauchi, S., & Yoshida, T. (n.d.). *Synthesized Analyses of Meso-Micro and Indoor Climates-Evalutation on the Spatial Distribution of Wind Potential inside a City for Reducing the Cooling Load of Residential Buildings by means of Cross-ventilation*.

Tian, W., & De Wilde, P. (2011). Uncertainty and sensitivity analysis of building performance using probabilistic climate projections: A UK case study. *Automation in Construction*, *20*(8), 1096–1109. https://doi.org/10.1016/j.autcon.2011.04.011

Tong, Z., Chen, Y., & Malkawi, A. (2016). Defining the Influence Region in neighborhood-scale CFD simulations for natural ventilation design. *Applied Energy*, *182*, 625–633. https://doi.org/10.1016/j.apenergy.2016.08.098

Tucker, L. R. (1966). Some mathematical notes on three-mode factor analysis. *Psychometrika*, *31*(3), 279–311. https://doi.org/10.1007/BF02289464

Urban Resilience + 100 Resilient Cities Partnership | Resilient Chicago. (n.d.). Retrieved November 7, 2020, from https://resilient.chicago.gov/urban-resilience

US Department of Commerce, N. N. W. S. (n.d.). *June 16-18, 2018: Mid-June Heat Wave*.

Wilcox, S., & Marion, W. (2008). *Users Manual for TMY3 Data Sets (Revised)*. https://doi.org/10.2172/928611